Inhibition of a Mycothiol Biosynthetic Enzyme and a Detoxification Enzyme as Anti-Tubercular Drug Targets

Mohlopheni Jackson Marakalala

Thesis Presented for the Degree of

DOCTOR OF PHILOSOPHY

Department of Clinical Laboratory Sciences

UNIVERSITY OF CAPE TOWN

AUGUST 2008

Supervisor: Associate Prof: D.J Steenkamp

Declaration

I, Mohlopheni Jackson Marakalala, hereby grant the University of Cape Town free licence to reproduce this thesis in whole or in part, for the purpose of research.

I declare that this dissertation is based on my original work, both in concept and execution, and that apart from the normal guidance from my supervisor, I have received no assistance, except where acknowledgements indicate otherwise. I also declare that all sources that I have used have been indicated and acknowledged by means of complete references.

Signature:…….

Date:…….

ACKNOWLEDGEMENTS:

I would like to express my heartfelt gratitude to the following people for the great role they played in making this project successful:

My supervisor, Prof Daniel Steenkamp, whose supervisory skills and guidance have unearthed my desire for science and made me proud of the career field I have chosen.

Useful discussions and suggestions from our collaborators are hereby acknowledged for the noticeable contribution they made towards the success of this study. I am grateful to Prof David Gammon and the rest of the carbohydrates chemistry lab members (Chemistry department, University of Cape Town), especially Dr Theo Mudzunga, Christian Bolz and Freddy Munyololo for synthesizing the *O*-glycosides for our biological testing. Dr Anwar Jardine of Chemistry Department, University of Cape Town and Prof Spencer Knapp of Rutgers State University of New Jersey, for providing us with the Thioglycosides. I am also indebted to Prof Stefan Oscarson of University College Dublin for the generous offer of an α-d form of GlcN-Ins. I thank Dr Adele Thomas of Medical Biochemistry, UCT, for the useful discussions on enzymatics and providing Accelerys Discovery Studio 17 as well as the assistance on the docking experiments.

To the past and present members of my laboratory, Biochemistry of Pathogens, I am so blessed to have been with you during the course of my study, thank you for the useful discussions; Lumka Bhunguzana for the initial cloning of mshB, Dr Monique Williams for her willingness to share her experience and for motivating me with her undying love for science, Gabriel Mashabela for a true and fruitful friendship along the years, Vuyo Mavumengwana for useful discussions and for the successful synthesis of the naphthoquinones, Nicholas Watermeyer for a great fellowship we enjoyed during the write-up of this thesis, and all our laboratory visitors from Portugal, Germany and Sweden. To Naadia, the dream lives on and this is just the beginning, thank you for everything my friend. To the rest of Chemical Pathology division, the H.O.D Prof Pillay and your team, thank you for being my second family and for providing a healthy learning environment. To the students, including the

registrars, in this division, it was really a journey worth travelling, may you all grow to become successful scientists.

I am grateful to Fr Graham for continuous spiritual support and for the guidance during the retreat and to my friends in fellowship at UCT Catholic Chaplaincy, for making my spiritual life blossom to the heights. To my friends at UCT choir for Africa, thank you for sharing the talent of music with me, this is a tribute to the choir chairperson and friend Oletlile. To so many people I am blessed to have as my friends, Dr Tshepo Bodiba, Mosiuwa, there are too many to mention, but I know I am richer for having you all in my life.

To my mother, who is my inspiration and the reason for my prosperity, Mrs Nancy Raisibe Marakalala, here are the fruits of the patience and courage you planted in me. I say all these could not have been possible without your encouragement and your uncompromised support emotionally, materially and financially. To the rest of my family, Joseph, James, Elizabeth, Jan, Simon (his memories still live) and Herbert, you are the reason I believe that a family built in the love of God will never go apart, I thank God everyday for bringing you into my life. To my love, my angel, Remoneilwe-Bontle, daddy loves you unconditionally.

I am grateful for financial assistance provided by the National Research Foundation of SA, Canon Collins Trust and the UCT Postgraduate Funding and their donors.

Glory to the sovereign God and His son Jesus Christ, my saviour, for with His gracious mercy I had enough strength to complete this study. His loving kindness is to time indefinite, and the favour He exercises upon His children endures for everlasting.

ABSTRACT:

Mycobacteriuam tuberculosis, the bacillus that causes tuberculosis (TB), utilizes mycothiol (MSH), a low molecular weight thiol, as its main antioxidant and a protectant against toxins. MSH maintains the bacterial intracellular redox homeostasis and is essential for the growth of *M. tuberculosis*. MSH reacts with toxins to form MSH *S*-conjugates which are cleaved by MSH *S*-conjugate amidase (mca), in the detoxification pathway which excretes drugs such as rifamycin and cerulenin from the cell as mercapturic acids. The biosynthesis of MSH proceeds in four steps catalyzed by enzymes denoted mshA, mshB, mshC and mshD. MSH-deficient mutants are hypersensitive to alkylating agents, free radicals and antibiotics like streptomycin, and the protective roles facilitated by MSH are critical to the survival of *M. tuberculosis* in the hostile environments of activated alveolar macrophages. Thus the inhibition of MSH biosynthesis and of the MSH-dependent detoxification pathway is an attractive avenue for the development of new drugs against TB and drug-resistant TB. The work in this thesis was carried out with the aim evaluating the inhibition of both mca and mshB by a range of analogs of the pseudodisaccharide substructure of MSH.

MSH was purified from *M. smegmatis* and used to synthesize MSmB and Acetyl-GlcN-Ins, the natural substrates for mca and mshB, respectively. Mca was partially purified from *M. smegmatis*, while the recombinant mshB from *M. tuberculosis* was expressed in *E. coli* and purified to homogeneity. 8 structural analogs of Acetyl-GlcN-Ins which contain either a cyclohexane or a thiophenyl in place of inositol were evaluated as substrates of mshB. 21 novel compounds, including thioglycosides, *O*-glycosides and naphthoquinones, were evaluated as inhibitors against both enzymes.

The heterodisulfide, MSSNaph, was found to be a substrate for mca with a *K*m value of 328 μM. Amongst the Acetyl-GlcN-Ins structural analogs evaluated as substrates for mshB, MCL2 was the best giving *V*max value twice lower than that of the natural substrate and the *K*m 5-fold higher. The naphthoquinones were the best inhibitors against both enzymes, giving the inhibition of up to 44% and 95% for mca and mshB, respectively. A pattern was observed where naphthoquinones with longer carbon chains were better inhibitors of mca and mshB. The Ki values of the naphthoquinones, Vu2, Vu4 and Vu5, against mshB were 162.7, 93.9 and 16.8 μM, respectively. From the docking experiments, Vu2 and Vu5 occupied the active site of

mshB providing a hypothetical model for the binding mode of the naphthoquinones and the MSH biosynthetic enzyme. Vu5 was the best mshB inhibitor because its longer carbon chain extends the molecule such as to allow interaction of the naphthoquinone group with the hydrophobic dipeptide of Val 184 and Leu 185. For future research on identifying potential drug targets, an evaluation of compounds bearing apolar groups, attached through spacers of variable length to the glucosamine moiety, as potential inhibitors of both mca and mshB will be especially fruitful.

Abbreviations:

Å	angstrom
AccQ-Flour	6-aminoquinolyl-*N*-hydroxysuccinimidyl carbamate
AcCysSR	acetylcysteine *S*-conjugates
Acetyl-GlcN-Ins/GlcNAc-Ins	1-*O*-(2-acetamido-2-deoxy-α-D-glucopyranosyl)-D-*myo*-inositol
AIDS	acquired immune difficiency syndrome
AMP	adenosine monophosphate
APS	ammonium per sulphate
ATP	adenosine triphosphate
BCG	Bacille Calmette-Guérin
Bp	base pairs
CDNB	1-chloro-2,4-dinitrobenzene
CoA	coenzyme A
CPM	7-diethylamino-3-(4'-maleimidylphenyl)-4-methylcoumarin
Cys-GlcN-Ins	1-*O*-[2-[[(2*R*)-2-amino-3-mercapto-1-oxopropyl]amino]-2-deoxy-α-D-glucopyranosyl]-D-*myo*-inositol
CySmB-GlcN-Ins	1-*O*-[2-[[(2*R*)-2-amino-3-mercapto-1-oxopropyl]amino]-2-deoxy-α-D-glucopyranosyl]-D-*myo*-inositol-bimane
Dabsyl chloride	4-dimethylaminoazobenzene-4'-sulfonyl chloride
DCM	dichloromethane
DEAE	diethylaminoethyl
DMSO	dimethyl sulphoxide
DNA	deoxyribonucleic acid
DnsCl	5-dimethylamino-1-naphthalenesulfonyl chloride
DOTS	directly observed treatment, short-course
dTdP	dithiodipyridyl
DTNP	5,5'-dithiobis(2-nitrobenzoic acid)
DTT	dithiothreitol
IL-2	interleukin 2
IL-12	interleukin 12

IMAC	Immobilized Metal Ion Affinity Chromatography
INF-γ	gamma interferon
INO1	inositol 1-phosphate synthase
Ins-2-P	*myo*-inositol 2 phosphate
IPTG	isopropyl-beta-D-thiogalactopyranoside
k_{cat}	turnover number
k_{cat}/Km	specificity constant
*K*m	catalytic constant
Ki	inhibition constant
Da	dalton
LDH	lactate dehydrogenase
Lpd	lipoamide dehydrogenase
Mca	mycothiol *S*-conjugate amidase
MDMPI	mycothiol-dependent maleylpyruvate dehydrogenase
MDR-TB	multidrug resistant tuberculosis
Min	minute
ml/hour	millilitre per hour
ml/min	millilitre per minute
mM	millimolar
MscR	*S*-nitrosothiol reductase
MSH	mycothiol
MshA2	Acetyl-GlcN-Ins-P phosphatase
MshA	UDP-*N*-acetylglucosamine: 1L-*myo*-inositol-1-phosphate 1-α-D-*N*-acetylglucosaminyltransferase
MshB	1-*O*-(2-acetamido- 2-deoxy-α-D-glucopyranosyl)-D-*myo*-inositol deacetylase
MshC	ATP-dependent L-cysteine: 1-*O*-(2-amino-2-deoxy-α-D-glucopyranosyl)-D-*myo*-inositol ligase
MshD	mycothiol synthase
MSmB	monobromobimane derivative of mycothiol
MSNO	*S*-nitrosomycothiol
MSSM	mycothiol disulfide

MSSNaph	2'-s-(mycothiolyl)-6-hydroxynaphthyldisulfide
$M^{-1}.cm^{-1}$	Per molar per centimetre
NAD	nicotinamide adenine dinucleotide
NADH	reduced nicotinamide adenine dinucleotide
NADPH	reduced nicotinamide adenine dinucleotide phosphate
N-AcCys-Naph	acetylcysteine naphthyldisulfide
N-AcCys-Mb	N-Acetylcysteine-bimane
n	nano
NO	nitric oxide
OD	optical density
ORF	open reading frame
PAS	p-aminosalicylic acid
PCR	polymerase chain reaction
PI3P	phosphotidylinositol 3-phosphate
PMSF	phenylmethylsulphonyl fluoride
PPD	purified protein derivative
Redox	reduction-oxidation reactions
RNA	ribonucleic acid
RNI	reactive nitrogen intermediate
ROI	reactive oxygen intermediate
RPM	revolutions per minute
SDS-PAGE	sodium dodecyl sulphate polyacrylamide gel electrophoresis
[S]	substrate concentration
TB	tuberculosis
TEA	triethylamine
TEMED	N N N `N`-tetramethyl-1,2-diaminoethane
TFA	trifluoroacetic acid
TLC	thin later chromatography
TLCK	*N*-*p*-tosyl-L-lysine chloromethyl ketone
TPCK	*N*-*p*-tosyl-L-phenylalanine chloromethyl ketone
tRNA	transfer ribonucleic acid
TSH_2	trypanothione

UDP-GlcNAc	uridine diphosphate acetylglucosamine
UV	ultraviolet
v	initial velocity
*V*max	maximum rate of reaction
W/V	weight/volume
WHO	world health organizaton
XDR-TB	extensively drug resistant tuberculosis
Zn^{2+}	Divalent zinc cation
µ	micro

List of Figures:

List of Tables:

BRIEF CONTENTS:

DETAILED CONTENTS:

CHAPTER 1: GENERAL INTRODUCTION

CHAPTER 3: SYNTHESIS OF SUBSTRATES

CHAPTER 4:
EXTRACTION, PURIFICATION AND INHIBITION OF MYCOTHIOL S-CONJUGATE AMIDASE

CHAPTER 1:
GENERAL INTRODUCTION

1.1 TUBERCULOSIS

1.1.1 Tuberculosis Infection

Amongst all human diseases resulting from bacterial infection, tuberculosis (TB) remains the deadliest. TB is a contagious disease which is caused by *Mycobacterium tuberculosis,* a bacillus that is transmitted in air droplets when an infectious person coughs or sneezes. Because the immune system is capable of fighting the progression into active TB, not all people who are infected with the bacillus develop the disease. The bacillus can remain dormant inside the lungs for years without causing the disease but is activated when the immune system is weakened (WHO, 2008).

Symptoms of TB include chest pain, difficulty in breathing, loss of appetite, excessive sweating, fever and coughing with blood in mucus that lasts for over two weeks. The advanced pathology may also cause blood vessel disruption resulting in haemoptysis[1] (Bloom and Murray, 1992). Multiple symptoms of TB may lead to gradual debilitation and physical exhaustion; hence the disease is often referred to as consumption (Ducati, 2006).

1.1.2 History of Tuberculosis

The great white plague of man, Captain of death, King's Evil, Phthisis, consumption and lupus vulgaris are some of the names that have been used to describe TB in the past centuries. Archeological works from a number of neolithic sites from ancient Egypt to the Roman and Greek empires indicate evidence of a disease consistent with modern TB. TB was described by Hippocrates' work dated back in 400 BC and was clearly documented by Claudius Galen during the Roman Empire (Mathema *et al*., 2006).

[1] Haemoptysis is the coughing up of blood from the respiratory tract.

The presence of spinal tuberculosis was demonstrated on the fossil bones dated 8000 BC (Ayvazian, 1993) and there is evidence that bone and tissue cell samples from Egyptian mummies of people that lived around 2400 BC contained *Mycobacterium tuberculosis* (Zink *et al.,* 2003).

The study was done in which samples from the Egyptian mummies were analyzed for the presence of the ancient mycobacterial complex DNA and further characterized using spoligotyping. When the spoligotyping signatures were compared to those in the database they all showed either a *M. tuberculosis* or a *M. africanum* pattern, and none of the samples analyzed were indicative of *M. bovis*, the causative agent of bovine tuberculosis (Zink *et al.*, 2003). These findings contradicted the theory that *M. tuberculosis* evolved from *M. bovis* and were further comfirmed by Brosch *et al*. (2002) who showed that a progenitor of *M. tuberculosis* was a human pathogen (Brosch *et al.*, 2002)

A major breakthrough was made in 1882 when Robert Koch discovered *M. tuberculosis* from crushed tubercles[2]. He identified *M. tuberculosis* as a causative organism of tuberculosis and in 1890 developed the tuberculin test[3] for diagnosis of the disease. Following this, Koch discovered the staining methods for the identification of the bacillus. His work allowed more researchers to focus on the development of TB therapy and his staining technique was subsequently improved by Paul Ehrlich, whose method provided the basis for the popular Ziehl Nielsen staining technique (Ducati, 2006).

1.1.3 Tuberculosis Infection and Epidemiology

1.1.3.1 Global TB incidence

According to the WHO global TB control report released in March 2008 (table 1.1), the largest number of new TB cases reported in 2005 occurred in the South-East Asia region and accounted for 34% of incident cases globally. 1.58 million people died of

[2]Tubercles, also known as granuloma, are formed at the site of infection which has been remodelled into a cellular mass by host reponse to TB infection (Russell, 2007).
[3] The tuberculin test is explained in section 1.4.

TB in 2005. Of these mortalities, 544 000 deaths occurred in the Africa region followed by the South-East Asia region where 512 000 people died of the disease. In the 1990s, the TB epidemic increased rapidly in Africa, but current reports indicate that the incident rate has begun to stabilize (WHO, 2008).

In all six WHO regions, the estimated per capita incident rate was stable in 2005. However, the slow decrease in the incident rate was offset by the rapid population growth. As a result, the number of new cases arising each year is still increasing globally (WHO, 2008). Thus TB is still a global problem that needs urgent attention and advanced treatment strategies.

Table 1.1: Estimated TB Incidence, Prevalence and Mortality, 2005 (WHO, 2008)

	Incidence[4]				Prevalence[5]		TB Mortality	
	All forms		Smear-positive[6]					
WHO region	number (thousands) (% of global total)	per 100 000 pop	number (thousands)	per 100 000 pop	number (thousands)	per 100 000 pop	number (thousands)	per 100 000 pop
Africa	2 529 (29)	343	1 088	147	3 773	511	544	74
The Americas	352 (4)	39	157	18	448	50	49	5.5
Eastern Mediterranean	565 (6)	104	253	47	881	163	112	21
Europe	445 (5)	50	199	23	525	60	66	7.4
South-East Asia	2 993 (34)	181	1 339	81	4 809	290	512	31
Western Pacific	1 927 (22)	110	866	49	3 616	206	295	17
Global	**8 811 (100)**	**136**	**3 902**	**60**	**14 052**	**217**	**1 577**	**24**

Pop denotes population.

[4] ***Incidence - new cases arising in a given period.***

[5] ***Prevalence - the number of cases which exist in the population at a given point in time.***

[6] ***Smear-positive cases are those confirmed by smear microscopy, and are the most infectious cases.***

1.1.3.2 TB Incidence in South Africa

South Africa has one of the worst TB epidemics in the world, ranking fifth amongst the world's high-burden TB countries. According to the WHO global TB report 2006, South Africa had about 339 000 new cases in 2004 (table 1.2), with an incidence rate of 718 cases per 100 000 people. The incidence rate more than doubled in 6 years and in 1998 was estimated at 338 per hundred thousand (WHO, 2006).

In 1996, South Africa adopted the directly observed treatment, short-course (DOTS) approach as a strategy to minimize TB cases. The success rate of DOTS was estimated to be 67%, significantly lower than the WHO standard rate of 85% (Gandhi *et al*., 2006). The substantial increase in number of tuberculosis cases in this area is compounded with the high levels of HIV and the emergence of drug resistant strains, indicating an urgent need for chemotherapeutic intervention.

Table 1.2: TB statistics in South Africa, all data was taken in 2004. (WHO, 2006)

Country population	47 207 653
Estimated number of new TB cases	339 078
Estimated TB Incidence (all cases per 100 000 population)	718
DOTS population coverage (%)	93%
DOTS treatment success rate in 2003 (%)	67
Estimated adult TB cases HIV+ (%)	60
Multi-drug resistant TB cases (%)	1.8

1.1.3.3 Tuberculosis and AIDS

TB is the leading cause of death amongst people who are HIV-positive or have progressed into full-blown AIDS (hivforum.org, 2007). Globally, about 42 million people are infected with HIV and almost one-third of these are also infected with TB. The HIV/TB co-infection is more persistent in Africa, where in most countries more than 50 percent of patients with TB are also HIV positive. The HIV/TB co-infection is

also a growing concern in Asia where TB accounts for 40% of AIDS deaths. The former Soviet Union and Eastern Europe have the fastest growing HIV epidemic in the world, and this could exacerbate MDR-TB in the region (usaid, 2008; WHO, 2008).

The relationship between the HIV and TB epidemics is a complex one as each contributes to the prevalence and mortality of the other (Sharma *et al*., 2005). In later stages of HIV infection the immune system in the lung becomes compromised and is characterized by the recruitment of fewer lymphocytes to the site of infection and the less efficient activation of macrophages (Collins *et al.,* 2002).

Thus, people infected with both HIV and TB are 30-times more likely to develop the active TB disease. Conversely, TB infection enhances HIV replication and accelerates the HIV progression to AIDS (usaid, 2008).

1.1.4 *Mycobacterium tuberculosis*

M. tuberculosis is the main etiological agent of TB in humans and was first discovered in 1882 by Robert Koch. *M. tuberculosis* is a weakly gram positive rod-shaped bacterium that has a width varying from 0.3 to 0.6 μm and a height of 1 to 4 μm. Unlike other bacteria, for example *E. coli*, which have division times measured in minutes, the generation time of *M. tuberculosis* ranges from 15 to 24 hours in both synthetic media and infected animals (Cole *et al.,* 1998).

The cell wall structure of the mycobacterium is arranged in such a way that the peptidoglycan contains *N*-glycolylmuramic acid instead of the *N*-acetylmuramic acid common in other bacteria. About 60% of the cell wall is made up of mycolic acids, lipids which consist of fatty acids with 60 to 90 carbons (Brennan and Nikaido, 1995). The mycobacterial cell wall is believed to be important in the pathology of TB, but due to its complex characteristics it is difficult to identify critical genes which would lead to attenuation if inactivated (Cole *et al*., 1998).

There are about 60 known species in the genus *mycobacterium*, of which three species, *M. tuberculosis*, *M. bovis* and *M. africunum* are causative agents of TB while one species, *M. leprae* causes leprosy in humans. The *M. tuberculosis* complex

consists of *M. bovis*, *M. bovis* BCG, *M. africanum*, *M. microti*, *M. canetti* and *M. tuberculosis* (Pérez-Martinez *et al*., 2008). Of all these mycobacterial species, the mostly studied strain in the biomedical research is *M. tuberculosis* H37Rv (Mtb H37Rv) due to its virulence and resistance against drugs (Cole *et al*., 1998)

The complete sequence of the *M. tuberculosis* H37Rv genome was reported in 1998 by Cole and co-workers (Cole *et al.*, 1998).

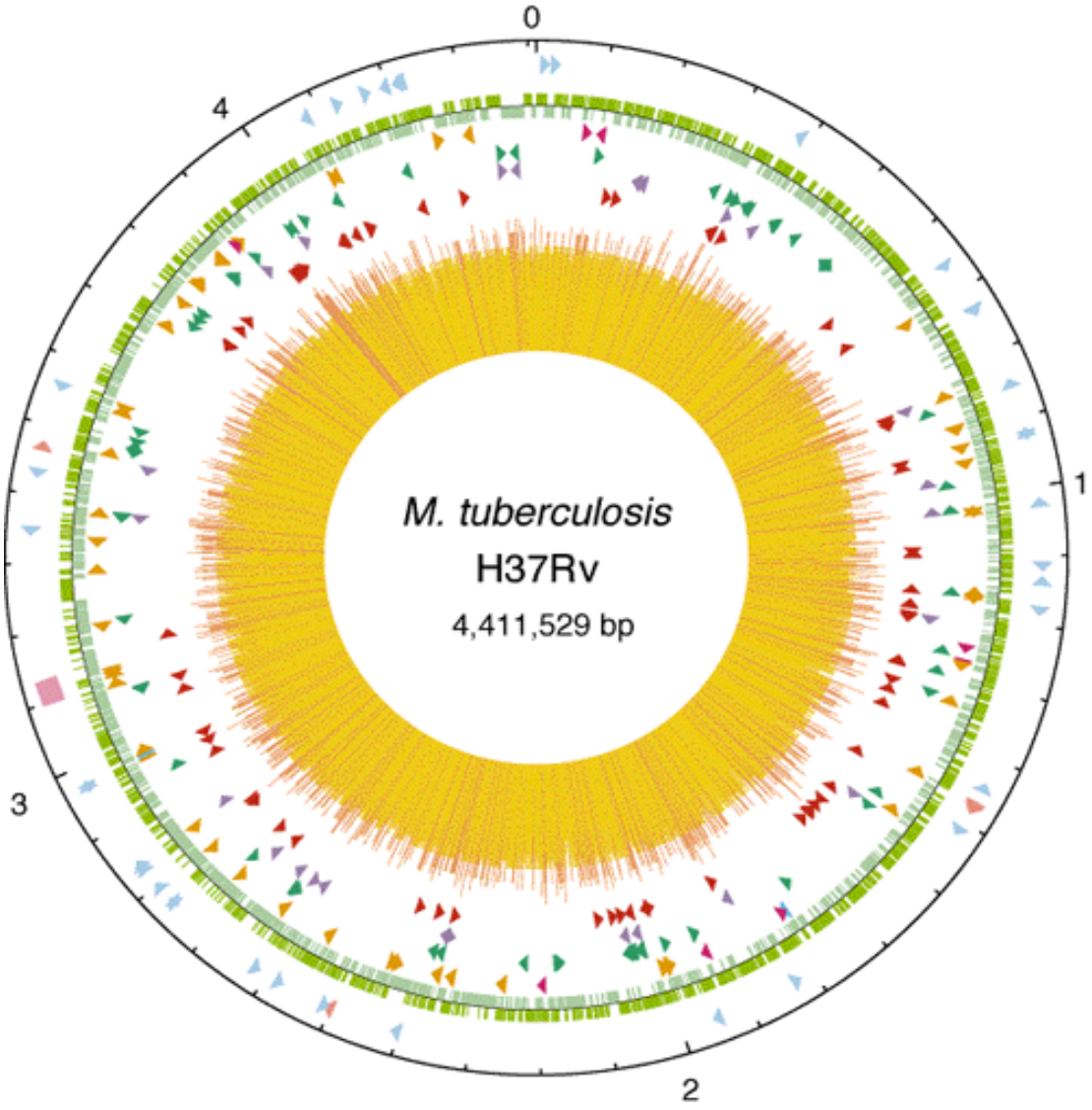

Figure 1.1: Circular map of the chromosome of H37Rv. The outer circle shows the scale in Mb, with 0 representing the origin of replication. The first ring from the exterior denotes the positions of stable RNA genes (tRNAs are blue, others are pink) and the direct repeat region (pink cube); the second ring inwards shows the coding sequence by strand (clockwise, dark green; anticlockwise, light green); the third ring depicts repetitive DNA. The histogram (centre) represents G + C content, with <65% G + C in yellow, and >65% G + C in red. (*Cole et al*., 1998)

Mtb H37Rv has a circular chromosome comprising 4 411 529 base pairs (figure 1.1). The genome contains about 4000 genes and 65.6% G+C content. Although Mtb H37Rv genome is smaller than *E.coli*, it codes for typical bacterial catabolic and anabolic pathways as well as for protein synthesis and degradation (Cole *et al*., 1998). About 16% of proteins in Mtb H37Rv have no similarity to any known protein, probably being involved in mycobacterial unique pathways. Another unique feature of Mtb H37Rv is that a very large portion of its coding capacity is devoted to the production of lipogenesis and lipolysis enzymes as well as to two families of glycine-rich proteins with a repetitive structure that may represent a source of antigenic variation (Cole *et al*., 1998; Camus *et al*., 2002).

Mtb H37Rv also contains enzymes required for processes such as glycolysis, the pentose phosphate pathway and glyoxylate and tricarboxylic acid cycles, thereby indicating that the pathogen has a dynamic metabolism (Ducati *et al*., 2006; Cole *et al*., 1998). All genes involved in the metabolism of mycothiol, the main antioxidant unique to actinomycetes, are present in the Mtb H37Rv genome (Steenkamp and Spies, 1994).

The completion of the genome sequence of *M. tuberculosis* has definitely opened gates for further research into the bacillus pathogenicity and its response against chemotherapy.

1.1.5 Clinical identification and Diagnosis of Tuberculosis

TB diagnosis involves detection of acid-fast bacilli in the sputum using Ziehl-Neelsen staining. The sputum sample is treated with NaOH to eliminate contaminating microoganisms, while mycobacteria survive these conditions as they are resistant to alkaline compounds due to their lipid layer. *M. tuberculosis* cultured from the sputum takes 4-6 weeks to form visible colonies. Another TB detection method is the Bactec system, which utilizes a medium containing radio-labelled palmitate as the sole carbon source. As *M. tuberculosis* multiplies, it breaks down palmitate to release radioactive $C0_2$. With the Bactec method, *M. tuberculosis* can be detected in 9-16 days (Todar textbook online, 2008).

The tuberculin skin test is the epidemiological surveillance method that can be used to detect infection through delayed hypersensitivity against mycobacterial antigens (Glickman and Jacobs, 2001). Purified protein derivative (PPD), which is employed as the test antigen in the tuberculin test, is generated by boiling a culture of *M. tuberculosis.* The PPD is intracutaneously injected in the forearm and the test results can be observed within 48 to 72 hours. The test is considered positive if the lesion, which is characterized by redness and swelling, is at least 10 mm in diameter (Todar, 2008). However this method is not reliable in patients vaccinated with BCG, since this vaccination also produces activity to PPD (Bloom and Murray, 1992).

More TB detection methods with sensitivity and specificity over 90% have been developed based on molecular techniques. These methods usually initiate with genomic sequence amplification, through PCR, which uses specific repetitive copy sequences, and can give sensitive results in few hours (Bloom and Murray, 1992; Ducati *et al*., 2006). Most of these methods are available commercially but are very expensive for some parts of the developing world to afford.

1.1.6 Protective immunity during tuberculosis infection

M. tuberculosis primarily infects alveolar macrophages[7], which represent the first line of defence against inhaled bacteria (Lohmann-matthes *et al*., 1994). Upon infection, the bacilli are ingested by phagocytic alveolar macrophages where they can be immediately eliminated or grow inside the intracellular environments in the localized lesions called tubercles. Two to six weeks after infection, cellular immunity is established in which lymphocytes and activated macrophages are infiltrated to the lesions where they eliminate bacilli and end the primary infection even before presentation of disease symptoms (Ducati *et al*., 2006). Phagocytosed bacilli are transported via the phagosomal and endocytic pathways to the lysosomes where they undergo degradation.

M. tuberculosis can parasitize macrophages by arresting the default process of phagosomal maturation into the phagolysosome (Vergne *et al*., 2003).

[7] Alveolar macrophages are located in the interphase between air and lung tissues. They are very actively involved in phagocytic and equipped to kill microorganisms.

Phosphatidylinositol 3-phosphate (PI3P) is a membrane trafficking regulatory lipid and is essential for phagosomal acquisition of lysosomal characteristics. PI3P was reported to be involved in the pathway that involves the maturation of phagosomes to become phagolysosomes (Chua and Deretic, 2004).

The immune system defence against infection includes activities of Th1 or Th2 cells which act in concert with $CD8^+$ and other numerous cell types including macrophages, B cells and stromal cells. Collectively, these interactions give rise to two patterns of cytokine release, type 1 and type 2 (Roitt *et al.,* 2001). Strong evidence exists that in mice the immunity correlates with type 1 response[8], a pattern of cytokine release dominated by gamma-interferon (INF-γ), interleukin-2 (IL-2) and interleukin-12 (IL-12) (Clerici *et al*., 1994, Salgame *et al*., 1991). Interferons and interleukins are group of molecules involved in signalling between cells of the immune system, the former are also involved in protection against viral infections (From immunology textbook by Roitt *et al*., 2001).

About two weeks after initial *M. tuberculosis* infection, growth of the bacteria is reduced due to the activation and differentiation of lymphocytes which supply INF-γ required to initiate the innate response. This leads to activation of macrophages which induce the production of nitric oxide (NO), one of the main mediators with antimycobacterial properties in mice (Ehlers, 1999). The NO production results in limitation of O_2 thereby inhibiting aerobic respiration. This impairs growth of *M. tuberculosis*, an obligate aerobe, and induces its dormancy program (Voskuil *et al.,* 2006). The importance of INF-γ in the immunity of mice was also established in some studies where its gene knockout resulted in an increased susceptibility to *M. tuberculosis* and death within 3 weeks (Dalton *et al*., 1993).

Although most of the bacilli are destroyed by the immune system, some will survive and establish primary infection in macrophages, residing in the phagosome (Glickman and Jacobs, 2001). The phagosome containing the living pathogen is able to resist the delivery to the degradation site in the lysosomes. The pathogen can therefore remain dormant in the alveolar macrophages embodied in the calcified structures of tubercles.

[8] Type 1 response refers to overall pattern of cytokine release by all cell types in the infected sites.

1.1.7 TB Vaccination

Bacillus Calmette Guérin (BCG) was first developed in 1924 by Albert Calmette and Camille Guérin and is currently the most widely used vaccine against TB. BCG vaccine, which is administered intradermally, is prepared from a strain of attenuated live *M. bovis* that has lost its virulence in humans. Since BCG vaccination produces PPD, the tuberculin skin test, which also relies on detection of PPD, gives false positive results in vaccinated patients (Bloom and Murray, 2002). This has led to some countries with low TB cases forbidding the BCG vaccination in favour of the more accurate disease detection test.

Studies by Weir and coworkers indicated that the BCG vaccination in infancy and adolescence induces an immunological memory to mycobacterial antigens that remains at measurable levels for at least 14 years (Weir *et al*., 2008). At best, BCG vaccine is 80% effective in preventing TB for about 15 years, although its protective effects seem to be variable according to geography (Colditz *et al*., 1994). Because of this variable efficacy as well as the loss of protective effects of BCG after a specific time there is a need for a search of more vaccines using recombinant modification and other attenuated live mycobacterial strains (Ducati *et al*., 2006).

1.1.8 TB Treatment

1.1.8.1 Directly Observed Treatment, Short-course

Directly Observed Treatment, Short-course (DOTS) is the treatment strategy that was launched by WHO in 1994 to tackle the global problem of inadequate TB control. This strategy is widely used globally, has an average success rate of 80% in curing TB (USAID, 2008) and remains at the heart of WHO TB treatment strategies. DOTS uses a 6 month course of drugs, including first line anti-tubercular drugs, isoniazid and rifampicin, and its implementation is dependent on 5 elements, namely, political commitment with sustained financing, case detection through quality-assured bacteriology, standardized treatment with supervision and patient support, effective drug supply and management system, and lastly, a system of monitoring and evaluation, and impact measurement (WHO, 2008). Although DOTS has been the

most effective strategy to combat TB, it may seem paternalistic to some patients as it involves direct observation by a health worker (Volmink and Garner, 2003). Fresh research is needed to shorten observed treatment duration, a measure that should make DOTS even more effective in controlling TB (Jawahar, 2004).

1.1.8.2 Anti-tubercular Drugs

In 1943 Selman Abraham Waksman, a microbiologist from Rutgers university who later won the Nobel prize, purified streptomycin from the soil bacterium *Streptomyces griceus.* The purified compound could kill a wide spectrum of bacteria, including *M. tuberculosis*, both in cultures and in animals (Shatz *et al.,* 1944a; Shatz *et al.,* 1944b). Streptomycin was quickly approved as an anti-tubercular drug by United States food and drugs administration and within 2 years about 25 000 kg per day of the drug was produced industrially. Although Waksman's discovery of streptomycin marked the beginning of the TB treatment era, single drug therapy using streptomycin, or other anti-tubercular drugs since then discovered, became ineffective due to the development of drug resistant strains of *M. tuberculosis* (Reviewed in Fox *et al*., 1999).

The development of streptomycin was followed by the discovery of another TB drug, para-aminosalicylic acid (PAS) (Reviewed by Sacchettini *et al*., 2008), by Jorgen Lehmen in 1948, followed by the introduction of Isoniazid and other antibiotics in the 1950s.

Today TB is curable with first line drugs, namely, isoniazid, rifampicin, ethambutol, pyrazinamide and streptomycin (figure 1.2). Isoniazid requires katG for activation and its mechanism of action includes inhibition of mycobacterial mycolic acids while rifampicin, ethambutol, and streptomycin inhibit transcription, arabinogalactan synthesis and protein synthesis, respectively. The mechanism of action of pyrazinamide is unknown but it is believed to inhibit membrane energetics and it requires pncA for activation (Sacchettini *et al.*, 2008).

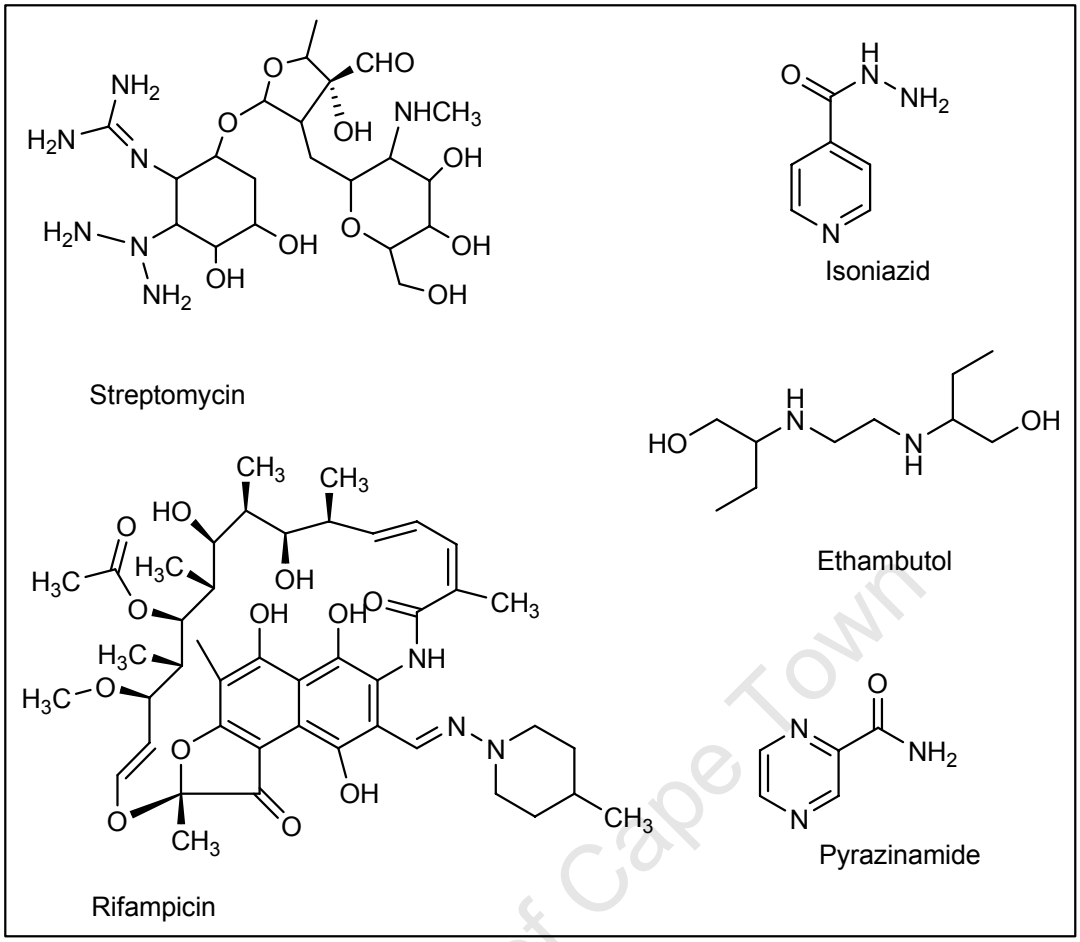

Figure 1.2: The commonly used first line anti-tubercular drugs

1.1.8.3 Multi Drug Resistant Tuberculosis

TB drug resistance is a global public health problem that hampers the progress of treatment strategies such as DOTS. Multi-drug resistant tuberculosis (MDR-TB) develops when *M. tuberculosis* becomes resistant to the first-line drugs, isoniazid and rifampicin. Resistance to any other combination of first line anti-tubercular drugs except these two is not classified as MDR-TB (WHO, 2008). In the Western Cape region of South Africa, DRF155, the *M. tuberculosis* strain that is resistant to rifampicin, isoniazid and streptomycin was identified. Factors leading to the development and spread of this resistant strain include inappropriate chemotherapy and poor adherence to treatment (Victor *et al*., 2007).

Resistance against anti-tubercular drugs is thought to be conferred by spontaneous chromosomal mutations which occur at a predictable rate in *M. tuberculosis*. Because

these mutations are unlinked, resistance against a particular drug is usually not associated to resistance against an unrelated drug. Thus, the fact that the primary mechanism of TB drug resistance is due to perturbations in the specific target genes, forms the basis for resistant TB chemotherapy (Ramaswamy and Musser, 1998; Sharma and Mohan, 2004). The molecular mechanisms for drug resistance are summarized in table 1.3 (Sharma and Mohan, 2004).

Table 1.3: Anti-tubercular drugs and the genes involved in their resistance

Drug	**Genes involved in drug resistance**
Isoniazid	Enoyl acp reductase (*inhA*) Catalase-peroxidase (*katG*) Alkyl hydroperoxide reductase (*ahpC*)
Ethambutol	Arabinosyl transferase (*emb A*, *B* and *C*)
Pyrazinamide	Pyrazinamidase (*pncA*)
Rifampicin	RNA polymerase subunit B (*rpoB*)
Streptomycin	Ribosomal protein subunit 12 (*rpsL*) 16s ribosomal RNA (*rrs*) Aminoglycoside phosphotransferase gene (*strA*)

Unlike with non-resistant strains which can be eliminated within 6 months using first-line drugs, MDR-TB requires prolonged and expensive treatment with second-line drugs (Sacchettini *et al*., 2008). The commonly used second-line anti-tubercular drugs

are shown in figure 1.3. More drugs and new treatment strategies are therefore needed to aid the control of MDR-TB.

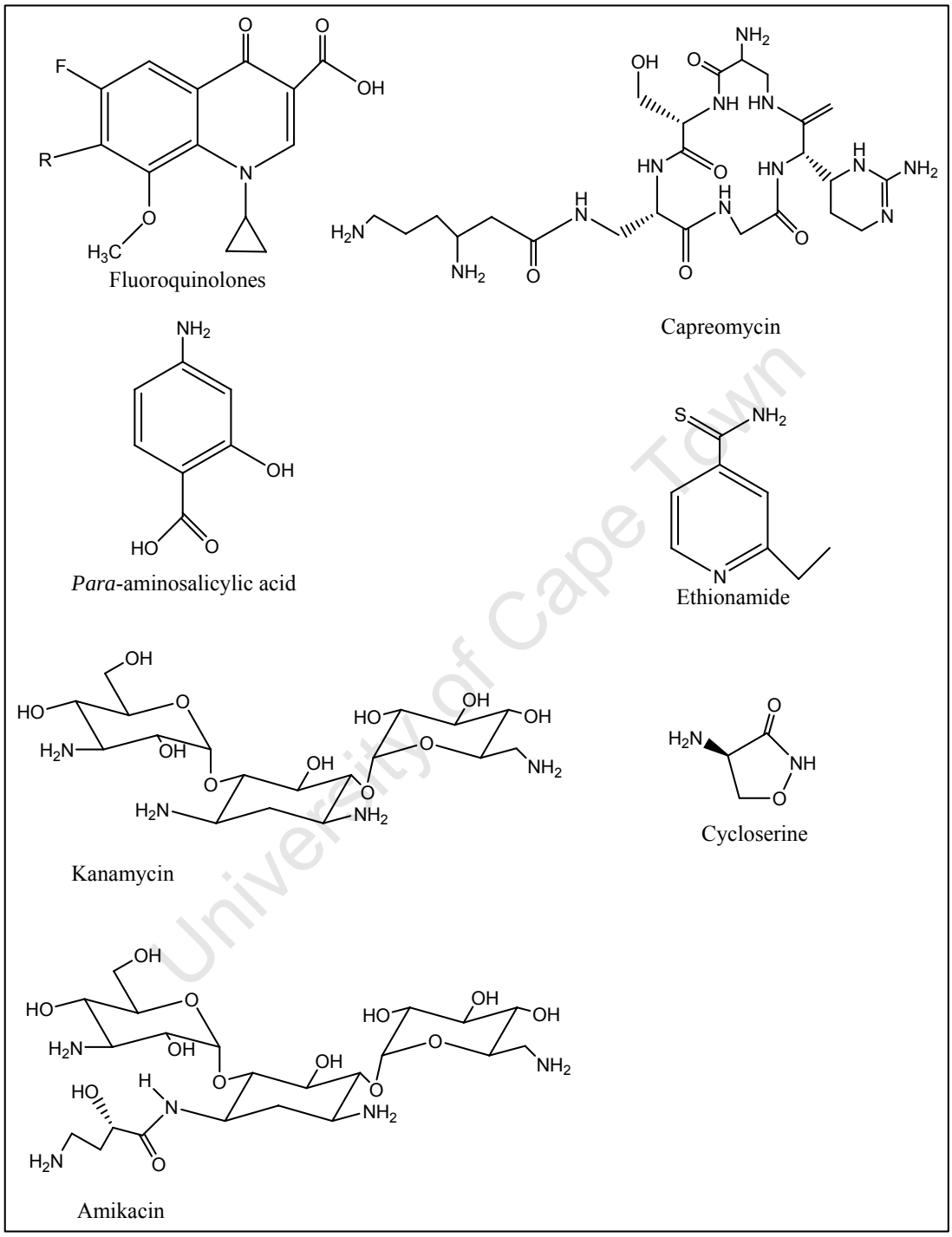

Figure 1.3: Second-line anti-tubercular drugs.

1.1.8.4 Extensively Drug Resistant Tuberculosis

Extensively drug resistant tuberculosis (XDR-TB) develops when *M. tuberculosis* MDR strains develop additional resistance to a fluoroquinolone and to at least one of the following second line drugs; kanamycin, capreomycin and amikacin (WHO, 2006). Because XDR-TB strains are resistant to most of the first and second line drugs, it remains extremely difficult to treat. It is understood that the high incidence of MDR-TB has arisen from factors such as poor patient compliance as well as the HIV co-infection. To prevent XDR-TB, it is crucial that the second line drugs are administered under controlled conditions so that they retain their potency (MRC-SA, 2006; WHO, 2006).

In the first detailed global XDR-TB survey, 18 000 individual isolates were tested. About 20% of the cases were MDR-TB, and 7% of these resistant strains were XDR-TB. Of MDR-TB isolated in South Korea and East Europe/West Asian, 15% were XDR strains while only one XDR-TB case was found amongst 156 MDR isolates from Africa/middle east (Centers for Disease Control and Prevention, 2006). Currently, the geographical spread of XDR-TB is still uneven. Although Sub-Saharan Africa has one of the highest TB incidences, XDR prevalence among the MDR isolates in this region is relatively low (Jones *et al*., 2008).

The first XDR-TB cases in South Africa were reported in 2006 (Gandhi *et al*., 2006) in the study carried out in Kwazulu Natal province. Of 1539 patients tested, 221 were diagnosed of MDR-TB, of which the 53 had XDR-TB. 52 patients with XDR-TB died within the median survival of 16 days after the disease was diagnosed (Gandhi *et al*., 2006). 44 of the 53 were tested for HIV and found to be HIV-positive (MRC, 2006). These observations indicate that XDR-TB is associated with high mortality and threatens the success of treatment programmes against TB and HIV (Gandhi *et al*., 2006). An urgent intervention in the form of controlled treatment programmes and the discovery of new drugs is needed.

1.1.9 New strategies for Drug Development

During infections like TB, a molecular understanding of host-pathogen interactions requires clear characterization of the mycobacterial defence against oxidative and nitrosative stress (Nathan and Shiloh, 2000). A large fraction of genes required for mycobacterial growth is specific to *M. tuberculsosis* and its closely-related species indicating that the bacillus uses survival strategies which are fundamentally different from other pathogens (Sassetti and Rubin, 2003). Understanding how *M. tuberculosis* evades harmful attacks in the hostile environments of the activated macrophages and how it detoxifies drugs could be essential in tackling the emergence of MDR- and XDR-TB.

Infected and lysed alveolar macrophages release reactive oxygen intermediates (ROI)[9], reactive nitrogen intermediates (RNI)[10] and other toxins which help to inhibit the replication of *M. tuberculosis* (Nathan and Shiloh, 2000; Clark-Curtiss and Haydel, 2003). In response *M. tuberculosis* employs various defence mechanisms to detoxify the stress caused by these harmful compounds.

AhpC is a mycobacterial protective gene that encodes alkyl hydroperoxide reductase (ahpC), a member of the peroxyredoxin family. An adaptor protein, ahpD, links ahpC to dihydrolipoamide dehydrogenase (lpd) and dihydrolipoamide succinyltransferase (SucB) which support mycobacterial antioxidant defence hydrogen and alkyl peroxides (Bryk *et al.,* 2002). AhpC, ahpD, lpd and SucB together constitute an NADH-dependent peroxidase and peroxinitrite reductase. Because of its antioxidation role ahpC could be a drug target (Bryk *et al.,* 2002).

Another important gene in the virulence of *M. tuberculosis* is *katG* which catabolizes the superoxides generated by phagocyte NADPH oxidase. However in the absence of the phagocyte oxidative burst, the role of *katG* is dispensable for the *M. tuberculosis*

[9] Reactive oxygen intermediates (ROI) are intermediate reduction products of O_2, namely, superoxide, hydrogen peroxide and hydroxyl radical (Nathan and Shiloh, 2000).

[10] Reactive nitrogen intermediates (RNI) refer to adducts of the nitrogenous products of nitric oxide synthases. These intermediates include nitric oxide (-NO), N_2O_3, N_2O_4, s-nitrosothiols, peroxynitrites and dinitrosyl-ino complexes (Nathan and Shiloh, 2000).

virulence. Also inactivating mutations in *KatG* confers resistance to isoniazid, because this enzyme has been implicated in activation of the drug. Similarly MSH-deficient *M. smegmatis* is less sensitive to Inh and is somehow also involved in its activation (Ng *et al*., 2004).

1.1.10 Low molecular weight thiols: an avenue for chemotherapeutic intervention

While defence mechanisms like those by *katG* and *ahpC* serve as an effective response to specific dangers in the host cells, there is also a need for an effective, immediate, and universal response to the wide spectrum of threats a bacillus may encounter during its life cycle (Ung and Av-Gay, 2006). Low molecular weight thiols may serve such a role, since they are involved in cellular redox potentials and protein-disulfide ratios, as well as for the protection of cells against reactive oxygen species (Hand and Honek, 2005). Therefore, the inhibition of key enzymes in the metabolism of low molecular weight thiols represents a new area for drug development

Mycobacteria contain two major low molecular weight thiols, namely, ergothioneine (ESH) and Mycothiol (MSH). Most important, MSH was shown to be essential in *M.tb* grown in culture, but no enzyme involved in ESH biosynthesis has ever been isolated and so its role is unknown (Williams M.J, 2007).

1.2. MYCOTHIOL

1.2.1 Mycothiol is the major low molecular weight thiol in Mycobacteria

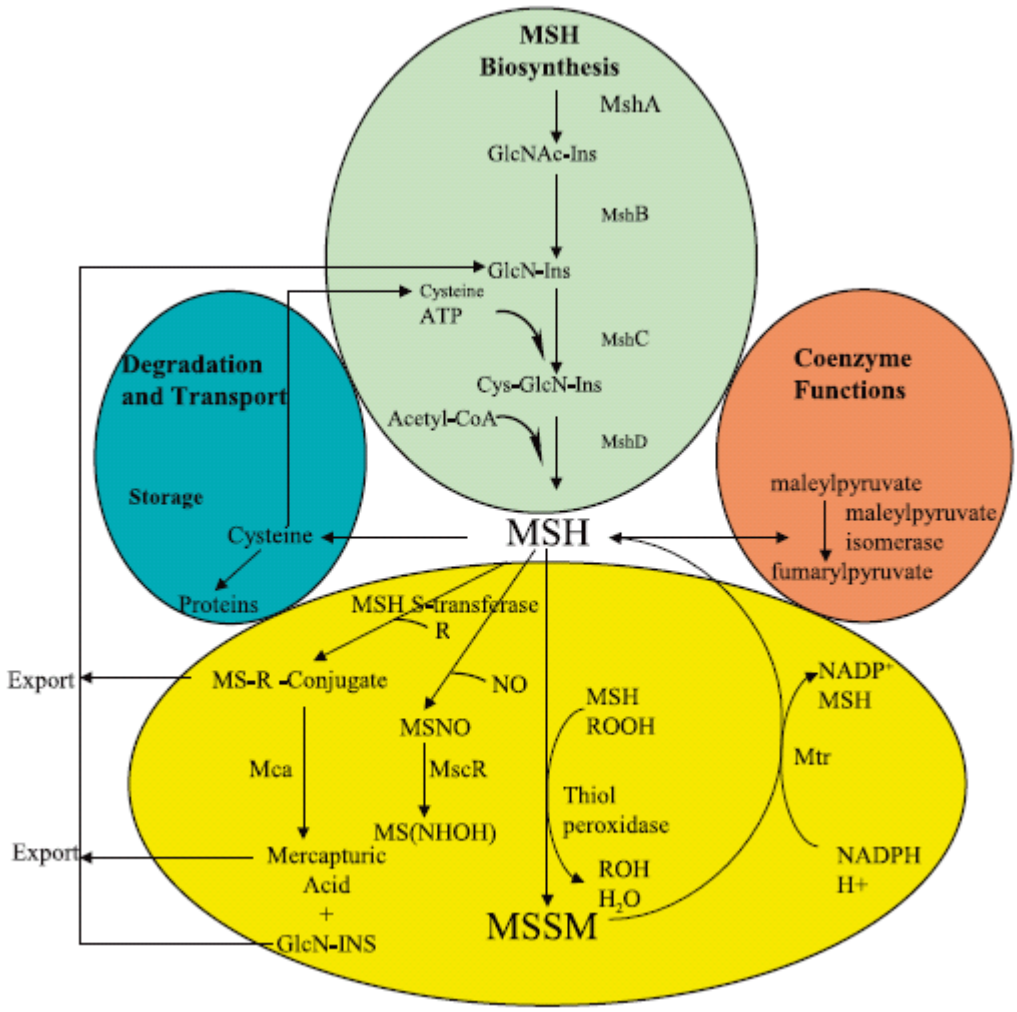

Figure 1.4: Overview of mycothiol metabolism. Green: biosynthesis of mycothiol catalyzed by mshA, mshB, mshC and mshD. Blue: degradation reactions to scavenge mycothiol for cysteine in times of nutrient starvation. Yellow, protective reactions catalyzed by: mycothiol amidase (mca) and nitrosothiol reductase (mscR) and thiol peroxidases or peroxiredoxins involved in oxidative and nitrosative stress protection and mycothiol reductase (mtr), which maintains mycothiol in a reduced form within the mycobacterial cell. Red, metabolic reactions catalyzed by enzymes such as maleylpyruvate isomerase requiring mycothiol as a cofactor for growth on diverse carbon sources. Permission to reproduce this figure was granted by the corresponding author of the published article (Rawat and Av-Gay, 2007).

1-D-*myo*-inosityl-2-(N-acetyl-L-cysteinyl)amino-2-deoxy-α-D-glycopyranoside was identified in its disulfide form in *Streptomyces* sp AJ 9463 by Zhou and co-workers (Sakuda *et al.,* 1994), and in an independent study at about the same time, Spies and Steenkamp discovered it as a free thiol in *Mycobacterium bovis* and assigned it the name mycothiol (Spies and Steenkamp, 1994). From the structure analysis of this thiol, it came out that MSH was the compound which was identified as U17 by Newton *et al*. (Newton *et al*., 1993; 1995). MSH is a major low molecular weight thiol produced in virtually all actinomycetales, a group which includes streptomyces and mycobacterium (Newton *et al*., 1996). Since actinomycetales do not produce glutathione (GSH) and trypanothione (TSH_2), it seems that MSH is responsible for the protective roles performed by these thiols in their respective organisms.

Pathogens which produce MSH seem to use this thiol as a protectant against electrophilic attack and alkylating agents as well as for the detoxification against ROI and RNI (Hand and Honek, 2005). *M. tuberculosis* utilizes MSH to detoxify toxins in a manner similar to mercapturic acid derivatives formation in the GSH detoxification pathway (Newton *et al*., 2000b). MSH in conjunction with mycothiol disulfide reductase controls cellular homeostasis by maintaining the reducing intracellular environments in *M. tuberculosis* (Patel and Blanchard, 1999).

1.2.2 Structure of MSH

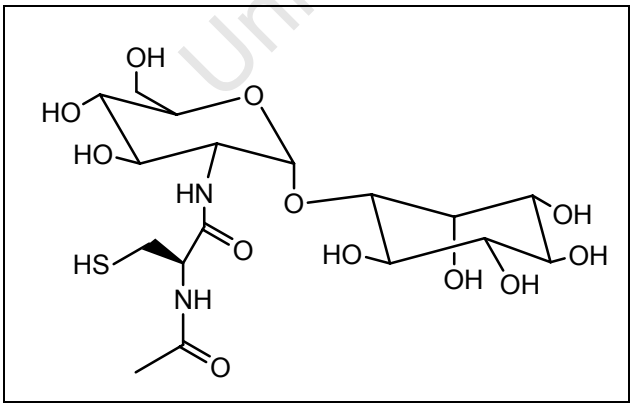

Figure 1.5: Structure of MSH

MSH is a glycothiol made up of *myo*-inositol, D-glucosamine and N-acetyl-cysteine. The most reactive group with which MSH forms *S*-conjugates is the sulfhydryl of the cysteine moiety.

1.2.3 Overview of MSH Biosynthesis

Acetyl-GlcN-Ins is the ultimate product of a sequence of reactions involved in the first step of the MSH biosynthetic pathway catalyzed by mshA and mshA2 (Newton *et al*., 2006), its deacetylation to form GlcN-Ins is catalyzed by Acetyl-GlcN-Ins deacetylase (mshB) (Maynes *et. al*., 2003), which was identified in *M. tuberculosis* as a homolog of MSH *S*-conjugate amidase (mca) (Newton *et. al*., 2000a,b). The ligation of cysteine to the amino group of GlcN-Ins is catalyzed by GlcN-Ins:Cys ligase (mshC) in an ATP-dependent reaction that produces AMP, pyrophosphate and Cys-GlcN-Ins (Sareen *et al*., 2002). The final step in the MSH biosynthesis involves the acetylation of Cys-GlcN-Ins by acetyl-CoA and is catalyzed by MSH synthase (mshD) (Koledin *et. al*., 2002).

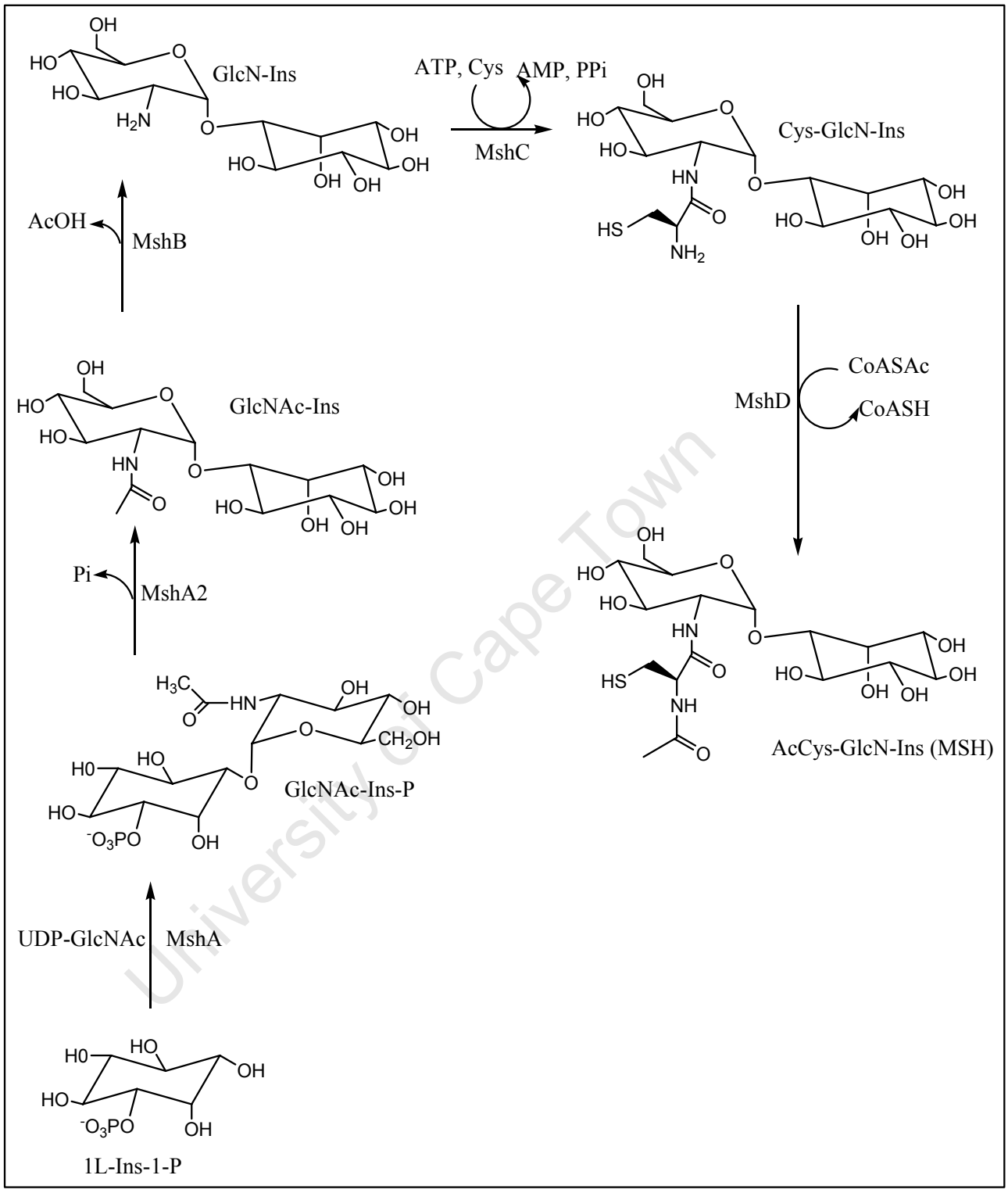

Figure 1.6: MSH biosynthetic pathway

1.2.3.1 MshA

1.2.3.1.1 MshA catalyzes the initial steps in mycothiol biosynthesis

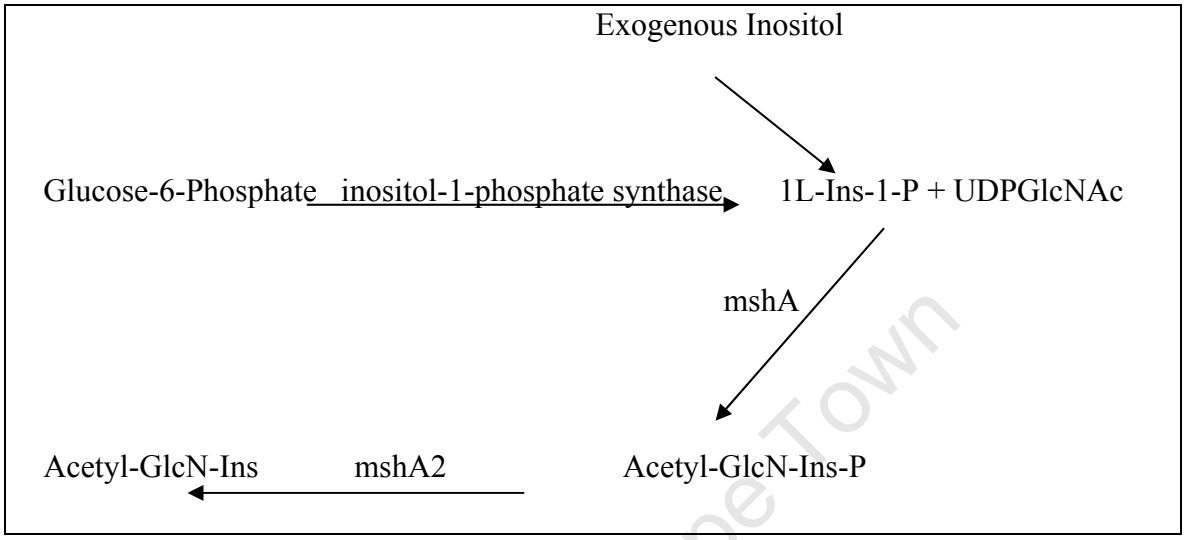

Figure 1.7: The initial steps of MSH biosynthesis

Based on amino acid sequence similarities, *mshA*, a gene encoding UDP-*N*-acetylglucosamine:1L-*myo*-inositol-1- phosphate 1-α-D-*N*-acetylglucosaminyl-transferase (mshA), was identified as a member of the glycosytransferases family 4 which includes enzymes such as sucrose synthase, sucrose phosphate synthase, mannosyl transferase and GlcNAc transferase. These enzymes catalyze the transfer of a sugar moiety from an activated donor to a specific acceptor, resulting in the formation of a glycosidic bond (Campbell *et al*., 1997).

The mshA-catalysed step was characterized in a work that completed a full elucidation of the MSH biosynthetic pathway. This step proceeds through two reactions leading to the formation of a pseudodisaccharide Acetyl-GlcN-Ins, an intermediate precursor of mycothiol (Newton *et al*., 2000a). In the first part of the reaction, UDP-GlcNAc donates a sugar moiety to 1L-Ins-1-P resulting in the formation of Acetyl-GlcN-Ins-P. 1L-Ins-1-P serves as the best optimal acceptor in this reaction compared to other inositol-containing compounds such as 1D-Ins-1-P and Ins-2-P which were inefficient substrates when used as acceptors. In the second part

of the reaction, Acetyl-GlcN-Ins is produced by dephosphorylation of Acetyl-GlcN-Ins-P by a phosphatase called MshA2 (Newton *et al*., 2006).

Bacchawat and Mande reported that L-myo-inositol-1-phosphate is produced from glucose-6-phosphate in a reaction catalyzed by inositol-1-phosphate synthase, encoded by *INO1*. This is also the case in other organisms. Inositol-1-phosphate is then dephosphorylated by inositol-1-phosphatase and the resultant free inositol is subsequently used by the host to produce inositol-derived metabolites (Bacchawat and Mande, 1999). Thus 1L-Ins-1-P is an acceptor in mshA catalyzed reaction and also a precursor in the biosynthesis of inositol. Alternatively, 1L-Ins-1-P can be derived from exogenous inositol (Reviewed in Newton *et al*., 2006).

1.2.3.1.2 MshA as a drug target

Both streptomycetes and mycobacteria belong to Actinomycetes, a group which produces mycothiol as a low molecular weight thiol (Spies and Steenkamp, 1994; Sakuda *et al*., 1994). Park *et al.* (2006) identified the homologues of *mshA, B, C* and *D* in the genome of *Streptomyces coelicolor* which were found to serve the same role as their counterparts in Mycobacteria. The disruption of *mshA* by PCR gene targeting mutagenesis resulted in no production of MSH. In addition, when the mutant was complemented with the *mshA* gene, MSH synthesis was fully restored to the same levels as in the parent strain indicating that MSH production was indeed shut down by gene disruption of *mshA*. This indicates that mshA is essential for MSH biosynthesis in *S.coelicolor* (Park *et al*., 2006). Newton *et al* showed that *mshA* is also essential for production of mycothiol in *Mycobacterium smegmatis,* but not for growth of the organism (Newton *et al*., 2003). Recently, disruption of *mshA* in *Mycobacterium tuberculosis* Erdman showed that this gene is also essential for the growth of this pathogen (Buchmeier and Fahey, 2006), a similar effect as in the targeted mutagenesis of *mshC* in the same strain (Sareen *et al*., 2003). MshA is therefore a target for development of compounds that could block MSH biosynthesis.

1.2.3.2 Acetyl-GlcN-Ins Deacetylase

The formation of GlcN-Ins from the deacetylation of Acetyl-GlcN-Ins is catalyzed by mshB. Although mshB is not essential for the growth of mycobacterium, it is the key enzyme in the biosynthesis. The *mshB*$^-$ mutants of Mtb produces about 15% of wildtype MSH suggesting that the loss of deacetylase activity might be compensated for by another gene, most probably mca due to its homology with mshB (Newton *et al*., 2000a; Maynes, 2003). Because this study is aimed at inhibiting both mshB and mca, they will both be discussed in details at the end of this chapter.

1.2.3.3 GlcN-Ins:Cysteine ligase

The activity of GlcN-Ins:Cysteine ligase from mycobacterial crude extracts was first identified by Bornemann and coworkers in the work that elucidated the final steps of MSH biosynthesis. They reported the synthesis of GlcN-Ins and showed that it is enzymatically linked to L-cysteine in ATP- dependent ligation to form Cys-GlcN-Ins. The acetylation of Cys-GlcN-Ins with acetyl-CoA produces MSH (Bornemann *et al.*, 1997). GlcN-Ins:Cysteine ligase has been purified to homogeneity from *Mycobacterium smegmatis* from which apparent *K*m values for Cys and GlcN-Ins were determined to be 40±3 and 72±9 μM, respectively. The gene, *mshC,* was also identified from the N-terminal sequence in *Mycobacterium tuberculosis* (Sareen *et al.*, 2002). MshC is related to cysteinyl-tRNA synthetases due to its mode of activating cysteine through the formation of a cysteine-AMP derivative which subsequently undergoes an attack by the amino group of GlcN-Ins (Meinnel *et al.*, 1995).

The absence of MSH and its metabolic enzymes in eukaryotes suggests that their inhibition is a possible avenue for drug development. The evidence of MSH involvement in the protection of mycobacteria was demonstrated in MSH-dependent detoxification mechanism facilitated by MSH *S*-conjugate amidase in which the toxin moiety is eventually excreted out of the cell as a mercapturic acid (Newton *et al.*, 2000b).

Rawat *et al*. (2002) found that the depletion of MSH in *M. smegmatis* increases its susceptibility to toxins and antibiotics. MSH-deficient mutants of *Mycobacterium smegmatis* created by both chemical and transposon mutagenesis are sensitive to alkylating agents such as Diamide, iodoacetamide and mBBr. They are also sensitive to oxidative stress and a range of antibiotics indicating that MSH is important in protection of the *M. smegmatis* against stress caused by those compounds. A chemical mutant I64 and two transposon mutants, Tn1 and Tn2 were shown to be 3 to 16-fold more sensitive to penicillin G, erythromycin, vancomycin, and azithromycin than the wild-type strain. Both transposon mutants, Tn1 and Tn2 were reported to be more susceptible than chemical mutant I64 to anti-tubercular drugs, rifamycin and rifampin. However I64 and both transposon mutants are respectively 16-fold and 125-fold more resistant to isoniazid than the wild type strain. These mutants also lack cys:GlcN-Ins ligase activity. The absence of ligase activity in the chemical mutant is due to the point mutation in *mshC*. The complementation of this mutant with *mshC* restored the MSH production in the mutant and revert its antibiotic susceptibility (Rawat *et al.*, 2002). This indicates that lack of MSH production was due to the mutated mshC gene.

In the other work which confirmed the importance of mshC in the growth of mycobacteria, Sareen *et al* found that no viable clones possessing MSH were produced after the targeted disruption of a native *mshC* in *M. tuberculosis* Erdman. However, when *mshC* gene was incorporated into the chromosome, the clones produced normal levels of MSH demonstrating that *mshC* gene and the production of MSH are essential for the growth of this strain (Sareen *et al*., 2003).

1.2.3.4 Acetyltransferase (mshD) catalyzes the reaction that produces MSH

Mycothiol synthase (mshD) belongs to the N-acetyltransferase superfamily, a group of enzymes which use acyl-CoA to acylate their substrates (Vetting *et al*., 2005). The presence of mycothiol synthase activity was first demonstrated in *M. smegmatis* (Bornemann *et al*., 1997), later identified in as ORF Rv0819 and cloned in *E. coli* (Koledin *et al*., 2002). Rv0819 has orthologs in the genomes of other actinomycetes, a group to which MSH production is confined (Newton *et al*., 1996). Orthologs with sequence identities of 62%, 75%, 46% and 34% to the M.tuberculosis enzyme are

present in *M. smegmatis*, *M. leprae*, *Streptomyces coelicor* A 3(2) and *Corinebacterium diphtheriae* respectively.

MshD catalyzes the final step in the production of MSH, where Cys-GlcN-Ins is acetylated with acetyl-CoA. The *MshD*::Tn5 mutant of *M. smegmatis*, accumulates high levels of Cys-GlcN-Ins and accumulates all of the intermediates in the biosynthetic route to MSH but produces only ~1% MSH indicating that mshD is important in the biosynthesis of MSH (Koledin *et al.*, 2002). Cys-GlcN-Ins exists as a disulfide form at different growth stages of *MshD*::Tn5 suggesting that the cells are susceptible to autooxidation due to the extremely low levels of MSH. The *MshD*::Tn5 mutant produces two novel thiols related to MSH, namely, *N*-Succinyl-Cys-GlcN-Ins and *N*-formyl-Cys-GlcN-Ins. The latter substitutes MSH in helping mutant cells to resist the peroxides stress (Newton *et al*., 2005). Although *N*-formyl-Cys-GlcN-Ins serves as a weak surrogate of MSH, in mshD-deficient mutant of *M. tuberculosis*, it is not sufficient to support the normal growth of the cells under stress conditions similar to those in macrophages (Buchmeier *et al*., 2006).

1.2.4 Mycothiol-Dependent Enzymes

1.2.4.1 Redox status of MSH

Oxidation is harmful to vital cellular components such as the nucleic acids, lipids and proteins (Chae *et al*, 1994). Thiols tend to be oxidized to disulfides when exposed to extracellular environments. MSH also undergoes oxidation to form mycothiol disulfide (MSSM). NADPH dependent mycothioldisulfide reductase (mtr) maintains MSH in a reduced state and thus contributes to the intracellular redox homeostasis of the mycobacterial cell. Mtr from *M. tuberculosis* was cloned and expressed in *M. smegmatis* using a shuttle vector with hsp60 promoter. This 50 kDa subunit enzyme is NADPH-dependent and it utilizes MSSM as a substrate. The *K*m values of MSSM and NADPH were reported to be 73 and 8 μM respectively. Mtr requires FAD as a cofactor (Patel and Blanchard, 1999).

AcCys-GlcN is also a substrate for mtr, although with a five-fold larger *K*m value than MSSM (Patel and Blanchard, 1998). This indicates that although mtr is selective

for MSSM, the removal of the inositol residue from MSH does not eliminate the reductase activity. Alpha-configured methyl- and benzyl-glycosides have also been described as alternate substrates of mtr (Stewart *et al*., 2008). *M.tuberculosis* mtr is a flavoenzyme and is a member of pyridine nucleotide-disulfide reductase superfamily, which contains proteins such as glutathione reductase, thioredoxin reductase and trypanothione reductase (Patel and Blanchard, 2001). Inspite of its broad similarity to GSH and TSH_2 reductases, mtr does not display activity against disulfides of GSH and TSH_2 indicating its specific importance to the stability of MSH in mycobacteria (Patel and Blanchard, 1999).

Because of its protective role against oxidation in mycobacteria, mtr is an attractive drugable target. The properties of 7-methyljuglone derivatives as potential subversive substrates have been reported (Mahapatra *et al*., 2007), providing the basis that more specific naphthoquinones could serve as good subversive substrates for mtr.

1.2.4.2 Maleylpyruvate isomerase

Gentisate (2,5-dihydroxybenzoate) and substituted gentisates serve as key intermediates in the aerobic pathways for the metabolism of compounds such as salicylate (Ohmoto *et al*., 1991), dichloromethoxybenzoate (Werwath *et al*., 1998), and naphthalene (Grund *et al*., 1992). In Gentisate pathway *p*-dihydroxylated aromatic ring is cleaved by gentisate 1,2-dioxygenase to form maleylpyruvate. Maleylpyruvate isomerase catalyzes the conversion of maleylpyruvate to fumarylpyruvate. This enzyme requires GSH as a cofactor in GSH-containing organisms such as *Klebsiella pneumoniae* and *Ralstonia* strains (Zhou *et al*., 2001).
However, the identification of a gene (*ncgl2918*) with maleylpyruvate isomerase activity in *C. glutamicum* indicated that a different cofactor is employed since GSH is absent in this bacterium (Shen *et al*., 2005).

In subsequent studies, Feng *et al* established a link between MSH biosynthesis and GSH-independent gentisate pathway in *C. glutamicum.* It was reported that MSH is a cofactor of maleylpyruvate isomerase and also essential for growth of *C. glutamicum* when gentisate is used as a carbon source (Feng *et al*., 2006). *Ncgl2918* was cloned, expressed and purified in *E.coli*, and it is a monomer of 34 kDa with Km(app) of 148

μM when maleylpyruvate is used as a substrate and MSH as a cofactor (Feng *et al*., 2006). MSH-dependent maleylpyruvate isomerase (MDMPI) is a metalloprotease with a divalent metal-binding domain and its C-terminal domain possesses a folding pattern, αβαββα (Wang *et al*., 2007).

1.2.4.3 NAD/MSH-dependent Formaldehyde dehydrogenase

Detoxification of formaldehyde in various organisms is catalyzed by reductases differing in coenzyme/cofactor used. In larger eukaryotes and gram-negative bacteria, toxic formaldehyde is detoxified by NAD/GSH-dependent formaldehyde dehydrogenase. NAD/MSH-dependent formaldehyde dehydrogenase, the first enzyme of MSH metabolism to be identified, serves the same detoxification role in actinomycetes (Misset-Smits *et al*., 1997). MSH-dependent detoxification of reactive nitrogen species such as nitric oxide radical leads to intermediate formation of nitrosomycothiol (Vogt *et al*., 2003). NAD/MSH-dependent formaldehyde dehydrogenase catalyzes the oxidation of the thiohemiacetal group of MSH with formaldehyde which is present in aqueous solutions as a H_20 adduct (Norin *et al*, 1997; Misset-Smits *et al.*, 1997).

A class III alcohol dehydrogenase gene of Mtb, *Rv2259*, was cloned and expressed in *M. smegmatis* as the C-terminally His-tagged product (Vogt *et al*., 2003). This enzyme catalyzed two activities, the NAD-dependent conversion of *S*-hydroxymethylmycothiol into formic acid and MSH, as well as the NADH-dependent decomposition of *S*-nitrosomycothiol (MSNO). Hence, the enzyme is also denoted *S*-nitrosomycothiol reductase. The protective role of MscR in macrophages has not been fully established yet.

1.2.4.4 Mycothiol *S*-Conjugate Amidase

1.2.4.4.1 MSH-dependent detoxification pathway

In mammals the complete detoxification pathway is more complicated since more than one enzyme is involved. The conversion of alkylating agents to glutathione *S*-

conjugates is catalyzed by glutathione *S*-transferases and it occurs in various tissues (Ketterer *et. al*., 1988, Mannervik *et al*., 1988). Glutathione *S*-conjugates are exported to the plasma and transported into the liver and kidney where they are degraded by γ-glutamyltranspepetidase to form CySR-Gly which is cleaved by dipeptidase to produce CysR (Stevens and Jones, 1989). CysR is a Cysteine *S*-conjugate which is imported and acetylated by Acetyl CoA to produce AcCysSR, a mercapturic acid which is excreted in urine and bile.

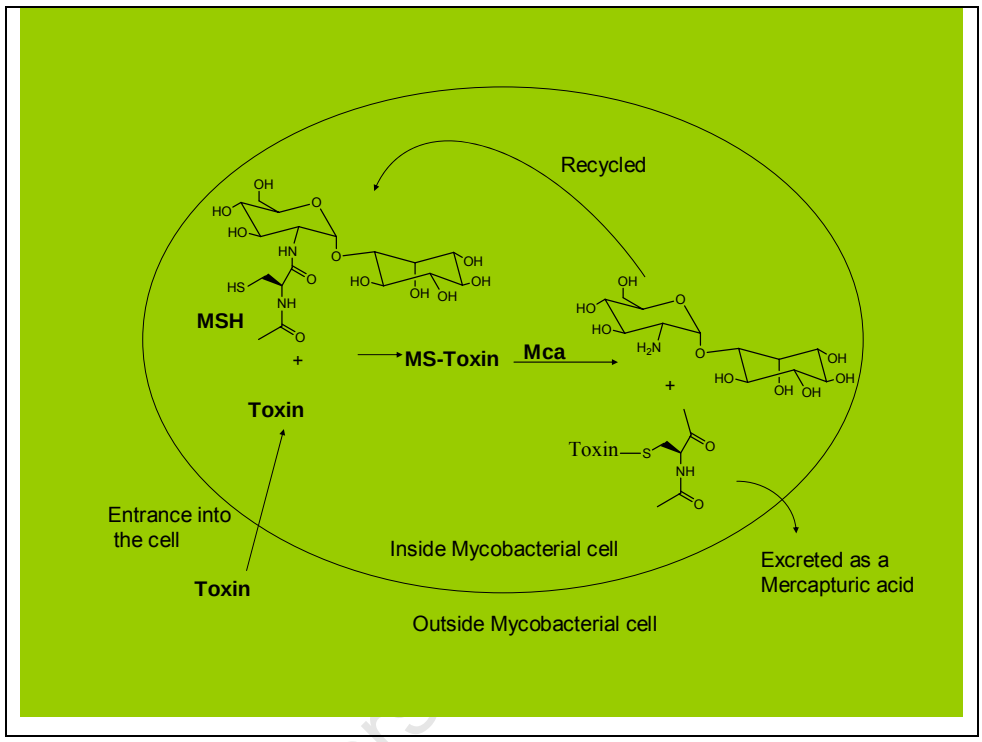

Figure 1.8: The detoxification pathway in Mycobacteria
(Modified from Newton *et al*., 2000b)

In mycobacteria, a single enzymatic activity is responsible for a detoxification pathway that leads to the excretion of AcCysSR. MSH reacts with a toxin to form a mycothiol *S*-conjugate which is cleaved by mycothiol *S*-conjugate amidase (mca) to form GlcN-Ins and a mercapturic acid. The latter is excreted from the cell while GlcN-Ins is used to resynthesize MSH (Newton *et al.*, 2000b). Mca was first isolated from *M. smegmatis* and its N-terminal sequence analysis revealed an orthologous gene in *M. tuberculosis* annotated as Rv1082. The *M. smegmatis* enzyme had a *K*m value of 95 μM and k_{cat} of 8 s^{-1} when the *S*-conjugate of a fluorescent alkylating agent, monobromobimane (MSmB), was used as a substrate (Newton *et al.*, 2000b).

Mca recognizes specifically the MSH moiety of conjugates and can accommodate different groups attached to the sulphur moiety in the MSH-toxin conjugate. However, mca does not have a significant activity with conjugates that lack the acetyl moiety present in mycothiol *S*-conjugates. MSH itself is a poor substrate of mca (Newton *et al*., 2006). Thus the thiol serves as a more autooxidation resistant reservoir of cysteine. The *M. tuberculosis* amidase, which was cloned and expressed in *E. coli* has a similar substrate specificity to the *M. smegmatis* amidase. It also utilizes MSmB as a substrate, albeit with a *K*m value of 160 μM and k_{cat} of 14 s^{-1}. Other substrates of mca include *S*-conjugates of iodoacetamide, N-ethylmalemide, and 7-diethylamino-3-(4'-maleimidylphenyl)-4-methylcoumarin (CPM) (Steffek *et al.*, 2003).

1.2.4.4.2 Bioinformatic analysis of mca

Mycobacterium tuberculosis mca is an 864-bp gene that codes for a metalloenzyme of 288 amino acids. Its product has a molecular mass of 32.7 kDa and an isoelectric point of 5.1. *Mycobacterium smegmatis mca* also codes for an 864-bp protein that contains 288 amino acids. The amino acid sequence of *M. tuberculosis* mca is 72% identical to that of the *M. smegmatis* enzyme (Newton *et al.*, 2000b; Steffek *et al*, 2003). This gene is present in all mycobacterial species sequenced so far. Comparable identity was also found in the orthologues of *mca* in *M. bovis* and *M. leprae*. In other actinomycetes, the amino acids identities between mca orthologues range from 51% for *S. avermitilis* to 72% for *N. farcinica*. There are at least four major domains that are highly conserved throughout the amidase family and histidine residues are conserved in three of these domains (Rawat and Av-Gay, 2007).

The *M. tuberculosis* genome contains two paralogues, Rv0323c and *mshB*. Rv0323c codes for a 24.2 kDa protein which is non-essential and is only present in pathogenic *M. tuberculosis* and not in *M. smegmatis* (Sassetti *et al.*, 2003). The second paralogue, *mshB,* codes for a deacetylase which catalyzes the second step in the biosynthesis of MSH (Newton *et al*., 2000a). The amino acid sequences of MshB and mca have a 36% identity in 299 amino acids and both enzymes are Zn-dependent metalloproteases. MshB possesses a weak amidase activity *in vitro* and, conversely, mca also displays the deacetylase activity when Acetyl-GlcN-Ins is used as a substrate (Newton *et al*., 2000a; Newton *et al*., 2006).

1.2.4.4.3 Mca is involved in the detoxification of antibiotics

The presence of *mca* homologs within the antibiotic biosynthetic operons for streptomycin, rifamycin and erythromycin indicates that the expression of these *mca* genes occurs at the same time as the antibiotic production. In order to understand whether mca plays a role in the detoxification of antibiotics, the presence of mercapturic acid derivatives of antibiotics in the fermentation broth of such mycobacteria should be investigated. Reports exist in which experiments were performed and numerous mercapturic acids of drugs were found in the broth (Supplementary material that came with a review by Newton and Fahey, 2002). These mercapturic acids are weaker in activity than the parent antibiotic. These findings gave a further evidence of mca involvement in the protection of the bacterial cell against its own antibiotics or those produced by its competitor. It was also reported that the *S*-conjugate of cerulenin, an antibiotic from actinomycete *Cephalosporin cerulens* which inhibits fatty acid synthetase, was a good substrate of mca (Newton and Fahey, 2002).

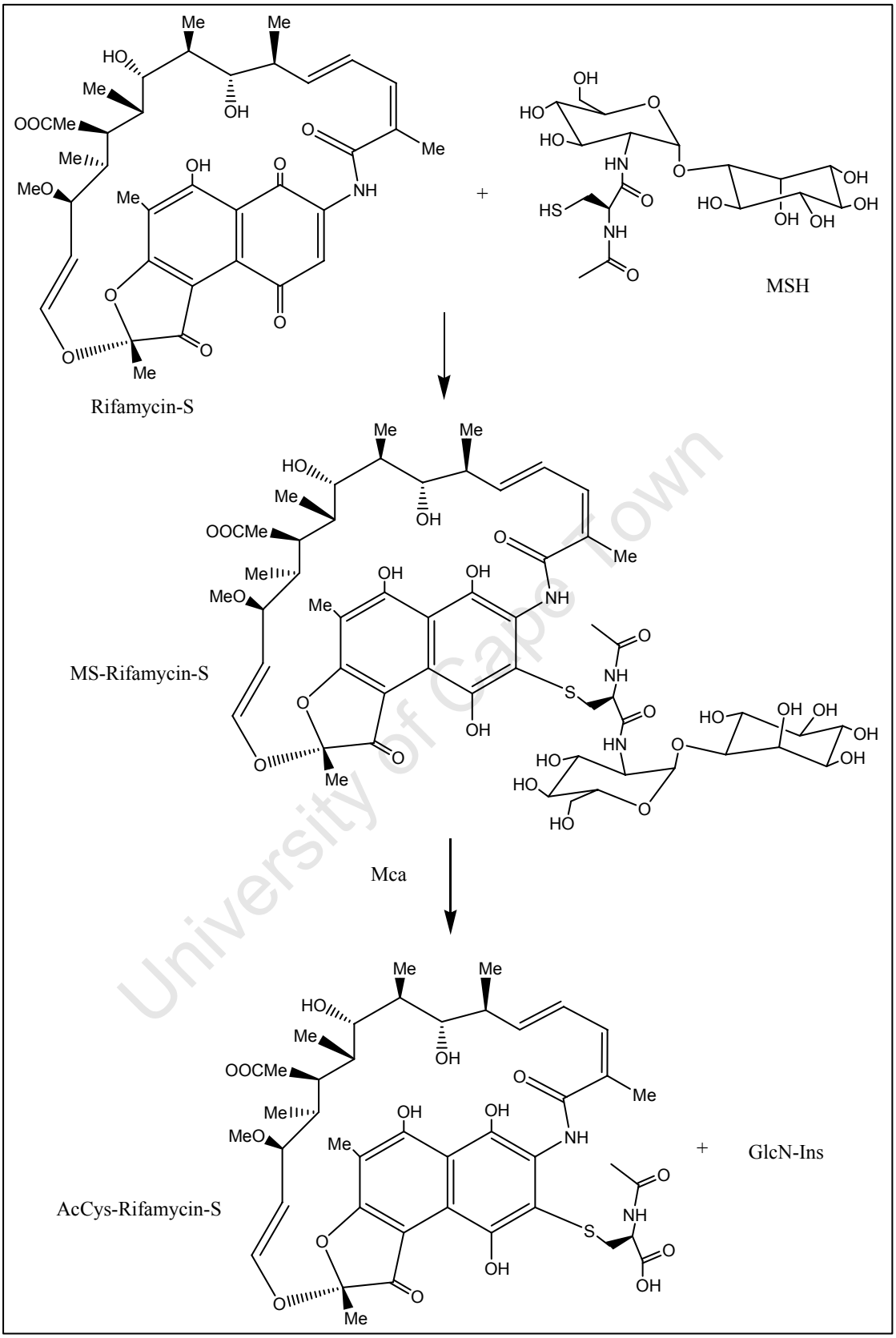

Figure 1.9: The formation of MS-conjugate of Rifamycin-S and its cleavage with Mca to release AcCys-Rifamycin-S and GlcN-Ins.

MSH-deficient mutants are more sensitive to alkylating agents and antibiotics like erythromycin, vancomycin, penicillin G, azithromycin and rifamycin (Rawat *et al.*, 2002). Rifamycin-S, a precursor of antituberculous rifampicin, also reacts with MSH to form an *S*-conjugate, which together with its oxidized form are substrates of mca. The *K*m values of mca when MS-Rifamycin-S reduced and oxidized forms are used as substrates are 190 μM and 450 μM respectively (Steffek *et al.*, 2003).

1.2.4.4.4 Mutant of a gene encoding mca

A targeted mutant of *mca* from *M. smegmatis* was generated and characterized (Rawat *et al.*, 2004). Unlike in the wild type strain where mercapturic acid is released after the cleavage of *S*-conjugates, the *mca* mutant does not possess an amidase activity. The *mca* mutant accumulates the *S*-conjugates of monobromobimane and rifamycin-S and also becomes more susceptible to electrophilic toxins such as N-ethylamalemide, iodoacetamide and chlorodinitrobenzene.
However the introduction of *M. tuberculosis mca* epichromosomally or *M. smegmatis mca* integratively into the mutant resulted in the complementation of the amidase activity and decreased levels of *S*-conjugates (Rawat *et al.*, 2004). The mca mutant also displayed similar phenotypic characteristics to the *mshC*-deficient mutant in that it was sensitive to drugs like streptomycin (Rawat *et al.*, 2002). However, it has not been established whether MSH can form *S*-conjugates with streptomycin, which could eventually be released as mercapturic acids.

1.2.4.4.5 Inhibitors of mca as potential drug targets

The involvement of mca in the mycobacterial detoxification of antibiotics makes it a promising target for drug development and indeed some efforts have been directed towards the synthesis of mca inhibitors. Bewley and coworkers screened 1500 natural products extracts and identified several inhibitors as lead candidates. Two bromotyrosine-derived alkaloids isolated from *Oceania sp.* were found to be competitive inhibitors of mca from *M. tuberculosis* (Nicholas *et al*., 2001; Nicholas *et al*., 2002). This was followed by the concise total synthesis of a bromotyrosine oxime which competitively inhibited mca with an IC_{50} value of 30 μM (Fetterolf and Bewley, 2004).

Based on the known structure of a naturally occurring alkaloid, a series of compounds were synthesized and tested as anti-infective agents against mycobacteria and other gram positive bacteria (Pick *et al*., 2006). EXEG1706 was identified as a lead compound that exhibited low minimum inhibition constants ranging from 2.5 to 25 $\mu g.ml^{-1}$ for methicillin-sensitive and methicillin–resistant *Staphylococcus aureus*, *M. smegmatis* and *M. bovis* whilst displaying minimum toxicity against mammalian macrophages and monocytes. EXEG1706 was also active against *M. smegmatis* mutant in which *mca* is deleted indicating that in addition to mca this compound possibly inhibits other target proteins in mycobacteria (Pick *et al*., 2006).

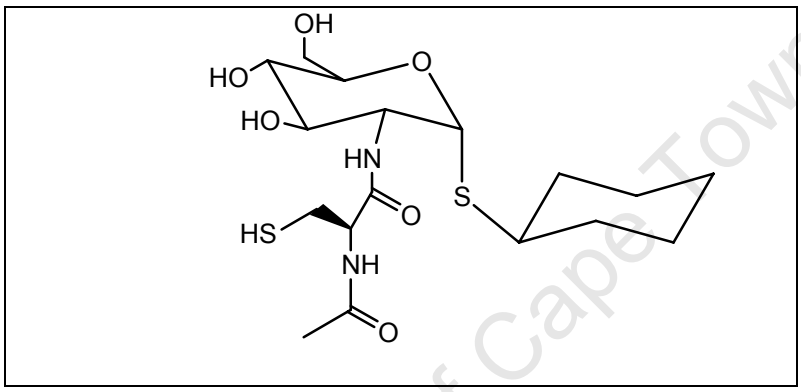

Figure 1.10: Thioglycosidic analog of MSH

The thioglycosidic analog of MSH has been synthesized and *S*-alkylated with monobromobimane (Knapp *et al.,* 2002). The evaluation of this analog as a substrate for mca revealed the specific activity of 7500 $nmol.min^{-1}.mg^{-1}$ versus 14200 $nmol.min^{-1}.mg^{-1}$ for MSmB (Knapp *et al.,* 2002). Although its specific activity was almost half that of the natural substrate, the thioglycoside can be used as an alternative substrate and its structure can serve as a starting material for anti-tubercular drug design.

The substitution of inositol with cyclohexane and replacement of *O* with *S* as a bridging atom seems to be an ideal approach for inhibitor designing. It combines several possible advantages because R-GlcNAc thioconjugates can be prepared stereoselectively and in good yield by *S*-derivatization (Knapp and Myers, 2002). Thioglycosides are more resistant to degradation by glycosidases than *O*-glycosides (Knapp *et al*., 1996; Bousquet *et al.,* 2000; Cohen and Halcomb, 2000).

Since inhibition of the MSH-dependent detoxification pathway could leave *M. tuberculosis* vulnerable to drugs, efforts are needed to generate more mca inhibitors. To this end, naturally occurring extracts have shown great promise as potential inhibitors of mca (Fetterolf and Bewley, 2004; Nicholas *et al*., 2001; Nicholas *et al*., 2002), however, there is still a need for the synthesis and testing of structure-based inhibitors against mca. Part of the current study is to evaluate several novel compounds as mca inhibitors. In an attempt to identify a single compound which can inhibit both the MSH biosynthetic and detoxification pathways, compounds which exhibit good inhibition against mca will also be evaluated as mshB inhibitors.

1.2.5 MSH B

1.2.5.1 1-D-myo-nosityl-2-acetamido-2-deoxy-α-D-glucopyranoside Deacetylase is the key enzyme in the biosynthesis of MSH

Rv1170, a gene which encodes mshB in *M. tuberculosis*, was first identified as a homolog of Rv1082, a gene encoding an MSH *S*-conjugate amidase (mca) (Newton *et al*., 2000b). Since mshB cleaves an amide bond similar to that hydrolyzed by mca, it was thought that mshB would be a broad spectrum enzyme involved both in MSH biosynthesis and in the detoxification pathway. However the comparison of mshB activities with MSmB and Acetyl-GlcN-Ins as substrates revealed that the deacetylase activity with Acetyl-GlcN-Ins as substrate was 23-fold higher than the amidase activity on MSmB. No deacetylation was detected with MSH and MSmB as substrate. This indicates that mshB does not possess significant activity for the degradation of MSH and it is not a broad spectrum deacetylase but is specific to Acetyl-GlcN-Ins (Newton *et al*., 2000a).

MshB catalyzes the deacetylation of Acetyl-GlcN-Ins to form GlcN-Ins in the second step of MSH biosynthesis. The level of Acetyl-GlcN-Ins in *M. smegmatis* at stationary and log phases is twice that of MSH and about 100-fold higher than that of other MSH precursors, GlcN-Ins and Cys-GlcN-Ins. This indicates that substantial amount of MSH can be produced upon demand from an endogeneous pool of Acetyl-GlcN-Ins under the control of mshB. It was shown that Acetyl-GlcN-Ins is absent in a MSH-deficient mutant strain 49 from *M. smegmatis,* and that this mutant strain can

assimilate Acetyl-GlcN-Ins from the medium and convert it to MSH (Newton *et al*., 2000a). This indicates that Acetyl-GlcN-Ins is a key intermediate leading to the biosynthesis of MSH.

The purification of recombinant mshB from *M. tuberculosis* was reported by Newton *et al* (Newton *et al*., 2006). The pure mshB had *K*m value of 340 +/- 80 μM and k_{cat} of 0.49 $s^{-1}$for its natural substrate, Acetyl-GlcN-Ins. As judged by activities at 0.1 mM substrate concentration, Acetyl-GlcN-Ins was 87-fold more reactive than GlcNAc on mshB indicating that inositol is important for binding (Newton *et al*., 2006). Other compounds which have been evaluated as mshB substrates were formyl-CySmB-GlcN-Ins and MS-acetophenone. Relative to Acetyl-GlcN-Ins, the activities of formyl-CySmB-GlcN-Ins and MS-acetophenone were 42 and 66%, respectively. MS-acetophenone was also cleaved by mca, indicating that a single inhibitor may inhibit both mshB and mca. The surprising finding by Newton and co-workers was that CySmB-GlcN-Ins proved to be a better substrate for mshB than its natural substrate with three times lower *K*m value (Newton *et al*., 2006). However, since the concentration of Cys-GlcN-Ins is almost undetectable inside the cells (Newton *et al*., 2000a), it seems highly unlikely that it could compete with MSH to form *S*-conjugates. Thus, the finding that mshB utilized CySmB-GlcN-Ins as a substrate better than Acetyl-GlcN-Ins is unlikely to have a physiological significance (Newton *et al*., 2006).

1.2.5.2 Crystal structure and Bioinformatics of mshB

Rv1170 (*mshB)* encodes a metalloenzyme consisting of 304 amino acid residues with a molecular mass of 33 000 kDa. The deacetylase activity of mshB is dependent on the divalent zinc ion (Newton *et al*., 2000a; Newton *et al.,* 2006). The sequence V10HAHPDDES is a conserved region in mshB orthologs of other actinomycetes including SCO5126, a gene encoding the MSH biosynthetic enzyme in *Streptomyces coelicolor* A(3)2 (Park *et al*., 2006) and TT1542 from *Thermus thermophillus* (Handa *et al*., 2003). *mshB* is a paralog of *M. tuberculosis* Rv1082 encoding the amidase, mca, which is also dependent on a divalent metal cation for activity (Newton *et al*., 2000a,b). MshB also possesses an amidase activity, albeit not as substantial as its deacetylase.

The crystal structure of mshB has been reported independently by Maynes *et al.* and McCarthy *et al.* (Maynes *et al*., 2003; McCarthy *et al*., 2004). The x-ray crystallographic structure of mshB reveals a folding pattern similar to lactate dehydrogenase (LDH) in the N-terminal domain. The zinc binding site in the N-terminal domain occupies a position equivalent to that of the NAD-cofactor in LDH and there are two water molecules which coordinate to the Zn^{2+} ion (Maynes *et al*., 2003).

MshB consists of a large nine-stranded mixed β-sheet and one small three stranded antiparallel β-sheet. The first five strands of the large β-sheet with the associated α-helices adopt a pattern that resembles Rossmann fold of LDH (White *et al*., 1976). McCarthy *et al.* also resolved a 3-D structure of mshB in which helices are packed against parallel β-sheets. Large loops emanating from the C-terminus of the β-strands form a cavity in which the active site is located (McCarthy *et al*., 2004).

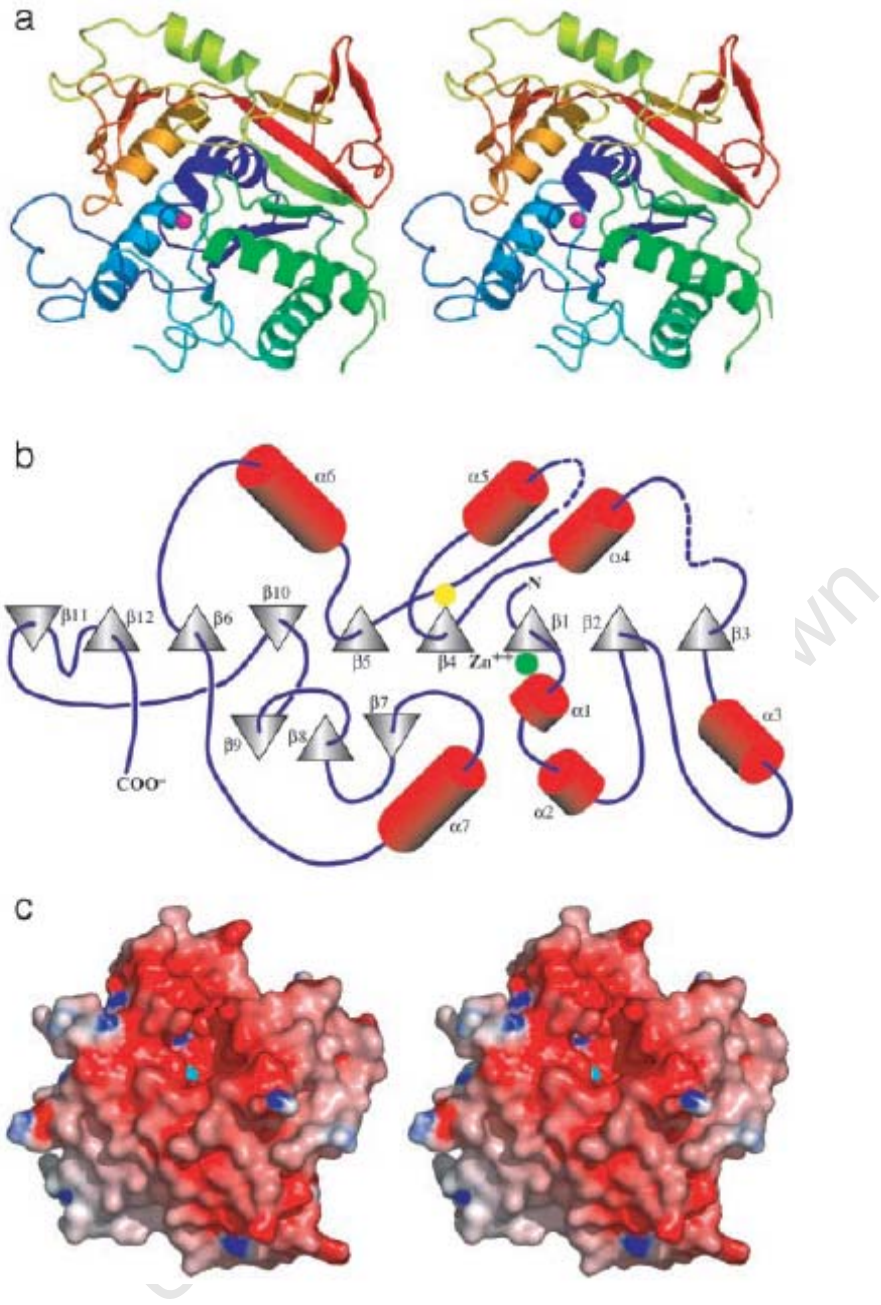

Figure 1.11: Overall structure of MshB.
A. One of the four MshB molecules present in the crystallographic asymmetric unit. The colouring is blue at the N terminus and red at the C terminus. The catalytic zinc is shown as a magenta sphere. **B.** Secondary structure present in the structure of MshB, showing the large central mixed β-sheet and lactate dehydrogenase (Rossmann) fold. The green sphere denotes the location of two of the zinc binding ligands (His-13 and Asp-16) and of the general base for the proposed catalytic mechanism (Asp-15). The yellow sphere represents the location of the third zinc binding ligand (His-147) and the electrophile for the catalytic mechanism (His-144). **C.** Electrostatic surface of mshB with positive electronegativity in blue and negative electronegativity in red **(**taken from Maynes *et al*., 2003). The permission to reproduce the figure was granted by the corresponding author of the paper, Prof M. James).

1.2.5.3 The mshB substrate binding pocket

Many molecules which bind carbohydrates contain hydrophilic residues which form hydrogen bonding with the sugar hydroxyl groups (Quiocho, 1993). Because Acetyl-GlcN-Ins is a very hydrophilic molecule, its binding pocket in mshB is expected to be hydrophilic. It was indeed reported that the active site and substrate binding pocket of mshB is hydrophilic and electronegative. The binding pocket contains carboxylate groups (Asp-15, -95 and -146), three hydroxyl groups (Ser-20,-260 and Tyr-142), four main chain carbonyls (Gly-140, Tyr-142, Glu-213 and Ile-214), one amide from the side chain of Gln-247 and two positively charged amino acids (Arg-68 and His-144) (Figure 1.12). The zinc ion is attached to three ligands, His-13,-147 and Asp-16 and is in proximity with two water molecules. One of these molecules is near the general base Asp-15 and is a nucleophilic water molecule (McCarthy *et al*., 2004 and Maynes *et al*., 2003).

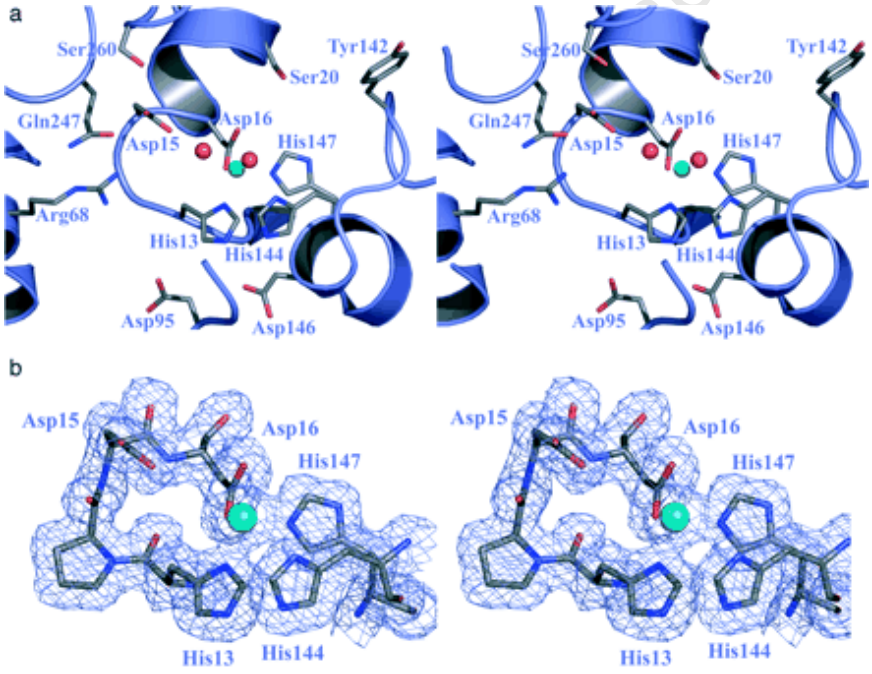

Figure 1.12: The active site of MshB. *a*, active site representation of one of the MshB molecules in the asymmetric unit. The catalytic zinc is shown as a *cyan sphere*, and two zinc-bound water molecules are shown as *red spheres*. The leftmost water molecule is within 2.83 Å of the catalytic Asp-15, and both water molecules are within 3 Å of the metal ion. The other metal ligands are 2.10 (His-13), 2.07 (Asp-16), and 2.13 Å (His-147) from the metal. *b*, Representative electron density from the active site region of MshB (Maynes *et al.*, 2003). (The permission to reproduce the figure was granted by the corresponding author of the paper, Prof M. James).

The 300-fold decrease in the mshB catalytic activity after the removal of the inositol moiety from Acetyl-GlcN-Ins indicates that inositol may also be interacting with mshB (Newton *et al*., 2000a). Although inositol does not participate in the deacetylation mechanism it is possible that its hydroxyl groups could interact via hydrogen bonding with the hydrophilic groups of mshB. To establish this, more compounds in which inositol is substituted with a spacefilling cyclohexane or phenyl group could be evaluated as mshB substrates.

1.2.5.4 Catalytic mechanism of mshB

The mechanism of Acetyl-GlcN-Ins deacetylation by mshB is very similar to that of a protease hydrolysing a peptide bond. The catalytic hydrolysis of Acetyl-GlcN-Ins involves displacement of the second water molecule on Zn^{2+} by the carbonyl oxygen of the acetyl group (Figure 1.13). This leaves the second water molecule activated for the nucleophillic attack of the carbonyl carbon of the acetyl group. The water-facilitated nucleophilic attack is assisted by a general base, the carboxylate of Asp-15, and the resultant tetrahedral transition state possesses a negatively charged oxygen which is stabilized by the positively charged Zn ion and the imidazolium chain of His144. Proton transfer to the nitrogen of the deacetylation product, GlcN-Ins, is through the general acid function of the carboxyl group of Asp-15 (Maynes *et al*., 2003). This mechanism is similar to that of typical zinc metalloproteinases such as carboxypeptidase (Christianson and Lipscomb, 1989). However in most zinc proteinases the role of a general base and general acid is accomplished by glutamate rather than Asp-15.

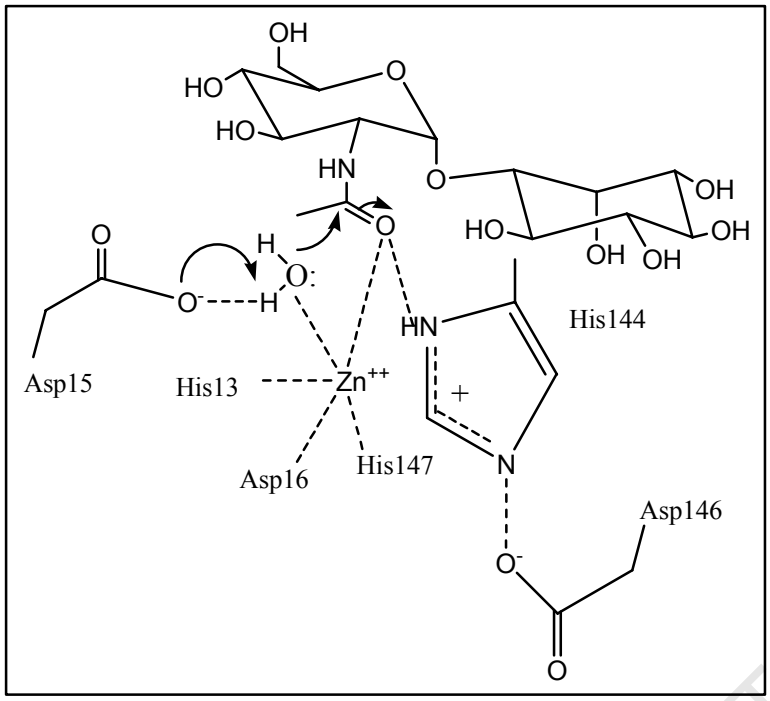

Figure 1.13: Catalytic mechanism of mshB (modified from Maynes *et al*., 2003).

1.2.5.5 Disruption of *mshB* results in decreased production of MSH

A *mshB*$^-$ mutant strain of *M. smegmatis*, Myco504, was constructed and analyzed for MSH content. The disruption of the *mshB* gene resulted in a substantial decrease of MSH production, yielding only 5-10% of the level produced by *M. smegmatis* wild-type mc^{2}155 (Rawat *et al*., 2003). Complementation of Myco504 with the *mshB* gene resulted in increased MSH production to the parental level confirming that the decrease of MSH production was indeed due to the disruption of *mshB* (Rawat *et al*., 2003).

The same scenario was observed with a mutant strain created by knocking out the *mshB* homolog in *Streptomyces coelicolor* A(3)2, annotated as SCO5126. The SCO5126 deficient mutant produced only 10% MSH but when it was complemented with the SCO5126 gene, the MSH production was restored to the levels similar to that of the wild type (Park *et al*., 2006).

Myco504 does not exhibit significant sensitivity to iodoacetamide, DTNP, cumene hydroperoxide and to antibiotics like vancomycin, cerulenin, rifampicin and erythromycin (Rawat *et al*., 2003). This was in contrast to the mshC$^-$ mutant which was reported to be sensitive to these antibiotics (Rawat *et al.,* 2002). Furthermore, unlike with other MSH mutants, Myco504 displayed the same resistance to isoniazid as the wild type strain. Myco504 was sensitive to ethionamide, mBBr and the glutathione *S*-transferase substrate, CDNB (Rawat *et al*., 2003).

The presence of 5-10% MSH, as compared to the wildtype, produced in Myco504 indicates that another gene compensates for the loss of deacetylase activity in the *mshB*$^-$ mutant. Since mshB and mca in *M. tuberculosis* share 36% identity, it is likely that mca is the enzyme responsible for the deacetylase activity in the mutant (Rawat *et al*., 2003). The inhibition of both mca and mshB could therefore result in the complete stoppage of MSH production.

AIMS AND OBJECTIVES

The aim of this study was to identify and evaluate structure-based compounds which can inhibit mshB, a key enzyme in the biosynthesis of MSH, and mca, an enzyme that catalyzes MSH-dependent detoxification pathway in *M. tuberculosis*. Due to the overlapping deacetylase activities of mca and mshB a complete disruption of MSH production at the deacetylase step can only be achieved by simultaneous inhibition of both these enzymes (Newton *et al*., 2006). Since MSH and its precursors are not commercially available, the synthesis of the natural substrates and the identification of alternate substrates for both mca and mshB was also the objective of the project.

CHAPTER 2:

MATERIALS AND METHODS

2.1. MATERIALS

Chemical/Reagent:	**Supplier:** (company details in Appendix B)
2,2-dithiodipyridyl	Aldrich
4,4'-dithiodypyridyl	Aldrich
2-mercaptoethanol	Merck
2-monobromobimane	Fluka
AccQ-Fluor	Waters
Acetic acid	Merck
Acetic anhydride	Aldrich
Acrylamide	Sigma
Ammonium persulfate	Merck
Ammonium sulphate	Riedel-de Haën
Ampicillin	Sigma
Bacto Middlebrook 7H9	Difco
Bis-acrylamide	Fluka
Chloramphenicol	Boehringer Mannheim
Coomasie Brilliant Blue R250	Merck
Dithiothreitol	Roche
DnsCl	Sigma
EDTA	Sigma-Aldrich
Glycerol	Sigma
Glycine	Merck
HCl	BDH
HEPES	Fluka
Imidazole	Fluka
IPTG	Fermentas
K_2HPO_4	Fluka

KH_2PO_4	Merck
Li_2CO_3	Sigma
$LiOH.H_2O$	Aldrich
Methylene Blue	Sigma
N-Acetyl-L-cysteine	Fluka
NaCl	Fluka
$NaHCO_3$	BDH
NaOH	Fluka
N N N `N`-tetramethyl-1,2-diaminoethane	BDH
Perchloric acid	BDH
PMSF	Boeringer Ingelheim
Ready Flow III Scintillation fluid	Beckman Coulter
SDS	BDH
Sodium borohydride	Aldrich
TLCK	Sigma
TPCK	Sigma
Tris	Merck
Tween 80	Sigma
$ZnSO_4$	BDH

Solvents:

Acetonitrile (HPLC grade)	Sigma
Butanol	Merck
Ethanol	Sigma
Methanol	Fluka
TEA	Sigma
TFA (HPLC grade)	Sigma

Chromatography Resins:

Iminodiacetic acid agarose	Sigma
Deae Sepharose	Sigma-Aldrich
Sephacryl S300	Pharmacia
Hydroxyapatite	Bio-Rad
DEAE Cellulose	Pierce

Vydac C-18 resin	Vydac
C-18 SepPack Cartridges	Waters
Normal phase TLC Silica G60	Macherey-Nagel
G-60 Desalting columns	Pierce

Dialysis:

Dialysis tubing	Sigma

Radio-chemicals:

^{3}H-*Myo*-inositol	Perkin Elmer

HPLC columns:

Biosep SEC-S2000 column (250 x 4.6 mm)	Phenomenex
Phenyl-hexyl HPLC column (250 x 4.6 mm)	Phenomenex
Phenyl-hexyl HPLC column (250 × 22 mm)	Phenomenex
Luna 5µ C-18 HPLC column (250 x 4.6 mm)	Phenomenex
Vydac TP1022 HPLC column (250 × 22 mm)	Vydac

2.2. GENERAL METHODS

2.2.1 Preparation of Middlebrook media

4.7 g Bacto Middlebrook 7H9 broth (Difco) was dissolved in 800 ml H_20[11], 50 ml glycerol and 0.5 g Tween 80 (Sigma) were added to the medium and more water added to make up 1000 ml. The medium was autoclaved at 121^0C, 15 psi for 20 minutes.

2.2.2 Maintenance of *M. smegmatis* in Middlebrook media

Mycobacterium smegmatis cells were maintained on Löwenstein–Jensen slants and stored at -4^0C. Liquid cultures were grown on Middlebrook medium which was shaken in Erlenmeyer flasks at 200 rpm at 37 °C. For primary cultures, a lump of bacteria was transferred from stock culture to 50 ml of liquid medium and grown for up to 3-5 days. For secondary cultures, 5 ml of densely grown primary culture was inoculated into 250 ml of medium and incubated overnight. The purity of the cultures was checked routinely with the Ziehl–Neelsen staining method. The cells were harvested by centrifugation at 7 000 g. The supernatant was discarded and the pellet frozen at -80 °C.

2.2.3 Ziehl-Neelsen staining

Mycobacterium smegmatis smear was dried on a slide for 3-5 min and then stained with Ziehl carbol fuchsin while applying enough heat for gentle steaming. The slide was washed with distilled water and decolorized in 95 % acid alcohol until only a suggestion of pink color remained. It was washed with tap water and counter-stained with Methylene Blue. The slide was then washed with tap H_20, dried and examined microscopically under 1000X magnification microscopy.

2.2.4 Radiolabelling of *M. smegmatis*

[11] Water used in this project was deionized. At some point, the water was sparged with argon but it did not make a difference.

M. smegmatis cells were inoculated in Middlebrook medium. 25 ml of cells was diluted to 100 ml, and 20 µl ^{3}H-myo-inositol was added. Incubation was continued for another 3 hours. The cells were harvested and stored at -80 °C.

2.2.5 Absorbance Spectrophotometry

Spectrophotometric analysis of thiols and their derivatives was performed using an Ocean Optics USB2000 spectrometer. For quantitation of 2-*S*-(2-thiopyridyl)-6-hydroxynaphthyldisulfide, 20 µL of the sample was added to 980 µl of 25 mM K_2HPO_4 buffer, pH 8,0 and the absorbance measured at 298 nm while reducing with dithiothreitol ($\Delta\varepsilon = 18500 M^{-1}.cm^{-1}$).

For the estimation of thiol content 20 µl of a sample was added to 970 µl of 25mM K_2HPO_4 buffer, pH 8.0, followed by the addition of 10 µl of 20 mM 4,4-dithiodipyridyl (dTdP). The thiol concentration was estimated from the resultant change in absorbance at 325 nm, due to the formation of pyridine-4-thione ($\Delta\varepsilon_{325} = 19800 M^{-1}cm^{-1}$), using an Ocean Optics Mini-diode array spectrometer. MSmB was also quantified spectrophotometrically by measuring absorbance at 396nm ($\Delta\varepsilon = 5300 M^{-1}.cm^{-1}$). Eluates from chromatographic steps used in the purification of enzymes were monitored by measuring absorbance at 280nm.

2.2.6 HPLC methods

Table 2.1: Method 1:

Time	0 minute	5 min	35 min	40 min	45 min
Buffer A%	95%	95%	10%	10%	95%
Buffer B%	5%	5%	90%	90%	5%

The column was eluted by running this gradient at a rate of 0.8 ml/min in which buffer A was 0.1% TFA in water and buffer B 100% acetonitrile. This method was

also used for analysis of the dansylation reaction with TEA:Acetic acid (0.088%:0.57%) as buffer A in place of 0.1% TFA.

Table 2.2: Method 2 (modified from Anderberg *et. al*, 1998):

Time	0 minute	10 min	50 min	53 min	57 min	60 min
Buffer A%	100%	100%	40%	0%	0%	100%
Buffer B%	0%	0%	60%	100%	100%	0%

Samples were injected into the Phenomenex phenyl hexyl C-18 HPLC column (250 x 4.6mm). The column was eluted by running the gradient at a rate of 0.8 ml/min in which buffer A was 0.1% TFA in water and buffer B 0.1% in methanol. UV detector was set at 250 nm and emission at 395 nm wavelength.

Table 2.3: Method 3:

Time	0 minute	5 min	35 min	40 min	45 min
Buffer A%	95%	95%	55%	10%	95%
Buffer B%	5%	5%	45%	90%	5%

The column was eluted for 5 mins with 5% B, for 30mins with a linear gradient to 45%B, for 5mins to 90%B, followed by a return to initial conditions (Solvent A: 0.1%TFA and Solvent B: acetonitrile). The flowrate was 0.8ml/min.

2.2.7 Preparation of Standard curves

2.2.7.1 Preparation of N-Acetyl-L-Cysteine-mB Standard curve

10 mM N-Acetyl-L-cysteine was prepared in 1 ml distilled water and derivatized with two-fold mBBr. The samples were injected into the Phenomenex phenyl hexyl C-18 HPLC column (250 x 4.6mm). The column was eluted by running method 1 at a rate of 0.8 ml/min in which buffer A was 0.1% TFA and buffer B was 100% acetonitrile. UV wavelength detector was set at 396 nm and emission at 482 nm wavelength. The amounts injected were plotted against the fluorescence area of the N-Acetyl-L-Cysteine.

2.2.7.2 Standard Curve of GlcN-Ins derivatized with AccQ-Fluor

GlcN-Ins was dissolved in water to make up 3.65 mM stock solution. Different concentrations ranging from 250 μM to 2000 μM were prepared in eppendorf tubes to the final volume of 30 μL with 200 mM Hepes buffer pH 8.0. 15 μL acetonitrile and 15 μL of 10 mM AccQ-Fluor were added to each eppendorf tube and the reactions were vortexed and left standing at room temperature for 1 minute. To complete the derivatization the reaction mixtures were heated for 10 minutes at 60 ^{0}C. They were then diluted 4-fold with water and stored at -80 ^{0}C. The samples were thawed and injected into the C-18 HPLC column (250 x 4.6mm). The column was eluted by running method 2 at a rate of 0.8 ml/min in which buffer A was 0.1% TFA in water and buffer B 0.1% in methanol. UV detector was set at 250 nm while the fluorescent detector was set at 250 nm for excitation and 395 nm for emission. The amounts injected were plotted against the area of the peaks of AccQ-Fluor derivatized GlcN-Ins.

2.2.8 Methods for Derivatization of Amines

The AccQ-Fluor method is more rapid and sensitive than the other amine derivatization methods, including dansylation and dabsylation of amines, used in this study. Thus, AccQ-Fluor was utilized throughout the kinetic analysis of inhibitors in

presence of Acetyl-GlcN-Ins. Dansylation was only used for the evaluation of Acetyl-GlcN-Ins structural analogs as alternate substrates of MshB.

2.2.8.1 AccQ-Fluor

6-aminoquinolyl-N-hydroxysuccinamidyl carbamate (AccQ-Fluor) is a derivatizing agent used to perform AccQ-Tag amino acid analysis (Cohen and Michaud, 1993). 10 mM AccQ-Fluor was purchased from Waters and reconstituted as instructed by the manufacturer. 50 µl of 200 mM Hepes buffer, pH 8 was added to the enzymatic reaction mixture and vortexed. The Hepes was found to be working better than borate buffer that came with the kit. 30 µl of 10 mM reconstituted AccQ-Fluor reagent was added and the fractions were vortexed for about 5 seconds. Fractions were incubated for 1 minute at room temperature followed by 10 minutes at 55^0C. The samples were analyzed by TLC or HPLC with the UV detector set at 250 nm and the fluorescent detector at 250 nm for excitation and 395 nm for emission.

2.2.8.2 Dansylation

Dansylation is one of the widely used methods for derivatization of amino acids (Gros and Labouesse *et al*, 1981). This method was used because AccQ-fluor is suitable for the analysis of polar amines. With apolar amines the derivatized amine co-elutes with a lot of interfering compounds, possibly reagent derived degradation products, and so the method fails. Therefore the derivatization with dansyl chloride was used as an alternate method for the analysis of the amide cleavage of alternate substrates of mshB, especially where the aglycon had no absorbance such as in the case of cyclohexane. 70 µL of mshB-treated Acetyl-GlcN-Ins samples were mixed with 80 µL of 40 mM Li_2CO_3 pH 9.0 and 200 µL of 40 mM DnsCl. The dansylation reaction was kept in the dark for 1 hour and 25 µL was diluted 5-fold with 50 µL TEA:acetic acid (starting buffer) and 50 µL and was injected in to a Luna 5µ c-18 HPLC column (250 x 4.6mm). The column was eluted by running method 1. On the fluorescent detector emmision was set at 578 nm and excitation at 254 nm while the UV detector was set at 254 nm.

2.2.8.3 Dabsylation

Derivatization of amino acids with 4-dimethylaminoazobenzene-4'-sulfonyl chloride (dabsyl chloride) was introduced by Lin and Chang, 1975. Dabsylation requires no fluorescent detector but only a UV detector set at 436 nm (Lin and Chang, 1975). An attempt was made to utilize this method for the evaluation of alternate substrates of mshB. However it was dropped since the product peaks were too small at lower substrate concentrations.

2.2.9 SDS-Polyacrylamide Gel Electrophoresis of Proteins

2.2.9.1 Preparation of materials

Resolving gel buffer

36.35g Trizma base (1.5 M) and 0.8g SDS (0.4%) were dissolved in 200ml distilled water. The pH was adjusted to 8.8 with concentrated HCl.

Stacking gel buffer

12.1g Trizma base (0.5 M) and 0.8g SDS (0.4%) were dissolved in 200ml distilled water. The pH was adjusted to 6.8 with concentrated HCl.

Acrylamide-bis-acrylamide stock solution

29.2g acrylamide and 0.8g bis-acrylamide were dissolved to 100ml distilled water. The solution was filtered through Whatman No 1 paper and stored in a bottle covered with foil at 4^0C.

Ammonium persulfate solution (APS)

10% APS was prepared by dissolving 0.05g in 500µl water.

N N N `N`-tetramethyl-1,2-diaminoethane(TEMED) Catalyst

TEMED Catalyst was used as a stock solution from BDH Chemicals Ltd.

Sample treatment buffer

2.5 ml stacking gel buffer, 4 ml of 10% (w/v) SDS, 2 ml glycerol, 1 ml 2-mercaptoethanol and 0.5 ml distilled water were mixed together in a bottle and stored at -20^{0}C.

Coomasie blue staining solution

1.25 g Coomasie Brilliant Blue –R250 (Merck) was dissolved in 227 ml methanol, 227 ml water was added and the contents were mixed. 46 ml glacial acetic acid was added and the mixture was left standing overnight and filtered.

Destaining solution

The destaining solution had the composition ethanol:acetic acid: water:: 2:1:7.

2.2.9.2 Loading the gel

SDS-polyacrylamide gel electrophoresis was performed on vertical slab gels (Laemmli, 1970). Resolving buffer was prepared according to the table and poured in to the plates. It was left for 1 hour to polymerize and overlaid by a stacking buffer (composition in the table).

Table 2.4: SDS Poly-acrylamide gel electrophoresis composition

Solutions	Resolving gel	Stacking gel
	12.5 % electrophoresis gel	
Resolving buffer	6.25 ml	-
Stacking buffer	-	3.75 ml
Distilled Water	8.25 ml	9.0 ml
Acrylamide solution	10.25 ml	2.25 ml
APS	75 µl	45 µl
TEMED	50 µl	30 µl

Protein samples were mixed with 1/10th the volume of Sample Treatment Buffer and heated at 80°C for 5min before loading. A tank buffer consisting

of 25mM Tris-Cl, 0.1% SDS, 0.19M glycine was used and gels were electrophoresed at 30mA. The electrophoresis Calibration Kit from Pharmacia and the Fermentas protein Molecular Weight Marker were used to estimate protein size.

2.2.9.3 Visualisation of Proteins Separated on SDS PAGE

Gels were stained overnight in the solution of 0.45% methanol and 0.18% glacial acetic acid, containing 0.25% Coomasie Brilliant Blue R250. Destaining was performed in the solution containing 20% ethanol and 10% acetic acid.

2.2.10 Detection of Bimane-derivatives

Samples derivatized with mBBr were injected onto a Phenomenex Phenyl-hexyl HPLC column (250 x 4.6mm). The column was eluted using Method 1 with the emission set at 482 and excition at 396 nm.

CHAPTER 3:

SYNTHESIS OF SUBSTRATES

3.1. INTRODUCTION

The fact that MSH or any of its immediate precursors are not commercially available is a serious impediment in studies of the metabolism of this thiol.

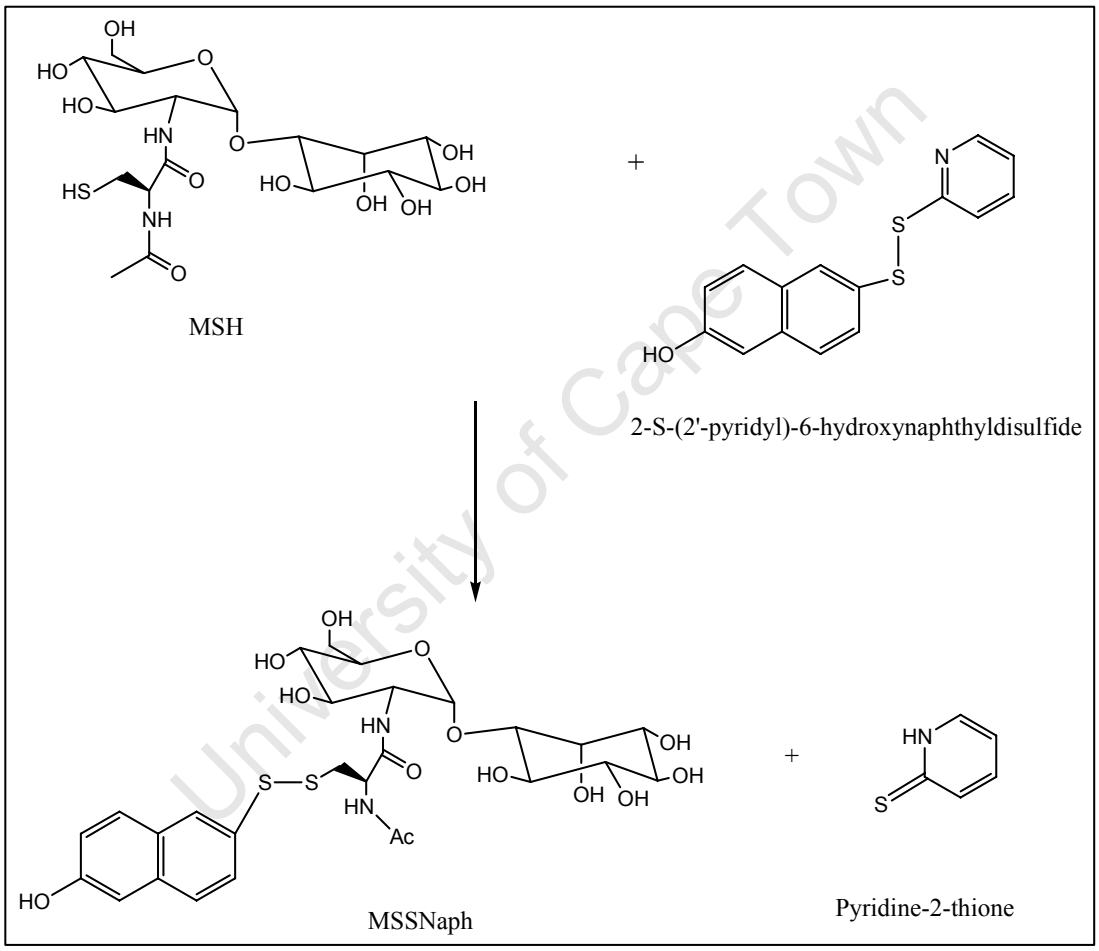

Figure 3.1: The reaction of 2-*S*-(2-thiopyridyl)-6-hydroxynaphthyldisulfide and MSH.

In previous studies, the chemical synthesis of MSH was reported (Jardine *et. al*., 2002). However, this approach yielded only relatively small quantities of MSH. Steenkamp and Vogt (2004) devised a methodology used for the isolation of MSH from *M. smegmatis* at milligram levels. The method has proved useful in producing

reasonable amounts of MSH for further biochemical studies. The protocol is based on the formation of an apolar heterodisulfide, 2'-s-(mycothiolyl)-6-hydroxynaphthyldisulfide, which is retained on C-18 reverse phase columns. After reduction the hydrophilic MSH is no longer adsorbed onto C-18 reversed phase resins while the apolar thionaphthol is retained (Steenkamp and Vogt, 2004). Because a quick and efficient method was required to generate substrates for the current study, the above procedure was used as a starting point for the purification of MSH

3.2. METHODS

3.2.1 Synthesis of 2-*S*-(2-thiopyridyl)-6-hydroxynaphthyldisulfide

The synthesis of 2-*S*-(2-thiopyridyl)-6-hydroxynaphthyldisulfide was performed with modifications of the previously described method by Steenkamp and Vogt, 2004. 6-Hydroxy-2-naphthyldisulfide (300 mg) was dissolved in 150 ml of a 1:1 (v/v) mixture of acetonitrile:water. The mixture was reduced by the addition of 900 mg sodium borohydride at room temperature, a yellow colour was observed due to the formation of the 2-thio-6-hydroxynaphthalene anion. The borohydride ions were destroyed by the addition of 3 ml glacial acetic acid and the pH of the resulting solution adjusted to 4.6 by the addition of dipotassium phosphate. The pH of 4.6 was chosen to be significantly below the p*K*a of 2-thio-6-hydroxynaphthalene, which was estimated to be approximately 6.4 by spectrophotometric titration (Steenkamp and Vogt, 2004).

The 2-thio-6-hydroxynaphthalene solution was added dropwise and with stirring over a period of 20 min to 75 ml of a solution containing 711 mg 2,2-dithiodipyridyl in a 1:1 mixture of acetonitrile and water. The mixture was left for 60 min and was then diluted with three parts of water to a final acetonitrile concentration of ~ 12.5% and left overnight at 4^0C. It was then cooled overnight at 4^0C. The resultant precipitate was collected by centrifugation and dissolved in a 60% (v/v) acetonitrile/water mixture. The precipitate consisted principally of 6-hydroxy-2-naphthalenedisulfide and 2-*S*-(2-thiopyridyl)-6-hydroxynaphthyldisulfide. These components were separated isocratically on a preparative Vydac TP1022 reversed-phase HPLC column (250 × 22 mm) with 65% acetonitrile and 35% of 0.1% Trifluoroacetic acid. The quantity of 2-*S*-(2-thiopyridyl)-6-hydroxynaphthyldisulfide was determined

spectrophotometrically as described in general methods using a molar extinction coefficient of 11184 $M^{-1}.cm^{-1}$ at 343 nm wavelength. The yield was 463 μmols in 470 ml.

3.2.2 Extraction of thiols from mycobacterial extract

Mycobacterium smegmatis mc^2 cells were purchased from the Center for Biocatalysis and Bioprocessing, University of Iowa, where it was grown in a 100 litre fermentor using the medium described by Isabelle *et al.* (2002). The cells (2.65kg) were harvested in the early stationary phase of growth and stored at -80^0C.

M. smegmatis mc^2 (138.7 g) was mixed with 1.0 g of ^{3}H-*myo*-inositol radiolabeled *M. smegmatis* and suspended in 300 ml of a solution containing 0.25 M perchloric acid, 2 mM EDTA, and 40% (v/v) acetonitrile/water. The cells were disrupted by sonication at an output control of 8 and duty cycle of 30 for 10 minutes. The mixture was clarified by centrifugation at 6 000 *g* for 15 minutes at Tmax of 4^{o}C using Beckman Rotor JA-3050. The pellets were discarded and the pH of the clear 335 ml supernatant was adjusted to 4.6 by the addition TEA. To get rid of hydrogen sulphide from the extract, the mixture was sparged for two hours with argon. The dithiodipyridyl-reactive thiols in the mycobacterial extract were estimated to be 462 μmols in a volume of 305 ml.

3.2.3 Synthesis of *S*-2-(Mycothiolyl)-6-hydroxynaphthyldisulfide

Because MSH tends to undergo oxidation reactions during storage and manipulations, it is usually difficult to maintain it in its reduced form. The best possible way to preserve this thiol at a stable form is to form the heterodisulfide, 2'-s-(mycothiolyl)-6-hydroxynaphthyldisulfide (MSSNaph) (Steenkamp and Vogt, 2004).

The solution that contained 462 μmols in a volume of 305 ml was added dropwise with stirring to 470 ml of 65% (v/v) acetonitrile/water solution containing 463 μmols 2-*S*-(2-thiopyridyl)-6-hydroxynaphthyldisulfide. The formation of *S*-2-(Mycothiolyl)-6-hydroxynaphthyldisulfide was monitored by injecting 25 μl aliquots of the reaction mixture onto a Luna 5μ C-18 analytical HPLC column (250 x 4.6mm) at different

times of incubation. The column was eluted using method 1 (Section 2.2.6). After 25 hours of the reaction, the mixture was diluted five-fold with water, filtered and then passed through SepPak C-18 cartridges. The cartridges were washed with water. MSSNaph was retained on the cartridge solid stationary phase and then eluted using a minimal quantity of 50% (v/v) acetonitrile/water. The *S*-2-(Mycothiolyl)-6-hydroxynaphthyldisulfide eluted from the cartridge was bubbled with air to reduce the excess acetonitrile concentration in the mixture to less than 10%. 10 µl was injected onto a Luna 5µ C-18 analytical HPLC column (250 x 4.6mm) and eluted with method 1. The peaks were collected and *S*-2-(Mycothiolyl)-6-hydroxynaphthyl disulfide (MSSNaph) identified by determining the radioactivity by scintillation counting. The concentration of MSSNaph was estimated spectrophotometrically and by recording the absorbance spectrum of an aliquot in 25mM K_2HPO_4 after reduction with 1mM dithiothreitol using molar extinction coefficient of 18500 mM^{-1} cm^{-1} at 298 nm.

3.2.4 Synthesis of MSH

The MSSNaph mixture was reduced with 25 mg sodium borohydride for one hour and 1 ml glacial acetic acid was used to get rid of borohydride. The reduced mixture was run through the C-18 SepPak cartridge which had been wet with 100% acetonitrile and then washed with water before use. Hydrophilic MSH ran through the C-18 SepPak cartridge while apolar thionaphthol was retained. Reduced MSH was then freeze-dried overnight and stored in glass vessels at 4^0 C. Since the addition of acetic acid in the sample of MSSNaph resulted in the formation of some ions such as sodium acetate, MSH which was now in powder form was redissolved in 5 ml water and injected on Vydac 218TP1022 HPLC reversed phase preparative column at 230 nm. The separation was achieved using the method which starts with 100% (0.1% TFA) until 10 minutes, followed by the gradient from 0% to 50% B (100% (CH_3CN) until 55 min and then back to 100% A at 60 minutes of the run.

The reduced MSH from HPLC was quantified as in section 2.2.5. Pure MSH was then freeze-dried overnight and stored at 4 ^{0}C.

3.2.5 Synthesis of Mycothiol-Bimane

MSH was redissolved in 4 ml distilled water and its pH converted to 8.0 with triethylamine. Monobromobimane (40 μmols) in 2 ml acetonitrile was mixed with 4 ml of 20 μmols MSH and the mixture was left in the dark until the derivatization was complete. The mixture was run on reverse-phase Vydac preparative column. Pure MSmB eluted was collected and freeze dried overnight. MSmB was redissolved in 2 ml distilled water and quantified spectrophotometrically using a molar extinction coefficient of 5300 $M^{-1}.cm^{-1}$ at 396 nm. The final MSmB concentration was 10.83 mM in 1.8 ml.

3.2.6a. Synthesis of GlcN-Ins

MSmB, 10.83 mM in 1.5 ml, was incubated with 1 ml of 25 mM Hepes buffer containing 1 mM Zn^{2+}, pH 7.5, at 37 °C with 1 ml of partially purified amidase. The reaction was monitored for the formation of N-AcCys-mB using TLC. Additional aliquots (0.6 ml) of enzyme were added as necessary to achieve complete hydrolysis of the MSmB over a maximum interval of 8 hours, after which the reaction mixture was acidified to a pH less than 3 with perchloric acid. A 1 ml SepPak, C-18 cartridge (Waters) was prepared by sequentially washing with 5 ml of methanol, 5 ml of 50% methanol, 5 ml methanol in 0.1% trifluoroacetic acid, and 20 ml 0.1% trifluoroacetic acid in water. The acidified reaction mixture was applied to the SepPak C18 cartridge, and material not retained was freeze-dried, and resuspended in 1 ml of water.

3.2.6b. Synthesis of GlcN-Ins from the thialysine derivative of MSH

MSH is more reactive at slightly alkaline pH. It can undergo derivatization and oxidation reaction at this pH, for instance, during oxidation with diamide and derivatization with monobromobimane. Bromoethylamine also reacts with MSH at the sulfhydryl group to give a product which has an analog of lysine in its structure, thialysine. Since trypsin cleaves next to arginine and lysine, its enzymatic action can be exploited for the synthesis of GlcN-Ins by cleaving at the thialysine residue.

The pH of MSH was adjusted to 8.0 with triethylamine. Ten-fold excess bromoethylamine was added into MSH under the steam of argon to avoid oxidation. The reaction was left standing at room temperature to ensure all MSH has reacted with excess bromoethylamine to form a thialysine residue. The resultant derivative of MSH was then cleaved at the thialysine moiety with trypsin to give GlcN-Ins.

3.2.7 Synthesis of Acetyl-GcN-Ins

Acetylation of GlcN-Ins was carried out using the modification of Newton *et al*, 2000. A solution containing 5.0 μmols of GlcN-Ins was prepared by dissolving 1.7 mg GlcN-Ins in 1 ml of 20 mM $NaHCO_3$ pH 8.7. A two-fold excess of acetic anhydride was added to the 5.0 μmols GlcN-Ins over a period of 20 minutes while stirring. The disappearance of amino group of GlcN-Ins was monitored by HPLC and TLC after derivatizing with AccQ-Flour.

3.2.8 Attempted Synthesis of Sulfonamides

In addition to the enzymatically synthesized GlcN-Ins, chemically synthesized GlcN-Ins was also donated as a generous gift by Prof Stefan Oscarson of University College Dublin. 5 μmols GlcN-Ins was prepared by dissolving 1.7 mg in 1.0 ml of 20 mM $NaHCO_3$ pH 8.7. Four-fold methanesulfonyl chloride was added over the period of 5 minutes while stirring. The disappearance of amino group of GlcN-Ins was monitored by HPLC and TLC. To optimize reaction conditions, the amounts of methanesulfonyl chloride were varied from 1 to 10-fold relative to the GlcN-Ins and the reactions incubated up to 10 hours.

3.3 RESULTS AND DISCUSSION

3.3.1 Isolation of MSSNaph and MSH using 2-*S*-(2-thiopyridyl)-6-hydroxynaphthyldisulfide

The methodology of isolating MSH at milligram levels involves the conversion of thiols in to a heterodisulfide in which a thiol partner is 2-*S*-(2-thiopyridyl)-6-hydroxynaphthyldisulfide, an apolar compound with strong affinity to hydrophobic stationary phase. 2-*S*-(2-thiopyridyl)-6-hydroxynaphthyldisulfide was synthesized by reacting 6-hydroxy-2-naphthyldisulfide and 2,2-dithiodipyridyl as previously described (Steenkamp and Vogt, 2004).

The mixture was loaded on a C-18 HPLC analytical column which was then eluted using method 1. 2-*S*-(2-thiopyridyl)-6-hydroxynaphthyldisulfide eluted at 31 minutes while the unreacted 6-hydroxy-2-naphthyldisulfide eluted later at the 34th minute as shown on the figure 3.2. The excess 6-hydroxy-2-naphthyldisulfide can be collected and recycled by freeze-drying.

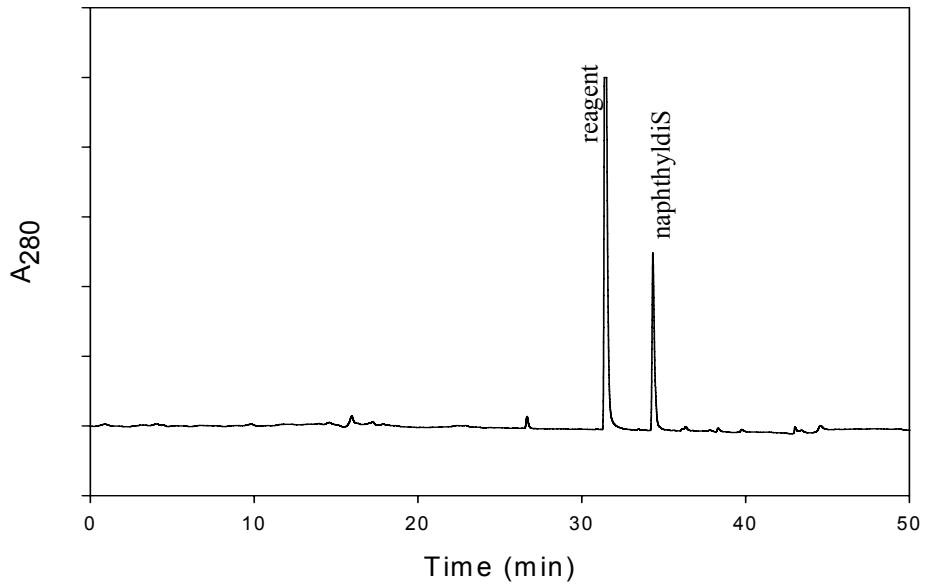

Figure 3.2: Analytical HPLC elution profile showing the reagent,
2-*S*-(2-thiopyridyl)-6-hydroxynaphthyldisulfide that is formed from the reaction of 2,2-dithiodipyridyl and 6-hydroxy-2-naphthyldisulfide (naphthyldiS). The reagent eluted at 31 minutes while the unreacted naphthyldiS eluted at 34 minutes.

2-*S*-(2-thiopyridyl)-6-hydroxynaphthyldisulfide clearly reacts specifically with MSH as it is evidenced by the formation of a prominent peak of MSSNaph eluting at 19 minutes in figure 3.3. At the end of the reaction of the *M. smegmatis* extract with 2-*S*-(2-thiopyridyl)-6-hydroxynaphthyldisulfide, several compounds were present in the mixture. Pyridine-2-thione eluted within 5 minutes at 5% acetonitrile followed by an uncharacterized peak at about 15th minute. This peak could possibly be attributed to the formation of either CoASSNaph or CysSSNaph. 2-thiopyridyldisulfide eluted at 27 minutes while excess 2-*S*-(2-thiopyridyl)-6-hydroxynaphthyldisulfide and 6-hydroxy-2-naphthyldisulfide eluted at 31 and 34 minutes respectively.

Based on the fact that the estimated amounts of the thiols in the mycobacterial extract were almost in equal proportion to the reagent in the reaction mixture, it was expected that the reagent would be consumed in the reaction. However, the size of the MSSNaph peak that eluted at 19 minutes did not increase any further when the reaction was left to continue beyond 21 hours while the reagent was still present. This suggests that 2-*S*-(2-thiopyridyl)-6-hydroxynaphthyldisulfide reacts specifically with MSH and that the equilibrium had been reached. Other possibilities may be that some of the MSH may have oxidised to MSSM and hence could no longer be trapped as a mixed disulfide.

The formation of heterodisulfides containing the 2-thio-6-hydroxynaphthalene chromophore can be monitored either by TLC or injecting aliquots on HPLC, in each case without any need for derivatization. Because the heterodisulfides exhibit excellent chromatographic properties, the quantitation of MSSNaph can be followed by measuring the area of the peaks in the HPLC profiles. The method of isolating thiols by derivatizing mycobacterial perchlorate extracts with 2-*S*-(2-thiopyridyl)-6-hydroxynaphthyldisulfide was described by Steenkamp and Vogt, 2004, in which 11.5 μmoles was recovered as MSSNaph while 10.7 μmoles was recovered as pure MSH from 4.0 mg of *M. smegmatis* cells. This proved to be a reasonable yield compared to chemical methods which are costly and can take long to prepare while yielding only small amounts of MSH (Jardine *et al.,* 2002).

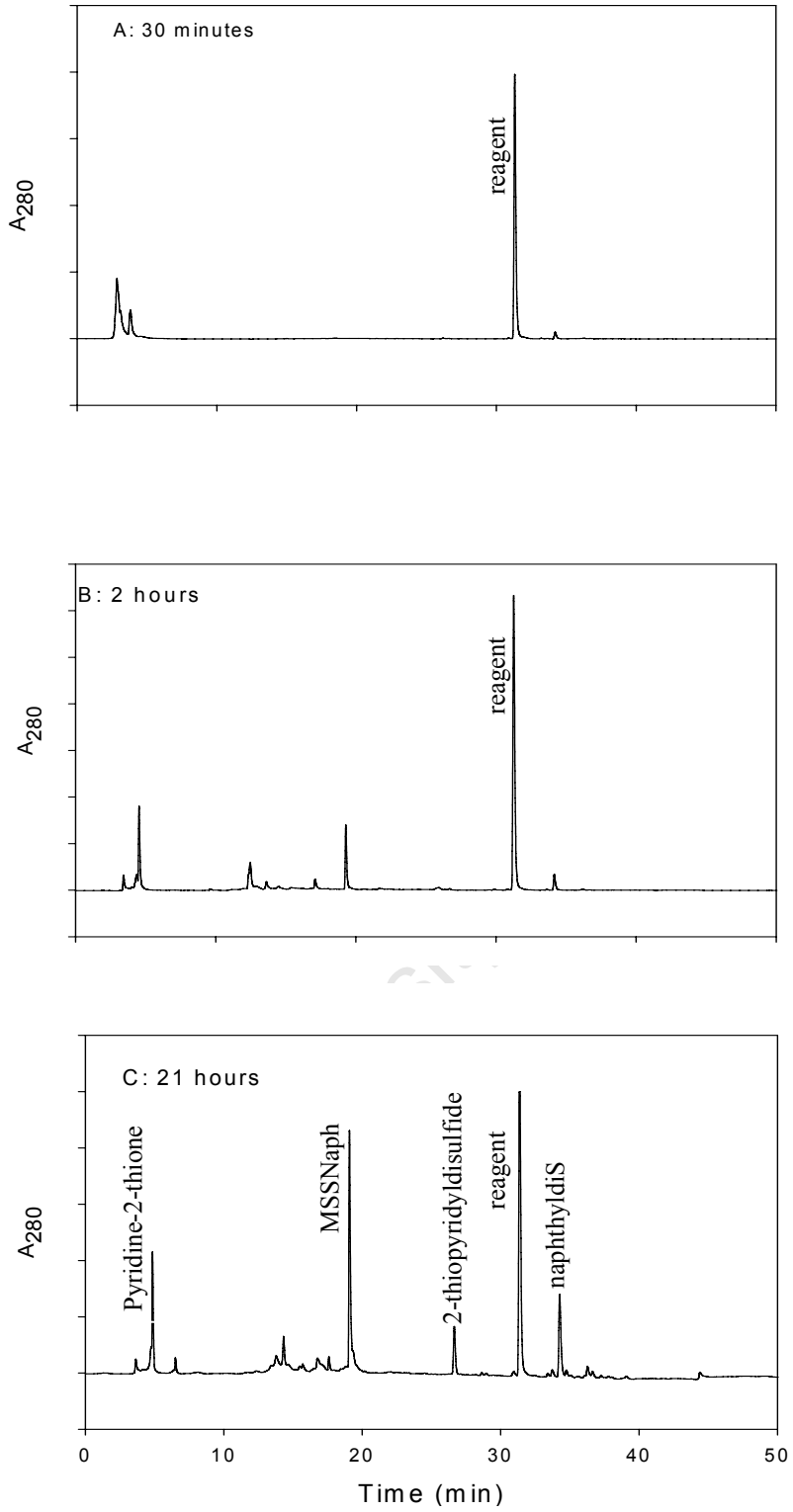

Figure 3.3: Analytical HPLC elution profile of a mixture containing perchlorate extract of *M. smegmatis* and 2-*S*-(2-thiopyridyl)-6-hydroxynaphthyldisulfide (the reagent). The reaction progress was monitored after 30 minutes, A; 2 hours, B and 21 hours, C. Method 1 was used for this analysis and MSSNaph eluted after 19 minutes.

The perchlorate extract of *M. smegmatis* grown to stationary phase in the medium described by Isabelle *et al.,* 2002, contained 462 μmols of 4,4-thiopyridyl reactive thiols from 138.7 g of cells. This was about twice the amount of thiols produced by the *M. smegmatis* cells utilized in the report by Steenkamp and Vogt, 2004, where 8.0 μmoles was obtained from 4.0 grams. The excellent amount of thiols in this work can be attributed to differences between the medium and conditions used during the fermentor growth as opposed to growth in shake culture.

The reaction of the perchlorate extract of *M. smegmatis* and 2-*S*-(2-thiopyridyl)-6-hydroxynaphthyldisulfide gave 137.5 μmoles of MSSNaph in 208 ml, about 30% recovery of the thiols initially present in the extract. Although, in addition to MSH, *M. smegmatis* contains other thiols such as free hydrogen sulphide, ergotheineine and coenzyme A[12], it is unlikely that these thiols could account for the 70% of thiols lost, as they are available in lower levels in the cells (Newton *et al*., 2006, Williams M.J, PhD Thesis, 2007).

Most of the product loss occurred during purification which involves several injections on HPLC preparative column where MSSNaph peak is separated from other eluates such as pyridine-2-thione, 2-thiopyridyldisulfide, 6-hydroxynaphthyldisulfide and the excess reagent as shown in figure 3.2.
Separation on an immobilized column packed with C-18 resin could overcome problems associated with poor yield of thiols. This method saves time and could allow the running of high volume of the mixture through the resin where the impurities can be separated from the desired compound by eluting with corresponding percentage of the solvent.

[12] MSH is over 10-fold more abundant than ergotheineine and hydrogen sulphide and about 6-fold more than coenzyme A (Newton et al,1996, Williams M.J, PhD Thesis, 2007).

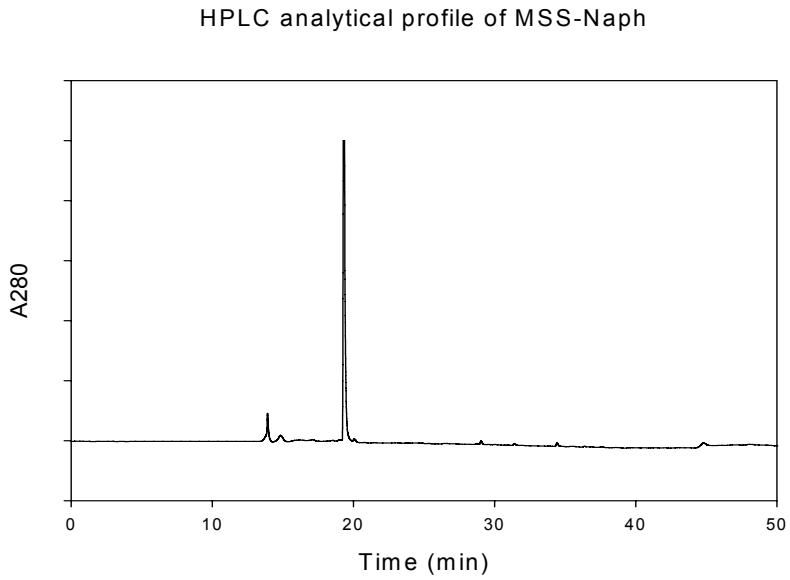

Figure 3.4: HPLC elution pattern showing MSSNaph at 19th minute.

MSH was obtained by reducing purified MSSNaph, shown in figure 3.3, with sodium borohydrate followed by acidifying the mixture with acetic acid. The mixture was separated on C-18 cartridges where hydrophilic MSH passes through while the apolar thionaphthol is retained. To get rid of ions such as sodium acetate, which formed when borohydride was destroyed with the acid, MSH that passed through the C-18 cartridge was run on a C-18 preparative column.

At the end, 120 μmols (58 milligrams)[13] of pure MSH was obtained from 138 grams of *M. smegmatis*. The yield is slightly higher than the estimation by Steenkamp and Vogt that it would require 250 g *M. smegmatis* to obtain 100 mg MSH (Steenkamp and Vogt, 2004).

Direct isolation and purification of thiols from natural sources is usually associated with problems such as oxidation, reversible oxidation to sulfinic acids as well as low concentrations of thiol species from cell-free extracts. The isolation of thiols is also complicated by their reactivity which result in undesirable addition reactions to aldehydes and activated double bonds.

To circumvent these problems thiols could be converted to less labile disulfide forms which can be concentrated selectively. Thus MSSNaph affords a form of MSH that is

[13] The molecular mass of MSH is 485 g/mol

stable to oxidation and the addition of alkylating agents. It is also considerably less hygroscopic than MSH and its disulfide form, MSSM.

3.3.2 Synthesis of Mycothiol-Bimane

mBBr is a highly efficient derivatizing agent with a broad application in biological procedures such as labelling of proteins, cells and thiols like GSH to form fluorescent derivatives (Kosower *et al.,* 1979). The separation method of mBBr-thiols derivatives with HPLC was reported by Newton *et al* in 1981 and is still used today (Newton *et al*., 1981). Mycothiol itself was also discovered as mBBr derivative by Spies and Steenkamp (Spies and Steenkamp, 1994).

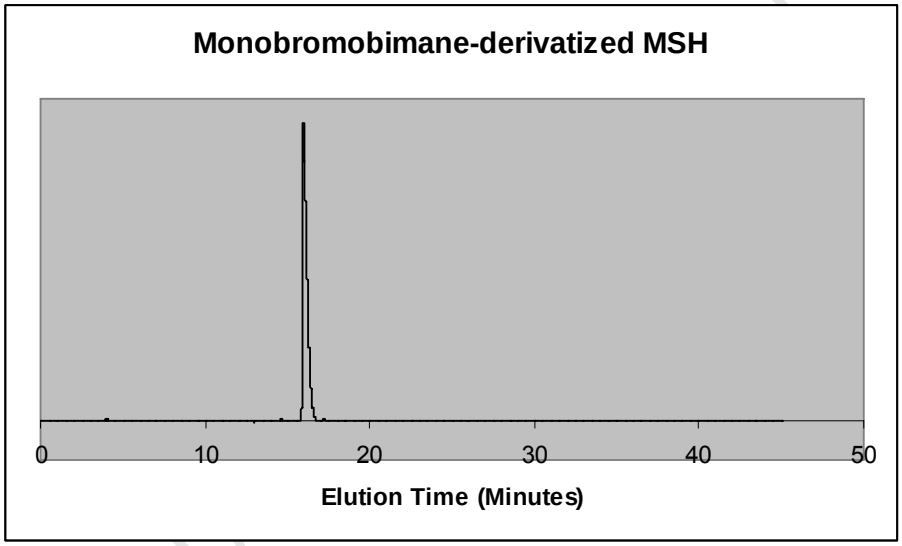

Figure 3.5: mBBr-derivatized MSH purified using Phenyl-Hexyl column on HPLC. Clear MSmB peak eluted at 17th minute.

MSmB (19.5 μmols) was synthesized by derivatizing 20 μmols MSH with 2-fold monobromobimane (mBBr) at pH 8.0. The complete derivatization was achieved within 30 minutes in the dark at room temperature, and the resultant MSmB eluted as a sharp peak at 17 minutes on the phenyl-hexyl analytical column eluted with method 1, figure 3.4. To get rid of excess mBBr which was still present in the mixture, the sample was run on a Vydac preparative column where the fluorescent peak was collected as pure MSmB.

MSmB is the best and most widely used substrate of mca not only because of its obvious benefit of low *K*m value, but because of its great separative characteristics on HPLC and fluorescence which makes it easily visible on the TLC under the UV light. The labelling procedures of thiols with mBBr are simple and can be carried out rapidly under physiological conditions (Kosower *et al*., 1979).

3.3.3 Investigation of different methods for GlcN-Ins synthesis

1-D-*myo*-inosityl-2-amino-2-deoxy-α-D-glucopyranoside (GlcN-Ins), a precursor in the biosynthetic pathway of MSH, was first synthesized chemically by Bornemann *et al*. In the same study it was reported that a cell-free extract of *M. smegmatis* catalyzes the ligation of cysteine, acetate and GlcN-Ins to produce MSH. In the absence of acetate, desacetylmycothiol, the precursor in the last step of MSH biosynthesis, accumulated in the reaction mixture indicating that MSH synthesis proceeds by sequential addition of cysteine and acetate to GlcN-Ins (Bornemann *et al*., 1997). GlcN-Ins can therefore serve as a starting point for the synthesis of several substrates needed to characterize MSH enzymes. Since the current study was also aimed at producing substrates for MSH enzymes, several methods to produce GlcN-Ins were investigated.

3.3.3.1 Trypsin-mediated Synthesis of GlcN-Ins from MS-thialysine

Trypsin is highly applied in enzymatic degradation of proteins into smaller peptides. This protease has high specificity, exclusively cleaving the C-terminal of arginine or lysine (Olsen *et al*., 2004).

Based on the proteolytic characteristics of trypsin, a method to synthesize GlcN-Ins was devised in which MSH was reacted with 10-fold bromoethylamine to form mycothiol-thialysine (MS-thialysine) conjugate, figure 3.6. Thialysine contains a functional group that mimics the structure of lysine, and could be cleavable by trypsin.

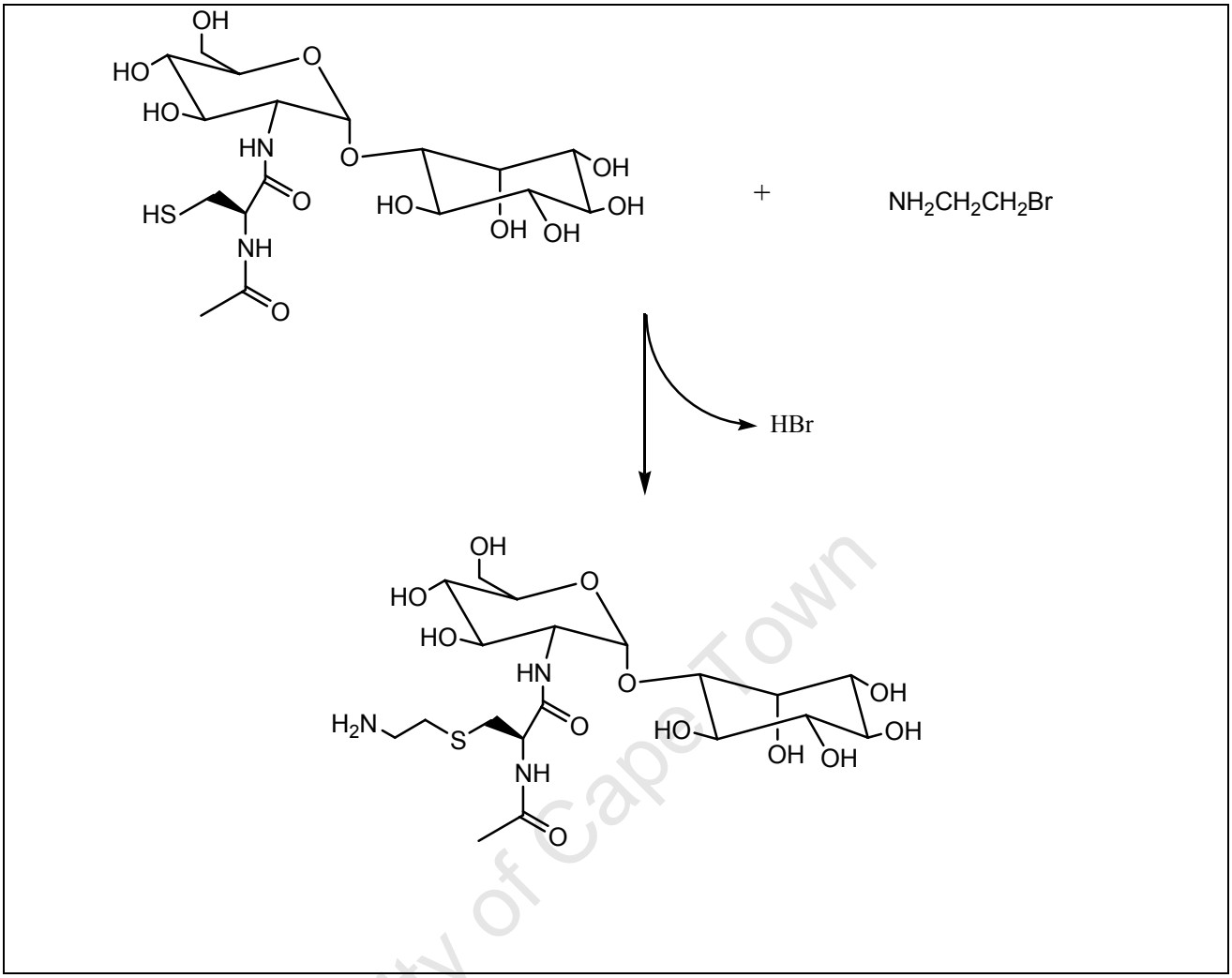

Figure 3.6: The reaction of bromoethylamine and MSH to form MS-thialysine. MS-thialysine has the functional group that mimics lysine and could therefore be cleaved by trypsin. HBr is released during the formation of MS-thialysine.

The HPLC elution profile of the bromoethylamine-MSH reaction is shown in figure 3.7, where MS-thialysine peak eluted after 21 minutes as judged by radioactive counting. The excess free reagent eluted as an off scale peak at 5 minutes. When trypsin was incubated with the mixture that contained thialysine, no GlcN-Ins formation was evident suggesting that the lysine moiety on the substrate was not a site of proteolysis for trypsin.

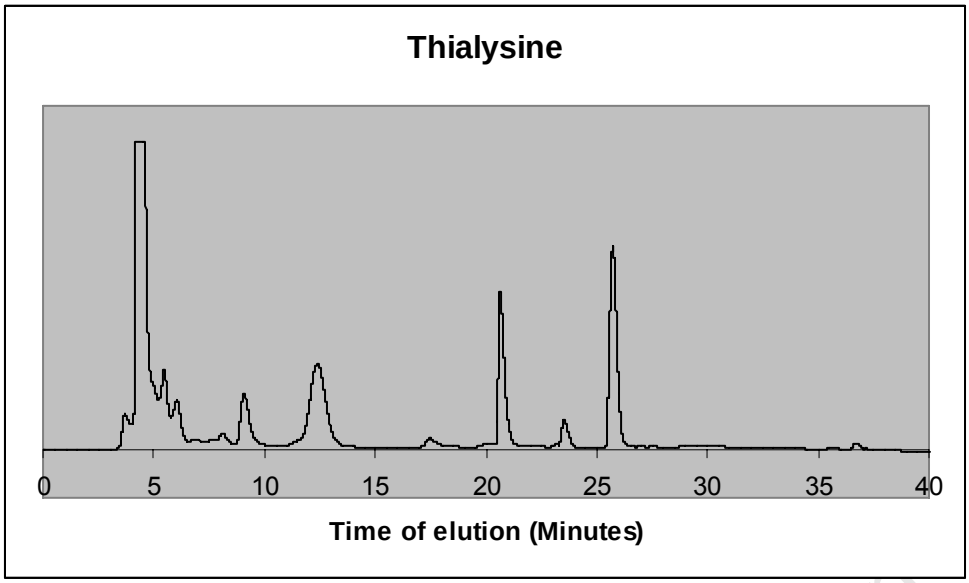

Figure 3.7: Formation of MS-thialysine from the reaction of MSH and excess bromoethylamine. MS-thialysine eluted at 21st minute. The cleavage of MS-thialysine was inhibited by abundant free bromoethylamine which eluted at 5 minutes.

It is well established that trypsin cannot cleave the C-terminal of a lysine or arginine that is followed by a proline (Keil, 1992). This indicates that trypsin cleavage can be affected by the nature of groups neighbouring the lysine, as it is also believed that the trypsin activity is suppressed by the presence of acidic residues on either side of the cleavage site (Rodrigues *et al*., 2008).

Accordingly, the disaccharide moiety of thialysine might have inhibited the proteolysis at the lysine cleavage site. On the other hand, it is possible that the presence of excessive free bromoethylamine in the mixture effected cleavage failure. To solve this problem, MS-thialysine should be purified first by HPLC. Thus, seeing that the production of GlcN-Ins by trypsin was not as quick and effective as expected, a different method was considered.

3.3.3.2 Hydrolysis of MSmB with *M. smegmatis* crude extracts

M. smegmatis cells which were radiolabelled with ^{3}[H]-*myo*-inositol during growth as described in general methods were lysed as described in section 4.2.1. After 50% overnight ammonium sulphate saturation, the crude extracts were run through G-60 desalting columns. The protein that eluted from these columns was used to hydrolyze

MSmB to GlcN-Ins and N-AcCys-mB as judged by the normal phase TLC analysis shown in figure 3.8.

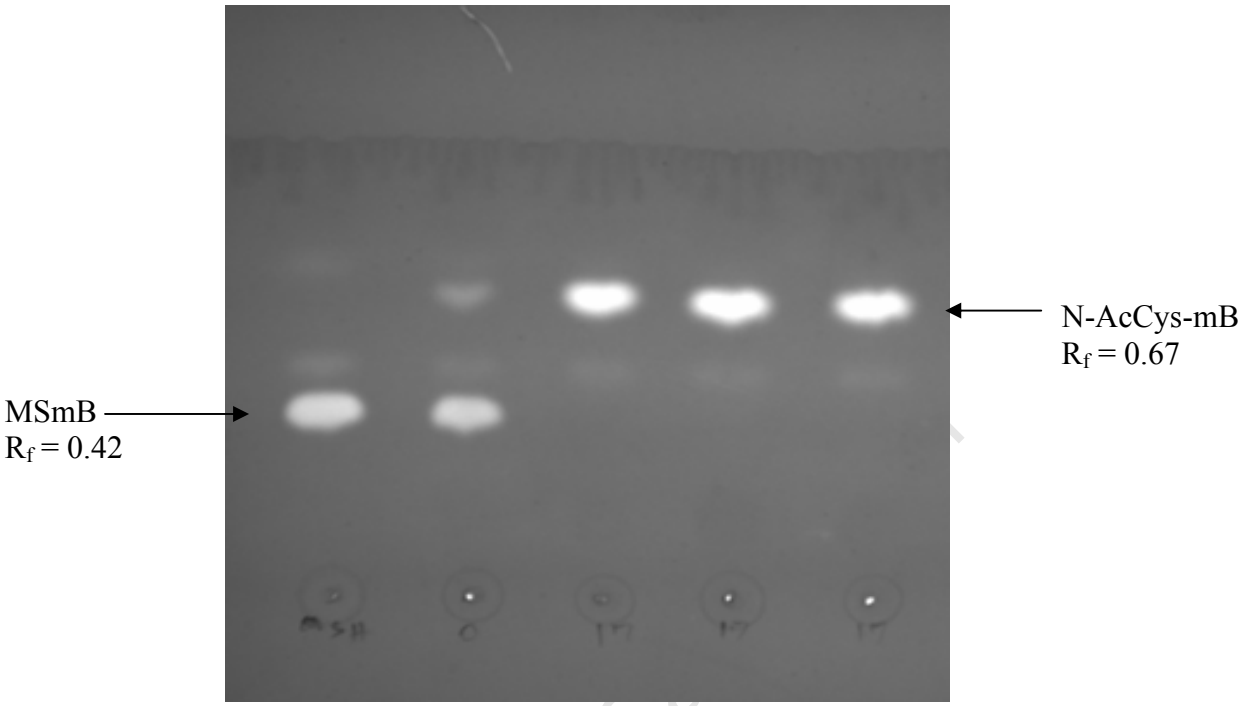

Figure 3.8: Normal phase TLC showing the hydrolysis of MSmB to form GlcN-Ins and N-AcCys-mB. The separation was carried out in a solvent system containing 2:1:1 of butanol:acetic acid:H_2O. In lane 1 is the MSmB before hydrolysis; lane 2 shows mixture of MSmB and *M. smegmatis* crude extract at time 0. All other lanes i.e, 3,4, and 5 show the product of the reaction after 17 hours of hydrolysis. GlcN-Ins, the other product of hydrolysis, is not visible in the TLC plate because it is not fluorescent.

From TLC results there was a complete conversion of the amidase substrate, MSmB, to the mercapturic acid, N-AcCys-mB. The spots of MSmB and N-AcCys-mB gave the R_f values of 0.42 and 0.67 respectively. Given that only samples attached to the fluorescent monobromobimane can be visualized on the TLC plate under the uv light, another method was needed to confirm the formation of non-fluorescent GlcN-Ins. Thus, the same enzymatic reaction mixture was injected on C-18 analytical HPLC column run at the rate of 0.8 ml/min and 0.8 ml aliquots were collected. The ^{3}H-radioactivity was determined on Beckman scintillation counter and the cpm (count per minute) units were exported and plotted on Microsoft-Exel.

Because the entire substrate was consumed in the reaction mixture as shown on TLC above, only GlcN-Ins was expected to have radioactivity. Indeed, the results in figure

3.9 confirm the presence of GlcN-Ins in fraction 17. Surprisingly, there was an extra peak which eluted in the 5th minute indicating that another radioactive compound was formed during the enzymatic reaction. Because polar compounds elute early on the reverse-phase resin, it was expected that the compound that eluted at 5 minutes should be highly polar and most likely inositol.

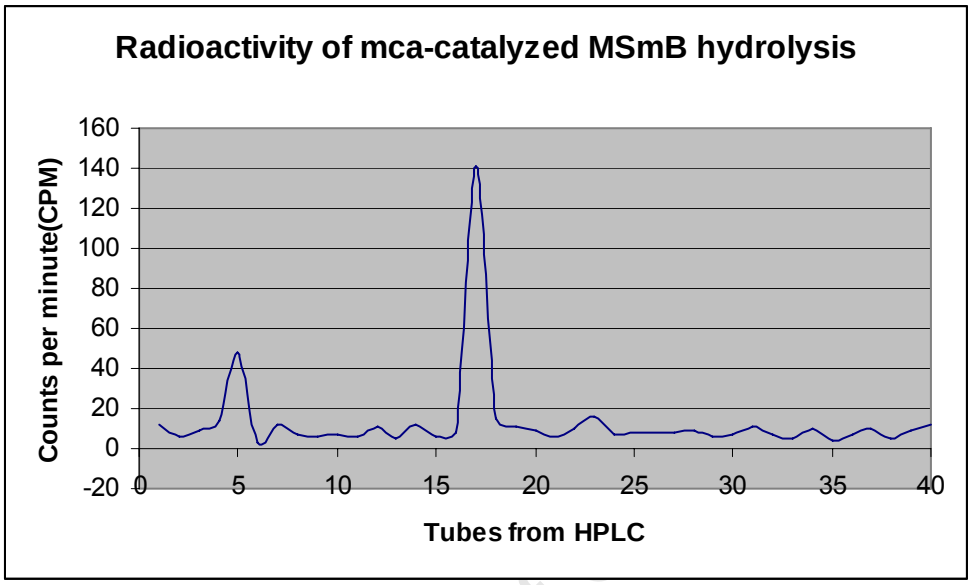

Figure 3.9: Radioactivity in the 17th fraction confirming the presence of GlcN-Ins after the hydrolysis of MSmB. The radioactive peak at 5th minute is free inositol which resulted from the glycosidase cleavage.

These results suggest that the release of free inositol during the hydrolysis of MSmB might have been due to glycosidase[14] activity present in the *M. smegmatis* crude extracts.

Although GlcN-Ins was produced using these crude extracts, substantial amount of yield was lost due to the release of inositol from both GlcN-Ins and MSmB. Thus, an extensive purification of mca was required to get rid of undesired proteins like the glycosidases.

[14] Glycosidases are enzymes which hydrolyze the glycosidic bond between two sugars.

3.3.3.3 Hydrolysis of MSmB with Amidase

The MSH *S*-conjugate amidase was purified with three different steps of chromatography, i.e, ion exchange, hydroxyapatite and size exclusion as described in chapter 4. 16.2 µmols of MSmB, 5.0 µmols Hepes buffer containing 1 µmol of Zn^{2+}, pH 7.5, and 1.54 mg of amidase in a final volume of 3.5 ml were incubated at 37 °C. At end of the reaction, as monitored by the TLC, the enzyme was deactivated by perchloric acid and discarded after centrifugation. The reaction mixture was applied to the SepPak C-18 cartridge. GlcN-Ins eluted with just water while the mercapturic acid was retained on the hydrophobic packing of C-18 cartridge. This method, which utilized purer enzyme, gave 15 µmols of pure GlcN-Ins (93% yield). A good yield of GlcN-Ins and the absence of free inositol at the end of enzymatic reaction indicate that the three-step purification of mca had been sufficient to separate mca from other proteins with a potential of yielding undesired results.
The successful synthesis of GlcN-Ins was a significant boost towards characterizing and inhibiting MSH enzymes, particularly mshB and mca which are the main focus of this project. GlcN-Ins is the product of both mshB and mca and can therefore be used as a standard for the assays of these enzymes; on the other hand, its acetylation produces the substrate of mshB.

GlcN-Ins can be reacted with sulfonyl chloride to form a sulfonamide which could be tested as mshB and mca inhibitor. Metaferia *et al* synthesized sulfonamides by attaching sulfonylchloride to the glycodic analog of MSH which contains cyclohexane instead of inositol and an S link in place of an O between two rings. Two of their compounds, 21 and 23, gave IC_{50} values of 90 and 120 µM against mca and 105 and 101 µM for mshB, respectively (Metaferia *et al.,* 2007).

The sulfonamides synthesized from GlcN-Ins could provide a clue about the significance of inositol in inhibitors. There is a precedence of inhibitors containing inositol, as it was found that the 2-deoxy-2-C-alkylglucosides of *myo*-inositol, inhibit the incorporation of ^{3}[H]-inositol by the whole cells of *M. smegmatis* into inositol-containing metabolites (Gammon *et al*., 2003).

3.3.4 Acetylation of GlcN-Ins to produce the substrate of mshB

Acetylation is the introduction of an acetyl functional group in to an organic compound, mostly, the substitution of an acetyl group for an active hydrogen atom. Acetic anhydride is the commonly used acetylating agent reacting with amines and free hydroxyls (Das *et al.,* 2007).

The acetylation of 5.0 µmols GlcN-Ins with two-fold acetic anhydride resulted in the formation of the Acetyl-GlcN-Ins, as confirmed by the disappearance of the amino group of GlcN-Ins. The HPLC results in figure 3.10 A, show the derivatized amino group of GlcN-Ins eluting at 24 minutes, while in B, the peak disappeared due to the complete acetylation of the amino group. The reagent, AccQ-Fluor, elutes as multiple peaks at 32 and 42 minutes, while the fluorescent by-product, 6-aminoquinoline (AMQ), eluted at 30 minutes.

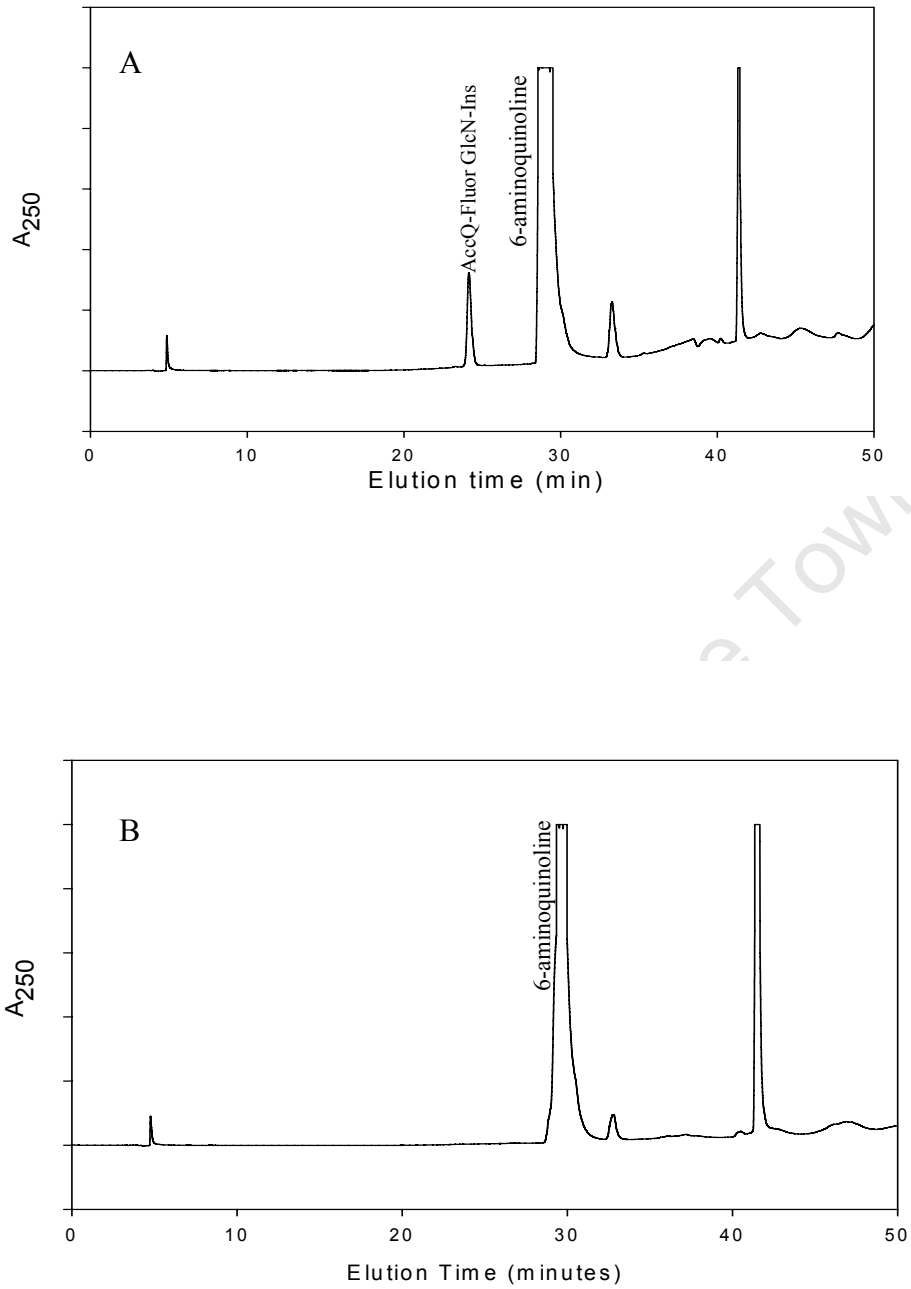

Figure 3.10: A. The HPLC elution profile showing the amino group of GlcN-Ins derivatized with AccQ-Fluor; the peak eluted at 24 minutes. B. After acetylation, the peak disappeared indicating that all the GlcN-Ins was converted to Acetyl-GlcN-Ins. The Samples were separated on the C-18 analytical column with method 2.

A previous synthesis of Acetyl-GlcN-Ins was reported whereby 10-fold acetic anhydride was used to acetylate GlcN-Ins (Anderberg *et al*., 1998). The disadvantage of substantial amount of acetic anhydride in a mixture is that when the amino group acetylation is complete, the excess acetylating agent can acetylate the hydroxyl groups

on the inositol and glucosamine rings. Thus, in order to avoid such effect, in the current study only two-fold acetic anhydride was used to acetylate GlcN-Ins. The successful acetylation of GlcN-Ins was important as the product of this step was required in reasonable yield to be able to evaluate a library of potential inhibitors against mshB.

3.3.5 Synthesis of sulfonamides as potential inhibitors

A successful synthesis of sulfonamides is indicated by the disappearance of the amino group of GlcN-Ins which is reacted with a sulfonyl chloride. GlcN-Ins was dissolved in sodium carbonate buffer and reacted with methanesulfonyl chloride. Aliquots were taken from the reaction mixture at 5 minutes intervals and derivatized with AccQ-Fluor. TLC and HPLC analysis of samples left to react up to 10 hours indicated that the reaction was unsuccessful. As part of optimizing reaction conditions, the amounts of the methanesulfonyl chloride were varied ranging from one to ten-fold relative to GlcN-Ins and yet no sulfonamide was formed.

Sulfonyl chloride derivatives are generally prone to hydrolysis in conjugation reactions, and methanesulfonyl chlorides, in particular, react with water and rapidly become unstable when exposed to aqueous environments (Lefevre *et al*., 1996).
The failure of the reaction could therefore be explained by the possibility that the methanesulfonyl chloride readily reacted with water in the sodium carbonate buffer faster than with the amino group of GlcN-Ins. As a result, several non-aqueous solvents such as DMSO, DCM and pyridine were tried in an attempt to dissolve GlcN-Ins but with no success.

It would be of great interest to evaluate GlcN-Ins-derived sulfonamides as inhibitors against mca and mshB, however this should start with identification of a relevant solvent in which to dissolve GlcN-Ins.

CHAPTER 4:

EXTRACTION, PURIFICATION AND INHIBITION OF MYCOTHIOL-*S*-CONJUGATE AMIDASE

4.1. INTRODUCTION

MSH forms *S*-conjugates cleavable by mca in the mycobacterial detoxification pathway which excretes drugs such as rifamycin and cerulenin from the cell as mercapturic acids (Newton *et al*., 2000b, Steffek *et al*., 2003). The mutant of *M. smegmatis* created by knocking out *mca* gene was more susceptible to electrophilic toxins such as N-ethylamalemide, iodoacetamide and chlorodinitrobenzene. The mutant was also found to be susceptible to oxidants such as menadione and plumbagin as well as to streptomycin (Rawat *et al*., 2006), indicating the protective role which mca serves in conjunction with MSH in the mycobacterial cells. Because of this role, mca inhibition has received significant attention from researchers in an attempt to discover new drugs for TB. Some naturally occurring extracts and substrate-mimic compounds have shown great promise as potential inhibitors of mca (Nicholas *et al*., 2002; Nicholas *et al*., 2003; Fetterolf and Bewley, 2004; Metaferia *et al*., 2006; Pick *et al*., 2006).

As part of ongoing efforts to identify more effective anti-tubercular drugs, one of the objectives in the current study was to evaluate novel structure-based chemically synthesized compounds as inhibitors of mca. This chapter, thus, focuses on the extraction, characterization with alternative substrate, MSSNaph, and inhibition of mca with the novel compounds.

4.2. METHODS

4.2.1. Cell lysis

50 grams *Mycobacterium smegmatis* was suspended in 160 ml of 50 mM Hepes buffer, pH 7.5, which contained 3 mM 2-mercaptoethanol and 0.1 Mm each of the protease inhibitors, TPCK, TLCK and PMSF. The cells were disrupted by sonication for 10 minutes with cooling on ice in 1 minute intervals and the mixture was clarified by centrifugation at the speed of 100 000g for 45 minutes at 4^0C. The pellet was discarded.

4.2.2. Ammonium Sulfate Saturation

The supernatant was brought to 15% saturation with ammonium sulphate by addition of the solid and incubated on ice for 1 hour. The mixture was centrifuged at 15 000g for 30 minutes at 4^0C. The pellet was discarded and the supernatant adjusted to 50% ammonium sulfate saturation and incubated overnight on ice. The mixture was centrifuged at 15 000g for 45 minutes at 4^0C, the supernatant was discarded and the pellet resolubilized in 120 ml of cold 50 mM Hepes, pH 7.5. A 1 ml stored with 20% glycerol at -80^0C for future assays.

4.2.3. Ion Exchange Chromatography

4.2.3.1. DEAE Cellulose column

DEAE resin was suspended in 0.5 M HCl and filtered on a Buchler funnel. The resin was washed with deionized water until the pH of the effluent was 7.0 and then with 100 mM and later 25 mM Tris-Cl, pH 8.0. The column was packed and equilibrated by elution with 5 volumes of 25 mM Tris-Cl, pH 8.0. 120 ml enzyme sample which had been dialyzed overnight against 25 mM Tris-Cl, pH 8.0 was loaded onto the column. The DEAE column (45 x 4.5 cm) was then eluted with a gradient from 25 mM NaCl in 25 mM Tris-Cl, pH 8.0 to 600 mM NaCl in 25 mM Tris-Cl, pH 8.0 at 48 ml/hour. 10 ml aliquots were collected and absorbance measured at 280 nm using an

Ocean Optics spectrophotometer. The elution profile was plotted from absorbance values against volume of eluent.

4.2.3.2. TLC and HPLC Assay of mca

Mca was assayed by following the appearance of the amino group of Gln-Ins, the product of amidase cleavage. Assay mixtures contained 54nmoles of MSmB, 0.25µmoles of Na-Hepes pH 7.5, 5nmoles of $ZnSO_4$ and the enzyme in a final volume of 20µl. The reactions were incubated for 1 hour at 37^0C. The reactions were terminated by the addition of 20µl of 5%TFA and 20µl of 100% acetonitrile. 2ul from each reaction mixture was spotted on Silica G-60 TLC plates and dried with a hair drier. The TLC plate was developed using butanol:acetic acid:water :: 4:2:2. MSmB and N-acetylcysteinylbimane migrated with Rf values of 0.42 and 0.67 respectively and were visualized with a UV lamp. Fractions which indicated the amidase activity were further analyzed by HPLC on a C-18 Reversed phase column using method 1 (See Chapter 2, p54). The activities for individual fractions were calculated and plotted to obtain a DEAE elution profile.

4.2.4. Hydroxyapatite

Active fractions from DEAE-Cellulose chromatography were pooled and concentrated by ultrafiltration using a membrane with 30 kDa exclusion limit. The concentrated enzyme preparation was dialyzed overnight against 10 mM potassium phosphate (KPi), pH 7.2 and was then loaded onto a hydroxyapatite column (2.2 x 30 cm) that had been equilibrated with 6 volumes of the starting buffer. The column was eluted with a 1000 ml gradient from 10 mM to 400 mM KPi, pH 7.2 at 48 ml/hour.
10 ml fractions were collected from the column and absorbance was measured at 280 nm wavelength. The elution profile was plotted from absorbance measurements versus volume of eluent. The active fractions were pooled together, concentrated by ultrafiltration and stored with 20% glycerol at -20^0C.

4.2.5. HPLC Biosep SEC-S2000

Active fractions were again concentrated by ultrafiltration and 100 µl mca was loaded onto a Biosep SEC-S2000 HPLC Column. The HPLC column was eluted with 100 mM KPi, pH 7.2 at 1 ml/min and all tubes assayed for activity.

4.2.6. Characterization of Mca

4.2.6.1. Activity of Mca with MSmB

Assay mixtures contained 5.65nmoles of MSmB, 0.1µmoles of Na-Hepes, pH 8.0, and the enzyme in a total volume of 80µl. The assay conditions were modified from those used for the TLC assays in section 4.2.3.2. $ZnSO_4$ was not added because the earlier experiments showed no change in the amount of mca activity with or without Zn^{2+}. Reaction mixtures were incubated at 37ºC for various lengths of time and the reactions stopped by the addition of 20µl of 0.5% trifluoroacetic acid and 20µl of 100% acetonitrile. A 2µl aliquot was spotted onto a Silica Gel G thin-layer plate which was then developed using n-butanol:acetic acid: water :: 4:2:2.

In the kinetic studies, the formation of N-AcCys-Bimane was quantified by HPLC. Reaction mixtures contained variable amounts of MSmB, 1.0 µmoles of Na-Hepes buffer, pH 8.0, and 7.7µg enzyme in 40 µl. Reactions were started by addition of the enzyme and were terminated after 10 mins by addition of 20µl of 5%TFA and 20µl of 100% acetonitrile. The mixtures were clarified by centrifugation and the supernatant were injected onto the HPLC column where method 1 was run.

4.2.6.2. Assessment of MSSNaph as a substrate of Mca

The formation of N-AcCys-Naph was quantified by HPLC. Reaction mixtures contained variable amounts of MSSNaph, 1.0 µmoles of Na-Hepes buffer, pH 8.0, 7.7µg of the enzyme in 80µl. Reactions were started by addition of the enzyme and were terminated after 10 mins by addition of 20µl of 5%TFA and 20µl of 100% acetonitrile. The mixtures were clarified by centrifugation and an aliquot was diluted 5-fold with 0.1%TFA before injection onto a Phenomenex phenyl-hexyl HPLC

column (250 x 4.6mm). Method 3 was run with the absorbance detector set at 280 nm. The amount of product formed was determined by measuring the difference the MSSNaph peak areas before and after the cleavage.

4.2.7. Mca inhibition reactions

MSmB which had been freeze-dried was dissolved in water to make 0.4 mM. 21 compounds, J1, J2, JDF1, JDF2, SP2, SP3, SP4, SP5, SP6, SP7, Th1, Th2, Th3, Th4, Th5, Th6, Th7, Vu1, Vu2, Vu3 and Vu4 were tested as inhibitors of mca. Each compound was tested in the presence of substrate and enzyme in a buffer. Assay mixtures contained 8.0 nmoles MSmB, 8.0 nmoles of an inhibitor and 1.0 µmoles of Na-Hepes buffer, pH 7.5, and 7.7µg mca in a final volume of 40 µl. The reaction mixtures were incubated for 10 minutes at 37 ^{0}C. 1.0 µmol NaCl was added to the assay reactions because the activities of mca with MSmB as a substrate were reported to be optimized at this level of ionic strength (Steffek *et al*., 2003).

The reaction was stopped by adding 20 µ1 acetonitrile and 20 µl 5.0% TFA. The mixtures were centrifuged for 3 minutes at 13 000 rpm and 75 µ1 of the supernatant was diluted four times with 0.1 % TFA and stored at -80^{0}C. 25 µl of the sample was injected into the Phenomenex phenyl hexyl C-18 HPLC column (250 x 4.6mm) which was eluted with method 1. The HPLC conditions were as described in general methods section. The inhibition percentage for each inhibitor was determined by calculating the amount N-AcCys-mB formed relative to the control reaction. For control reactions everything was added except the inhibitors.

4.3 RESULTS AND DICUSSION

4.3.1. Purification of Mycothiol *S*-conjugate Amidase

Mca from wild type *M. smegmatis* was partially purified 68-fold using a three-step procedure and the results are summarized in table 4.1. Dialysed ammonium sulfate fraction was loaded on DEAE cellulose column and eluted with 25-600 mM NaCl gradient.

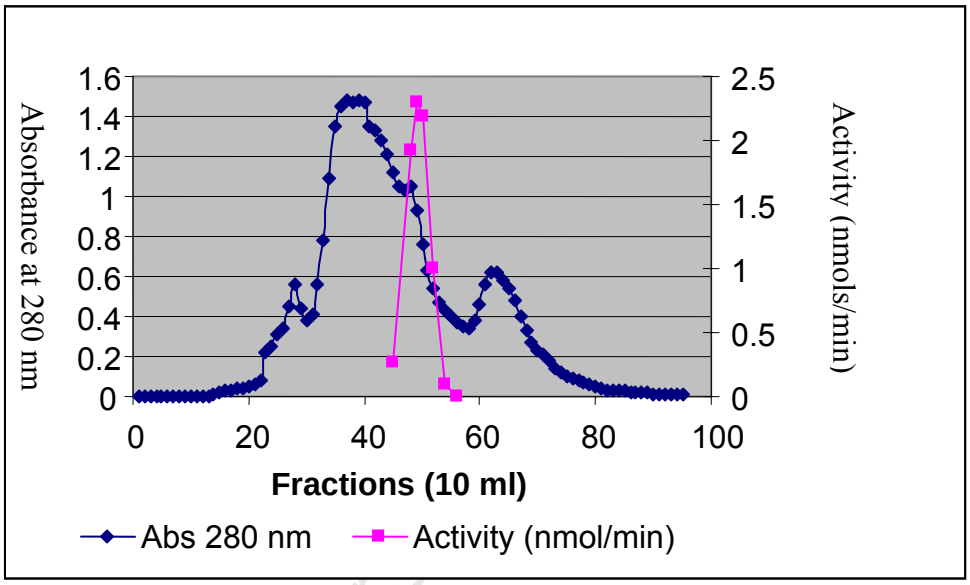

Figure 4.1: Elution pattern of mca eluted with 25-600 mM NaCl gradient on DEAE cellulose column.

The protein content from 10 ml gradient fractions is shown in figure 4.1 which also shows a band of activity spread between tubes 45 and 58. 59 mg of the protein with specific activity of 205.7 nmol/min/mg was generated in 138 ml from this purification step (table 4.1).

In view of the fact that the amidase activity eluted with the largest peak between tubes 30 and 60 where most of the bacterial protein content also eluted, more steps were required to further purify mca from other proteins present in the mixture (lane 3, figure 4.4). The active fractions were pooled, concentrated by ultrafiltration on an Amicon membrane with a 30kDa molecular size cut-off and dialyzed overnight against 10 mM Potassium phosphate (KPi), pH 7.2.

The enzyme preparation was then loaded onto a hydroxapatite column which had been equilibrated with the same buffer.

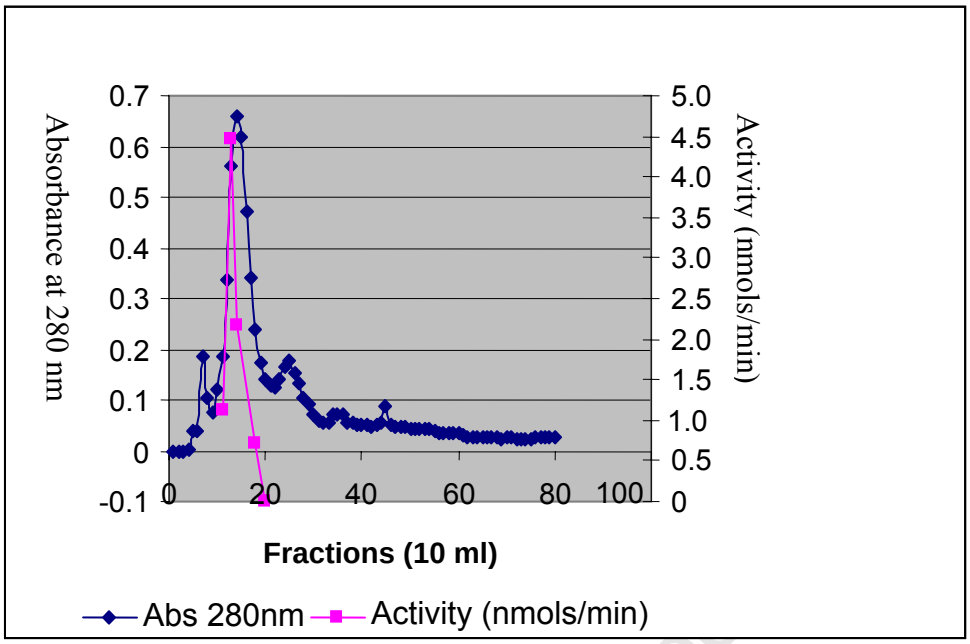

Figure 4.2: Amidase purification on Hydroxyapatite.

In the first isolation of mca from *M. smegmatis* by Newton and coworkers, DEAE 650C, phenyl sepharose and sephadex G-100 were used to purify the enzyme (Newton *et al*., 2000b). In the current work, hydroxyapatite was preferred in favour of phenyl sepharose because of a dramatic drop of activity encountered during the first purification attempt using the latter method. It was not surprising to lose activity during chromatography on phenyl sepharose, since partial denaturation of proteins during hydrophobic interaction chromatography is known to occur (Jungbauer *et al*., 2005).

Chromatography on hydroxyapatite was found to be useful in separating proteins which eluted in the first 10 fractions and between fractions 20 and 50 (figure 4.2). The amidase activity eluted in fractions 11 to 18 from which 27 mg of protein with a specific activity of 433 nmol/min/mg was recovered in 80 ml (table 4.1). Some activation of the enzyme occurred during purification as shown by increase of the total activity in the DEAE and hydroxyapatite step. In their work on mca from *M.*

smegmatis, Newton *et al* in 2000 also observed some activation, going through their DEAE and Phenylsepharose steps (Newton *et al*., 2000b).

Judged from the HPLC elution profile (figure 4.5), it seemed at this stage of purification that a glycosidase responsible for inositol cleavage, as dicussed in section 3.3.3.2, had been separated. Since the release of free inositol from MSmB was the main impediment, it appeared that the mca obtained from hydroxyapatite was sufficiently pure to be used for the synthesis of GlcN-Ins.

Table 4.1: Purification of Mycothiol *S*-conjugate Amidase (mca) from *Mycobacterium smegmatis*

Purification Step	Protein Concentration (mg/ml)	Volume of enzyme (ml)	Total Protein (mg)	Activity 3ul enzyme Assay (nmols/ min)	Total Activity (nmols/ min)	Specific Activity (nmol/mg/ min)	Purification Factor SA/SA 1
Extract	5,00	195 ml	975	0.0948	6162	6.32	1
50%AmSO4	21.8	20 ml	438	0.236	1576	3.59	0.57
Dialysis	15.6	19 ml	295.4	0.262	1662	5.63	0.89
DEAE	0.43	138 ml	59.1	0.264	12159	205.7	32
Hydroxyapatite	0.338	80 ml	27.07	0.45	12000	433	68

100 µl mca from hydroxyapatite was loaded onto a Biosep SEC-S2000 HPLC Column which was eluted at 1 ml/min with 100 mM KPi, pH 7.2. 1.0 ml aliquots were collected until 25 minutes and assayed for amidase activity, which eluted at the 8^{th} minute (figure 4.3).

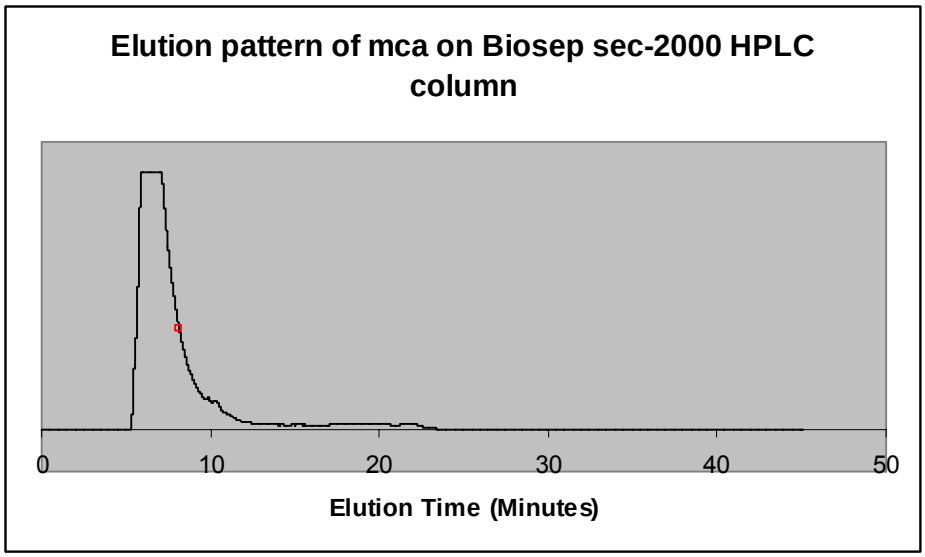

Figure 4.3: Elution pattern of 100 µl mca loaded on Biosep SEC-S2000 HPLC Column. The HPLC was run at 1 ml/min and all fractions assayed for activity. The activity was found in fraction 8 as indicated with a red dot in the chromatogram.

When analyzed by SDS-PAGE (which was performed as described in section 2.2.9 in the general methods), a significant separation was achieved on HPLC Biosep SEC-S2000 in which a dominant band was viewed at 36 kDa (lane 1, figure 4.4), corresponding to the molecular mass of mca (Newton *et al*., 2000b).

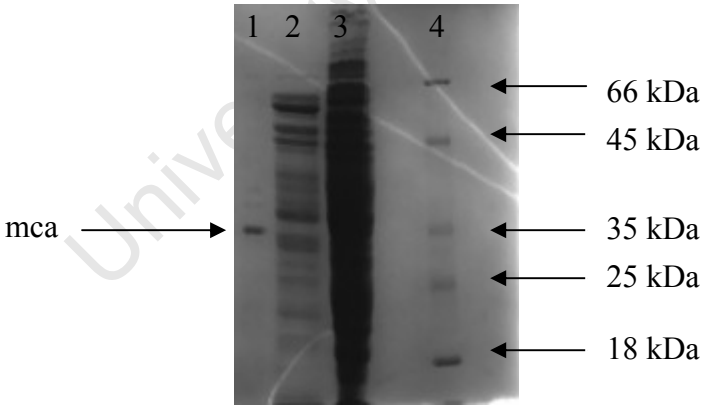

Figure 4.4: SDS-PAGE showing purification of mca from *M. smegmatis.*
The purification of mca is shown in lanes 1,2 and 3 corresponding to HPLC Biosep SEC-S2000, hydroxyapatite and DEAE cellulose, respectively. In lane 4 is the protein marker.

Judged by the HPLC analysis, the pure protein that eluted from Biosep SEC-S2000 gave significantly low levels of amidase activity, even after it was concentrated by ultrafiltration. Possible justification for the loss of activity may be that the HPLC and

the elution buffer, both at room temperature, were not set at optimal conditions for the enzyme activity. In some instances, during the assays of the activity, it was established in this study that extensive dilution of enzymes with water results in reduced activity. However, this effect was not expected with mca from Biosep SEC-S2000 since the dilution was done in the relevant buffer. Therefore, seeing that a lot of activity was lost in this step, the characterization of the enzyme was perfomed with the partially purified mca from the hydroxyapatite column.

4.3.2. Amidase activity assays

During isolation of the enzyme its presence in column effluents was ascertained by detection of the bimane derivative of N-acetylcysteine, as a product of the amidase cleavage of MSmB, by thin layer chromatography. MSmB and N-AcCys-mB migrated with Rf values of 0.42 and 0.67, respectively. For kinetic quantification, HPLC peak areas were used to determine the amount of product formed with reference to the standard curve constructed using N-AcCys-mB.

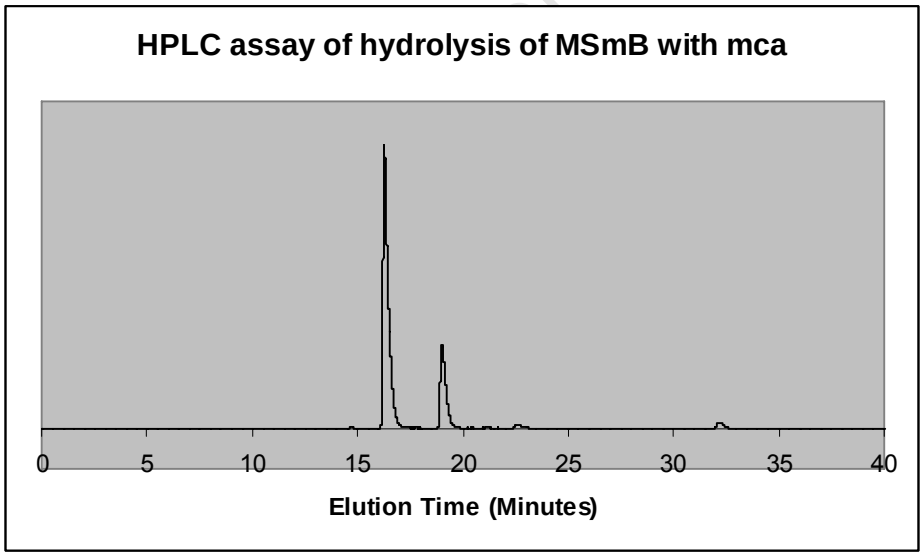

Figure 4.5: HPLC elution profile of MSmB after hydrolysis with mca.
On the reverse-phase column with method 1, MSmB and N-AcCys-mB eluted at 17 and 19 mins respectively.

Method 1 was run on a C-18 phenyl-hexyl analytical column at 0.8 ml/min with 0.1% TFA and 100% acetonitrile. Under these conditions MSmB eluted at 17 mins and the product, N-AcCys-mB at 19 mins.

4.3.3. Enzyme kinetics and substrate specificity

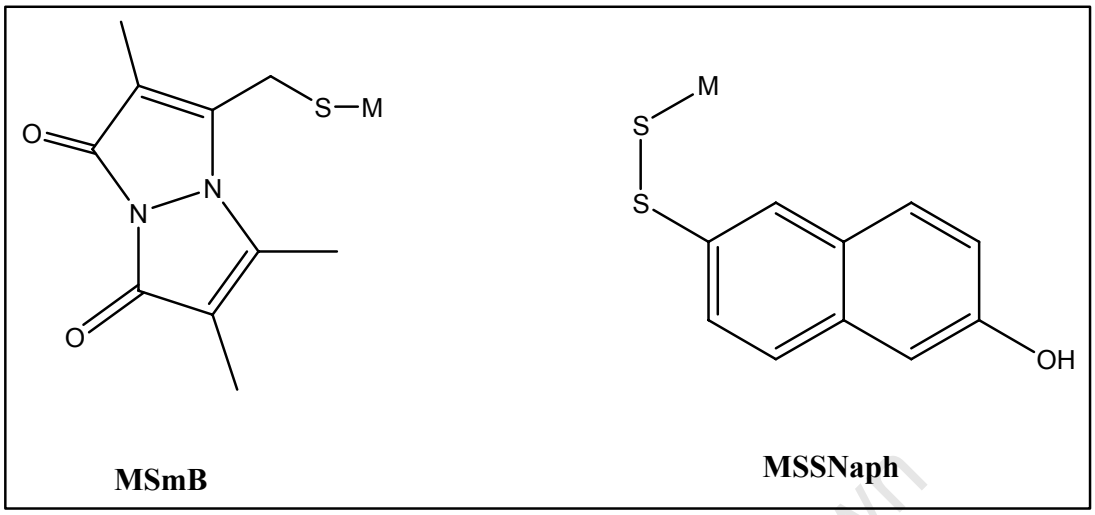

MSmB **MSSNaph**

Figure 4.6: Structures of bimane derivative of MSH, MSmB, and the heterodisulfide, MSSNaph.

4.3.3.1. Activity of mca with MSmB

Different values for the kinetic parameters of mca have been reported in the literature. The *K*m of mca from *M. tuberculosis* was almost two-fold higher than that reported for the same enzyme from *M. smegmatis* (Newton *et al*., 2000b; Steffek *et al*., 2003). In addition, the double reciprocal plots for the competitive inhibition of mca by bromotyrosine-containing natural products, compound 5 and psammaplysin A, in the presence of MSmB, intersected at the origin (Nicholas *et al*., 2002). This indicated that the *K*m value in their study would be different from the other two obtained in the studies by Newton *et al*. (2000) and Steffek *et al*. (2003). Kinectic parameters of MSmB cleavage with mca were reported to be sensitive to assay conditions, including temperature and the ionic strength (Steffek et al., 2003). The discrepancies may therefore exist due to different conditions used in different laboratories.

In the present study, the enzymatic assays were carried out at 37^0C in the presence of 50 mM Hepes and 50 mM NaCl, and the following kinetic values were obtained: *K*m = 187.6 ± 19.3 μM, *V*max = 64.2 ± 5.5 nmols/min/mg. The *K*m value is comparable to the 160 ± 40 μM previously obtained with the same conditions (Steffek *et al*., 2003).

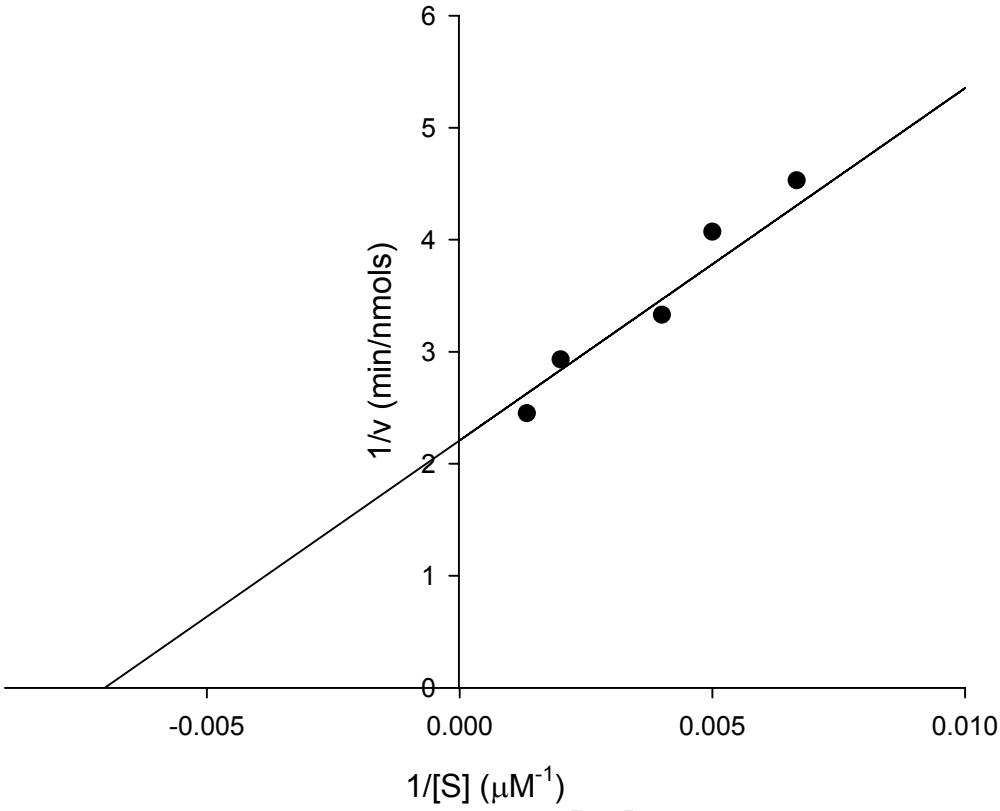

Figure 4.7: Lineweaver-Burk plot of mca with MSmB as a substrate.

4.3.3.2. Activity of mca with 2-S-mycothiolyl-6-hydroxynaphthyldisulfide

The evaluation of the heterodisulfide, 2-S-mycothiolyl-6-hydroxynaphthyldisulfide (MSSNaph) (figure 4.6) as a substrate of mca was carried out as described in the methods. The hydrolysis gave the two products, GlcN-Ins and N-AcCys-Naph, which are easily separated by means of SepPak cartridge. When analyzed by HPLC using Phenomenex phenyl-hexyl column and Method 3, MSSNaph eluted at 29 mins and the product, N-AcCys-Naph at 37 mins. The kinetic constants were determined from 5 substrate concentrations ranging from 88 to 350 μM using Lineweaver-Burk plot. The *K*m value was found to be 328 ± 22 μM, and the *V*max of 189.6 ± 33 nmols/min/mg.

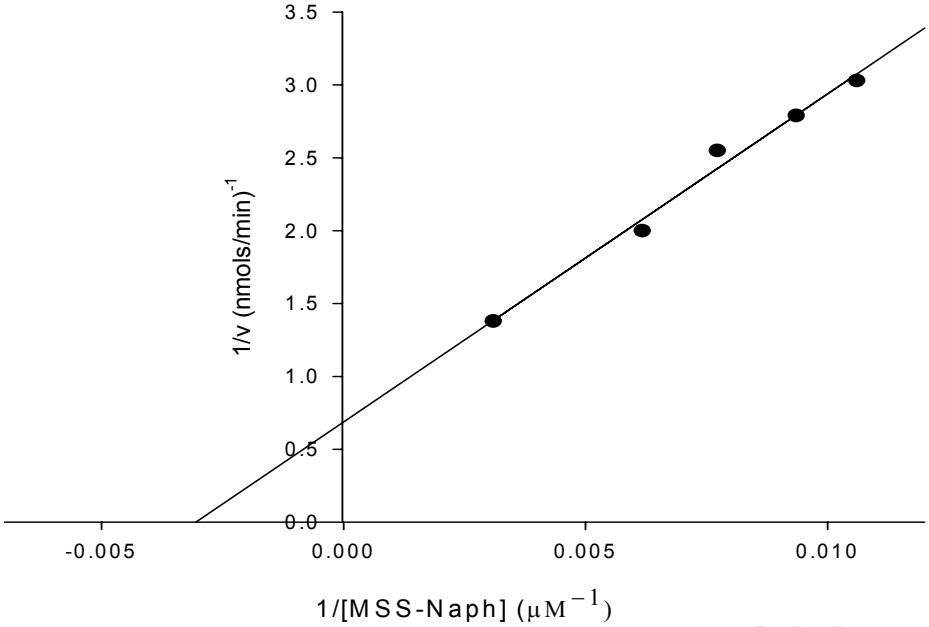

Figure 4.8: Lineweaver-Burk plot of mca with MSSNaph as a substrate.

MSSNaph is produced as a product of the thiol-disulfide exchange reaction in the first step of the preparation of mycothiol from natural sources (Steenkamp and Vogt, 2004). The synthesis of MSSNaph, as discussed in section 3.3.1, is simply achieved by reacting 2-*S*-(2-thiopyridyl)-6-hydroxynaphthyldisulfide with the perchlorate extract of *Mycobacterium smegmatis* followed by the purification on a reversed phase resin. It is, therefore evident that MSSNaph affords not only a convenient route to MSH by reduction, but also a convenient route to Gln-Ins by amidase cleavage using mca.

4.3.4. Inhibition of Mycothiol *S*-Conjugate Amidase

Table 4.2: Inhibition of Mca by Thioglycosides

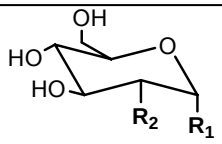

	R_1	R_2	Mca Inhibtion
J1	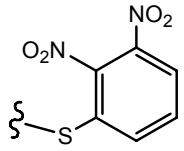	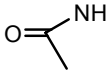	0%
A1120	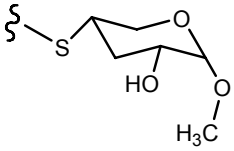	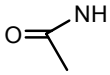	27%
JDF1	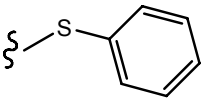	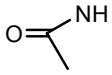	0%
JDF2	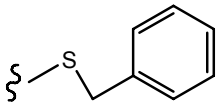	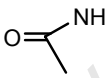	0%
SP2	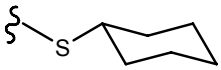	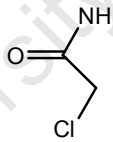	17%
SP3	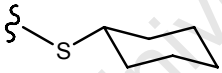		0%
SP4	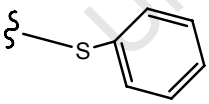		0%
SP5	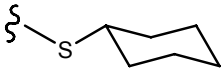	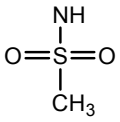	0%
SP6	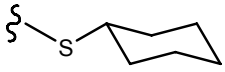	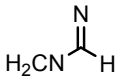	7%
SP7		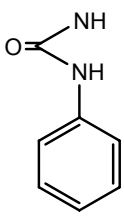	15%

Table 4.3: Inhibition of Mca by Naphthoquinones

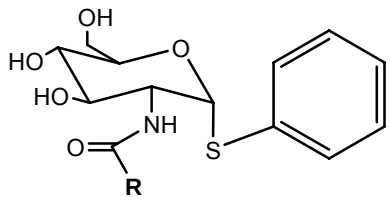

R	Mca Inhibition
Vu2 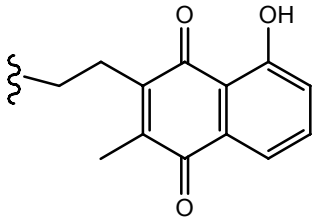	29%
Vu3 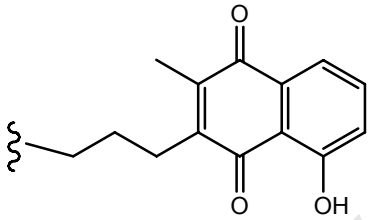	38%
Vu4 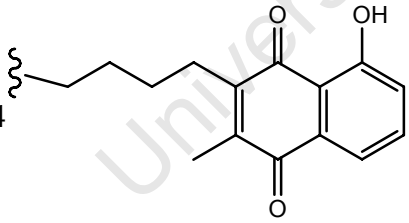	23%
Vu5 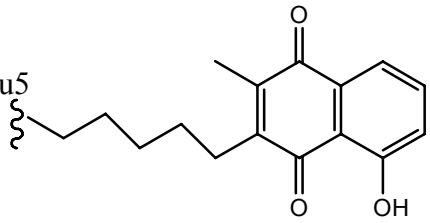	44%

Table 4.4: Inhibition of Mca by *O*-glycosides

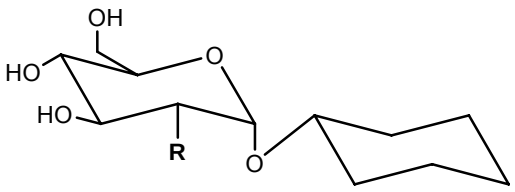

	R	Mca Inhibition
Th1 (β-linkage)	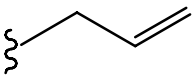	9%
Th2	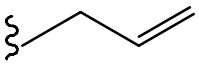	74%
Th3	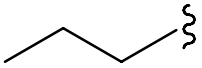	22%
Th4	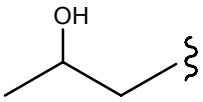	20%
Th5	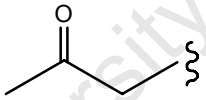	17%
Th6	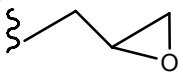	19%
Th7	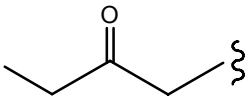	35%

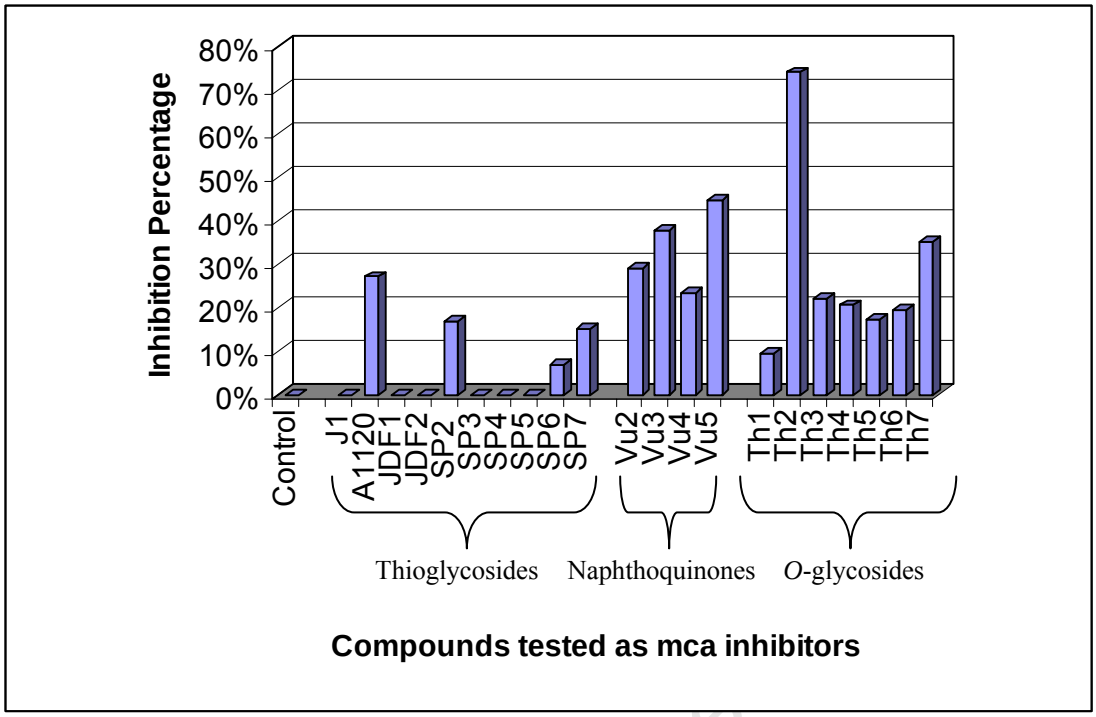

Figure 4.9: The inhibition of mca with MSH structural analogs.
Twenty one compounds were tested at 200 μM for inhibition of mca using HPLC assays. The experiments were performed in the presence of 200 μM MSmB. The bars represent the average of duplicate assays and the errors were within 10% of the indicated values.

A total of 21 chemically synthesized MSH analogs, grouped as thioglycosides, naphthoquinones and *O*-glycosides, were tested as inhibitors of mca at 200 μM using HPLC assays in presence of 200 μM MSmB as a substrate. Th2 exhibited the highest activity against mca giving 74% inhibition indicating that the substitution at position 3 of the glucose by an allyl group to form compounds like Th2 favours the binding of the scaffold to the mca active site. Nevertheless, Th1, which is similar to Th2 except that the cyclohexane is β-linked to the glucose moiety, exhibited poor inhibition of less than 10% against mca indicating that the α-linkage is preferable for the binding in the active site. The high inhibition exhibited by Th2 against mca clearly suggests an interaction with specific amino acids in the active site. Due to limited amount of the compound, further kinetic studies could not be carried out for Th2. Thus for future work, Ki determination and docking of Th2 in the active site of mca could establish its nature of inhibition.

The naphthoquinones, Vu5 and Vu3 which inhibited mca by 44% and 38% respectively, gave the second highest inhibition of mca after Th2, indicating that the quinone groups may be interacting with specific amino acids in the active site of mca. Also mca generally recognizes MSH conjugated to hydrophobic *S*-conjugates. So it is likely that the naphthoquinone motif, due to its hydrophobic characteristics, occupies the binding site where the *S*-conjugate of the natural substrate normally bind.

Because of the high homology and similarities in substrate preference between mca and mshB, the compounds tested as mca inhibitors were also evaluated against the activity of the deacetylase. The next chapter is therefore dedicated to the characterization and inhibition of mshB with chemically synthesized structure-based compounds.

CHAPTER 5:

EXPRESSION, PURIFICATION AND INHIBITION OF THE RECOMBINANT ACETYL-GLCN-INS DEACETYLASE

5.1. INTRODUCTION

Recently Metaferia and co-workers described the inhibition of mshB with natural product-inspired inhibitors which were grouped as heterocycles, amines and sulfonamides (Metaferia *et al*., 2007). The compounds tested by these researchers included structural features of groups which were previously shown to inhibit mca (Nicholas *et al*., 2003). These compounds inhibited mshB at micromolar concentrations, i.e, IC_{50} ranging from 105 to 7 μM and furher provide the basis for further development of more potent inhibitors against mshB (Metaferia *et al*., 2007). The synthesis of bicyclic thioglycoside mimics of N-acylated glucosamine has been described and these compounds were proposed to be potential inhibitors of the MSH biosynthetic enzymes (Slättegård et al., 2007). It remains to be explored whether these compounds are competitive inhibitors of mshB.

In the present study the structural analogs of Acetyl-GlcN-Ins were evaluated as alternative substrates of mshB. In addition a library of chemically synthesized structure-based compounds which include thioglycosides, naphthoquinones and *O*-glycosides were evaluated as inhibitors of mshB. The docking of best inhibitors to mshB is also reported.

5.2. METHODS

5.2.1. Induction of MshB

20 µL of *E.coli* BL21 pLysS glycerol stock was inoculated into 5 ml LB medium containing 34 µg/ml chloramphenicol and 50 µg/ml ampicillin. The cells were incubated at 37 ^{0}C on an orbital shaker until the OD_{600} reached 0.6. The cells were stored overnight at 4 ^{0}C and inoculated into 5 ml fresh medium containing the same amount of ampicillin and chloramphenicol.

The cells were then inoculated into 50 ml of the same medium and incubated at 37 ^{0}C until the $0D_{600}$ reached 0.6. IPTG was added to a final concentration of 0.4 mM and the incubation continued for 3 hours at 18 ^{0}C. Aliquots were withdrawn at 1 hour intervals for analysis. The flasks were placed on ice for 5 minutes and harvested by centrifugation at 5000 x g for 5 minutes at 4 ^{0}C. The supernatant was discarded and pellet stored at -80 ^{0}C.

5.2.2.1 Cell lysis

3.5 grams of induced *E.coli* BL21 pLysS cells were suspended in 20 ml of lysis buffer, which contained 50 mM NaCl and 1.0 mM each of the protease inhibitors, TPCK, TLCK and PMSF in 50 mM Hepes, pH 7.5. The cells were then sonicated on ice for 10 minutes while monitor the temperature at 30 seconds interval. The mixture was clarified by centrifugation at 15 000 g for 30 minutes at 4^{0}C and the supernatant was diluted twice with 25 mM Tris-Cl, pH 8.0.

5.2.2.2 Activity assay with Thin Layer Chromatography

The GlcN-Ins produced by deacetylation was determined using minor modifications of method reported elsewhere (Anderberg *et al*, 1998). 5 µl Acetyl-GlcN-Ins was alliquoted into 1.5 ml an eppendorf tube and 5 µl 20 mM Hepes buffer, pH 8.0 containing 5.0 µM zinc sulphate was added to each reaction mxture.
The derivatization with AccQ-Fluor was carried out as described in the general methods. 2 µl from each derivatized enzymatic reactions were spotted on the Silica

Gel TLC plates containing a 254 nm fluorescent indicator. The TLC was developed with 4:2:2 butanol:acetic acid:water and visualized under the UV light.

5.2.3. Ion exchange chromatography

DEAE sepharose column (45 x 4.5cm) was packed and equilibrated by washing with 6 volumes of starting buffer, 25 mM Tris-Cl, pH 8.0. 42 ml enzyme was loaded and eluted with 350 ml of 25 mM NaCl in 25 mM Tris-Cl, pH 8.0. And then with a 1 litre gradient from 25 mM to 600 mM NaCl in 25 mM Tris-Cl, pH 8.0. 9.0 ml fractions were collected. The enzymatic reaction was initiated by addition of 20 µl aliquots obtained from the fractions obtained from DEAE-sepharose. Every 5^{th} fraction was assayed until the 180^{th} fraction.

5.2.4. Immobilized Metal Ion Affinity Chromatography

Active fractions which eluted from the DEAE sepharose column were pooled and concentrated from 80ml to 18ml by ultrafiltration using a 30 000 daltons cutoff membrane. The preparation was then dialysed overnight against 1 litre of 50 mM phosphate buffer, pH 7.0 containing 0.5 M NaCl.

Iminodiacetic acid agarose resin was packed on to the column with the dimensions: 1.6 x 12.5 cm, and 50 mM $ZnSO_4$ was run through the column followed by equilibration with starting buffer, 50 mM phosphate, pH 7.0 containing 0.5 M NaCl. The preparation obtained from DEAE-Sepharose was applied to the column and washed with 75 ml of 1 mM imidazole in 50 mM K-phosphate buffer, pH 7.0 containing 0.5 M NaCl. The column was then eluted with a gradient from 1 to 20 mM imidazole in the starting buffer. Fractions were collected and assayed for protein by absorbance at 280 nm and for enzyme activity.

5.2.5. Size Exclusion Chromatography

The 32 ml fraction was ultrafiltered with 30 000 cut off membrane. The resultant 8.0 ml was loaded on Sephacryl 300 size exclusion column (95 x 0.9 cm) and eluted with 50 mM K-phosphate buffer, pH 7.0. 10 ml fractions were collected and the elution

pattern was plotted with absorbace at 280 nm. 7.0 ml of a pure mshB was mixed with 1.8 ml glycerol and stored at -20 ^{0}C.

5.2.6. *K*m determination of Acetyl-GlcN-Ins

Assay mixtures contained 1.0 µmoles of Hepes buffer pH 7.5, 1.0 µmoles of NaCl, 3.26 µg (2 µl of 1.63 mg/ml) of mshB and Acetyl-GlcN-Ins in a concetration range of 50-2000 µM in the final volume of 40µl. The mixtures were incubated for 10 minutes at 37^{o}C. The reaction was terminated by the addition of 20 µl acetonitrile and 20 µl 0.1% TFA were added to stop the reaction followed by the heating for 10 minutes at 60 ^{o}C. After cooling for 5 minutes on ice the mixtures were centrifuged for 3 minutes at 13 000 r.p.m. 70 µl of the supernatant was derivatized with AccQ-Fluor as described in the general methods. The samples were then analyzed by HPLC for Gln-Ins, as the AccQ-fluor derivative, using a C-18 column and method 2.

5.2.7. Evaluation of thiophenyl-containing compounds as mshB substrates

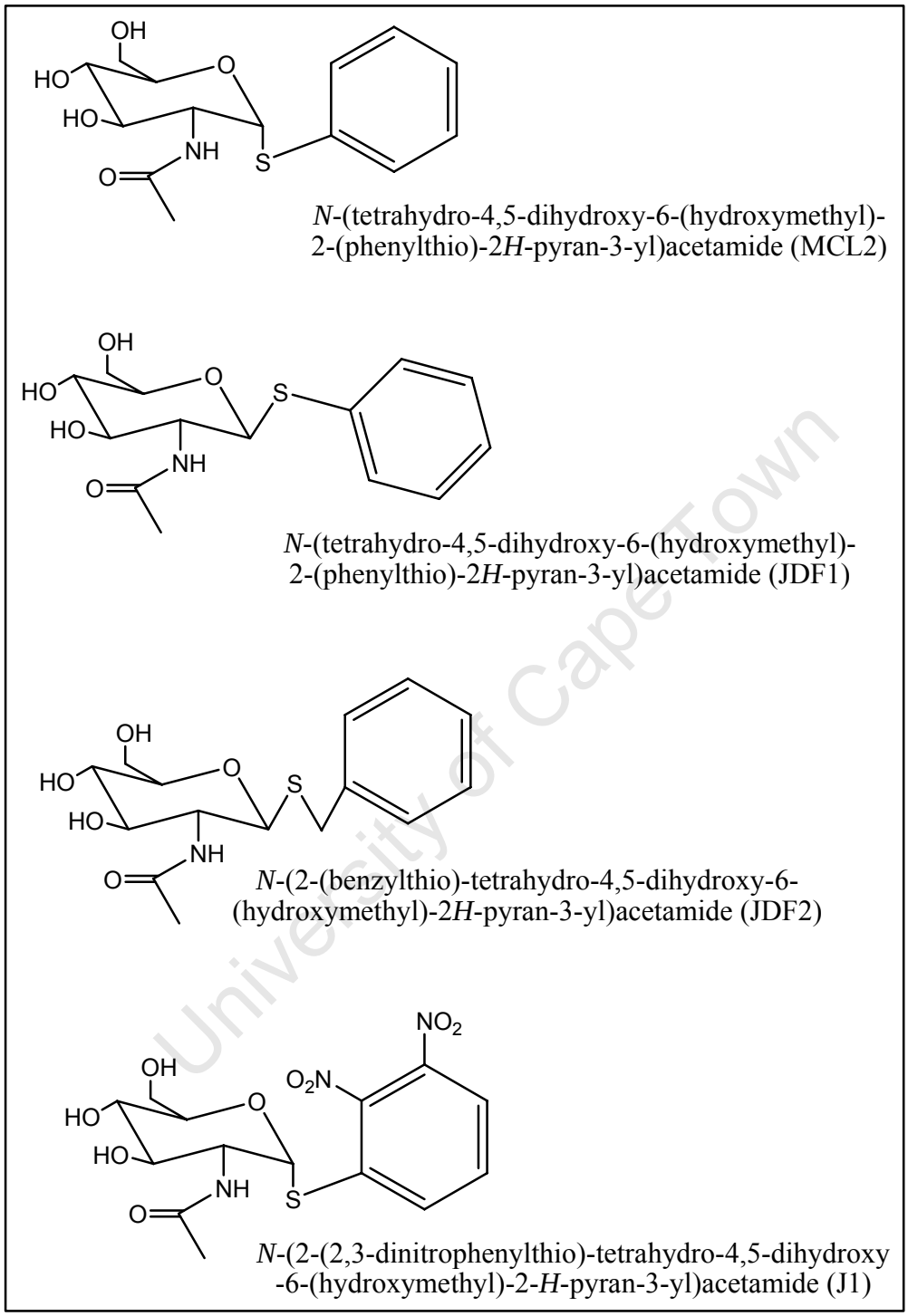

Figure 5.1: Compounds tested as substrates of MshB.

MCL2, JDF1 and JDF2 were chemically synthesized in the laboratory of Prof David Gammon, Chemistry department, University of Cape Town. J1 was synthesized in the laboratory of Dr Anwar Jardine, Chemistry department, University of Stellenbosch.

Stock solutions of MCL2, JDF1, JDF2 and J1 (5.0 mM of each) were prepared in 20% acetonitrile and distilled water. Each compound was evaluated separately as a substrate of mshB. For the compounds which were cleavable by the enzyme, the kinetic constants were determined by assaying at the following substrate concentrations: 250 µM, 500 µM, 750 µM, 1000 µM, 1250 µM, 1500 µM, 1750 µM and 2000 µM. The assay mixtures contained 1 µmol NaCl, 1 µmol Hepes buffer, pH 7.5, the substrate and 8.15 µg (5 µl of 1.63 mg/ml) of MshB in a total volume of 40 µl. The mixtures were incubated for 10 minutes at 37^0C.

The reactions were then terminated by addition of 20 µl TEA:acetic acid (0.088%:0.57%) and 20 µl of 100% acetonitrile and the samples were injected onto a Phenomenex Luna C-18 HPLC column (250 x 4.6mm) which was eluted using method 1. To quantify the amounts of product formed, the reactions were left to go to completion with known amounts of substrate to construct a calibration curve.

5.2.8. Evaluation of cyclohexane-containing compounds as mshB substrates

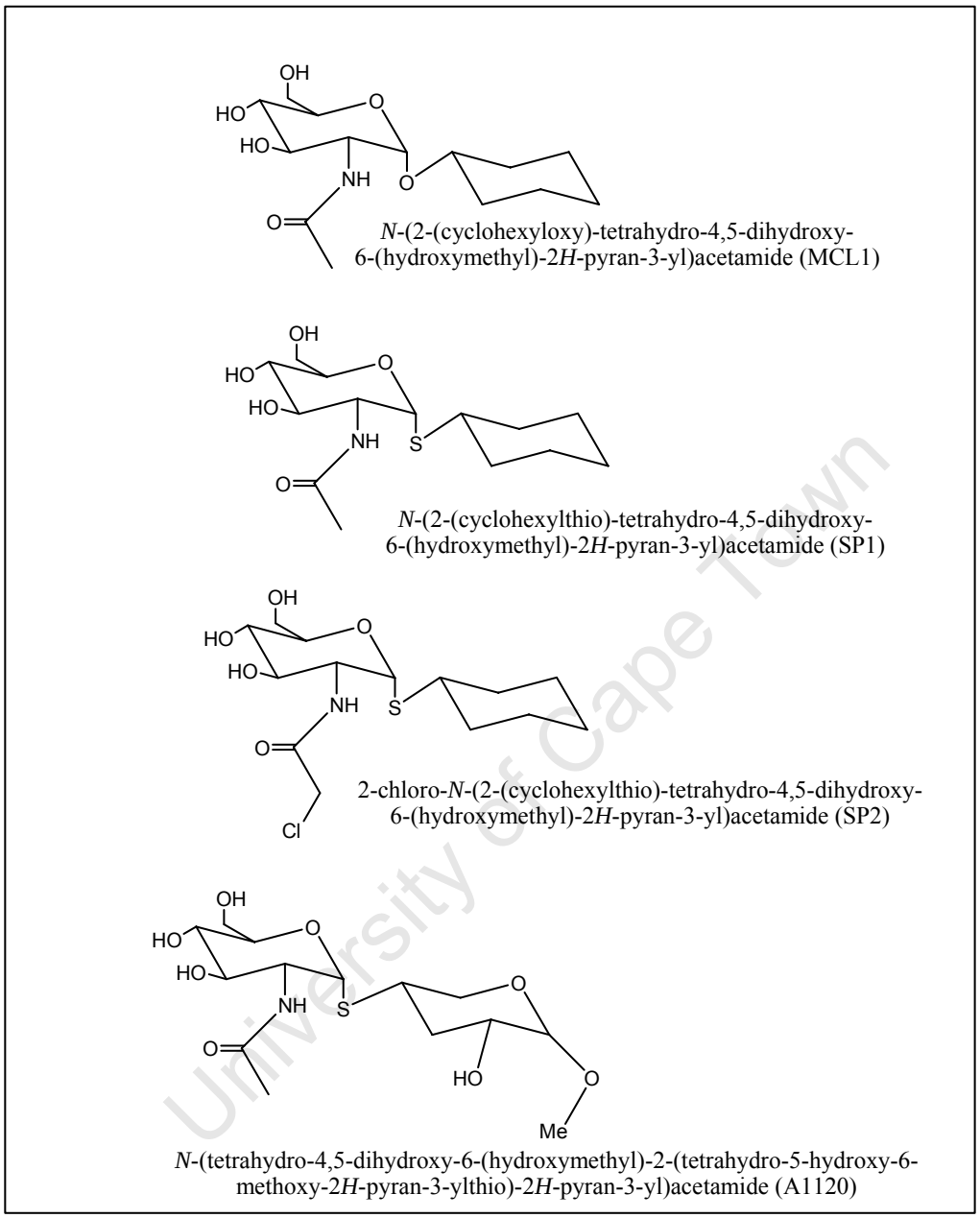

Figure 5.2: Compounds tested as substrates of MshB.

MCL1 was synthesized by Prof D. Gammon Chemistry department, University of Cape Town. SP1 and SP2 were chemically synthesized in the laboratory of Prof Spencer Knapp, Rutgers State University of New Jersey. A1120 was synthesized in the laboratory of Dr Anwar Jardine, Chemistry department, University of Stellenbosch.

Each of the cyclohexane-containing compounds, MCL1, SP1, SP2 and A1120 was evaluated separately as a substrate for MshB. The reaction mixtures contained variable substrate concentrations ranging from 150-2000 µM. The assay mixtures contained 1 µmol NaCl, 1 µmol Hepes buffer, pH 7.5, the substrate and 8.15 µg (5 µl of 1.63 mg/ml) of mshB in a total volume of 40 µl. The mixtures were incubated for 10 minutes at 37^0C. The reactions were terminated as described in section 5.2.7.
The dansylation reactions where carried out as described in the general methods. The column was eluted by running method 1 at a rate of 0.8 ml/min in which buffer A was TEA:acetic acid (0.088%:0.57%) and buffer B was 100% acetonitrile.

5.2.9. MshB Inhibition reactions

21 compounds, J1, J2, JDF1, JDF2, SP2, SP3, SP4, SP5, SP6, SP7, Th1, Th2, Th3, Th4, Th5, Th6, Th7, Vu1, Vu2, Vu3 and Vu4 were tested as inhibitors of mshB. In each reaction mixture, 5 µL of 1.63 mg/ml mshB, inhibitor at final concentration of 500 µM and the substrate, Acetyl-GlcN-Ins, also at final concentration of 500 µM were mixed with 1 µmol NaCl and 1 µmol Hepes buffer, pH 7.5 in a final volume of 40 µL. Mixtures were incubated for 10 minutes at 37^oC. 20 µL acetonitrile and 20 µL 0.1% TFA were added to stop the reaction followed by the heating for 10 minutes at 60 ^{o}C. After cooling for 5 minutes on ice the mixtures were centrifuged for 3 minutes at 13 000 rpm.

70 µL of the supernatant was mixed with 45 µL of 200 mM Hepes, pH 8.0, and 20 µL acetonitrile. After vortexing for 5 seconds 15 µL of 10 mM AccQ-Fluor was added to start the derivatization reaction. The mixture was vortexed briefly and left standing at room temperature for 1 minute followed by heating at 60 ^{0}C for 10 minutes. The samples were diluted 2-fold with distilled water and stored at -80 ^{0}C. 100 µL was injected injected on HPLC where method 2 was run. The inhibition percentage for each inhibitor was determined by calculating the amount of GlcN-Ins formed as an AccQ-Fluor derivative relative to the control reaction. Control reactions were treated the same way except for the addition of inhibitors.

5.2.10. Determination of Inhibition constants of MshB Inhibitors

The inhibtion constants (Ki) of compounds which gave more than 50% inhibition against mshB were determined by HPLC using the same procedure as in section 5.2.9. The inhibition assays were performed by keeping the enzyme concentration constant and varying the inhibitor concentrations. The Ki value for Vu2 was determined at the following inhibitor concentrations: 25, 50, 100 and 200 μM; and for Vu3 and Vu4, the inhibitor concentrations were 50, 100, 150 and 200 μM. For Vu5, the inhibitor concentration range was 10, 25, 50 and 100 μM. All assays were performed in presence of the substrate, Acetyl-GlcN-Ins, at the following concentrations: 50, 60, 80, 100 and 250 μM.

5.2.11. Docking of Inhibitors to MshB

The x-ray crystal structure of MshB (Maynes *et al*., 2003), was selected for docking of the inhibitors, Vu2 and Vu5. *In silico* experiments were performed using Accelrys Dicovery Studio 17 protocol.

5.3 RESULTS AND DISCUSSION

5.3.1. Expression of MshB

MshB was first cloned by Newton and coworkers in the expression vector pET16b, and found to be active in *E. coli* crude extracts. However, the protein lost activity during purification due to appearance of another smaller protein, 26 kDa, which was also found in elevated levels and was speculated to be a degradation product of the deacetylase (Newton *et al*., 2000). The degradation was circumvented when mshB was cloned to contain a C-terminal His-6 tag where a pure protein was obtained with 10-fold higher activity than the previous attempt (Newton *et al*., 2006).

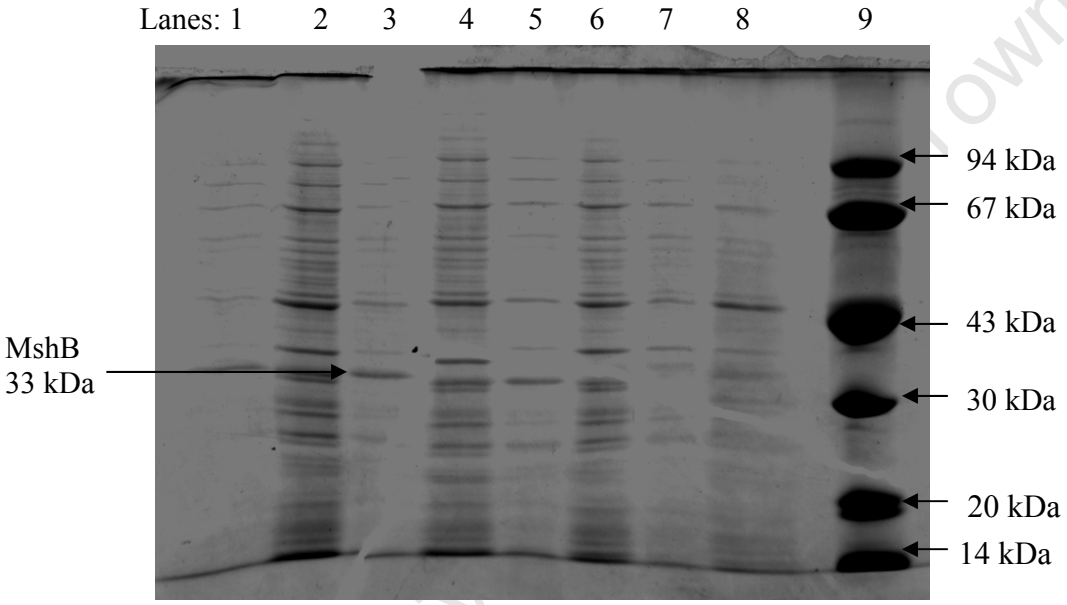

Figure 5.3: SDS-PAGE (prepared as described in section 2.2.9 in the general methods) of mshB before and after induction. The lanes 1 and 2 show the supernatant and pellet of samples induced with IPTG for 3 hours. Lanes 3 and 4 show the supernatant and pellet after 2 hour induction and 5 and 6 after 1 hour of induction. In lanes 7 and 8 is the supernatant and pellet of uninduced samples and the protein marker is in lane 9.

In the current study mshB, which had been cloned into the expression vector pET17b, was transformed into *E. coli* BL21 (DE3). After induction with IPTG for 3 hours the mshB band could be observed at 33 kDa on SDS-PAGE (figure 5.3)

5.3.2 Purification of MshB

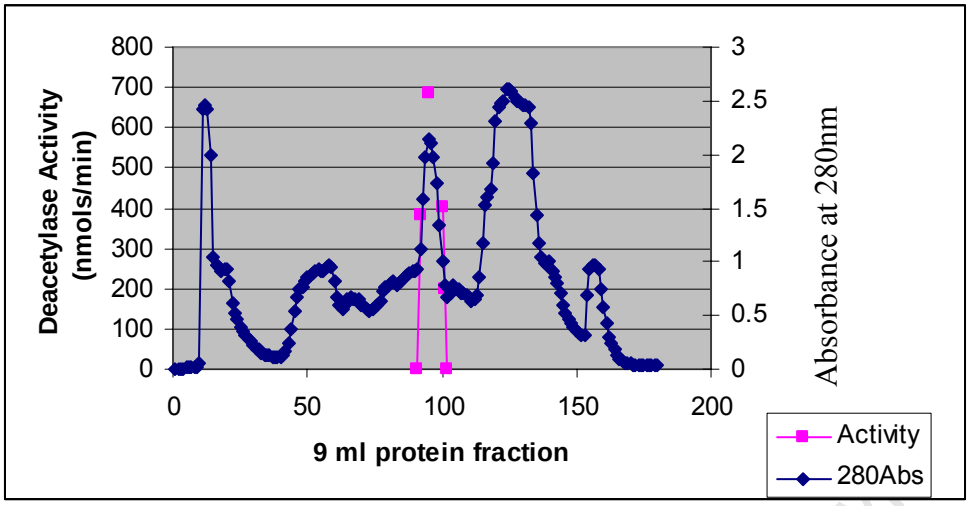

Figure 5.4: Elution of mshB from DEAE Sepharose column.

Recombinant mshB was purified 28-fold using a three-step procedure and the results are summarized in table 5.1. The crude extracts were applied to a DEAE Sepharose column and eluted with A 1 litre of a 25-600 mM NaCl gradient. The protein content from 9 ml gradient fractions is shown in figure 5.4 which also shows a peak of activity which eluted between fractions 92 and 101. The deacetylase cloned in the expression vector pET17b was previously reported to behave as a dimer (Newton *et al*., 2006), and in the current study an additional minor deacetylase activity was also found in a small peak from 103 to 110. However, only fractions from the sharp peak were pooled together for further analysis. From this purification step, 99.9 mg of protein with a total activity of 1321 nmol/min and the specific activity of 13.2 nmol/min/mg was obtained.

After overnight dialysis against 50 mM phosphate buffer, pH 7.0, containing 0.5 M NaCl, the enzyme was applied to a Zn-IMAC affinity column (1.6 x 12.5 cm) and eluted with 1 to 20 mM imidazole gradient.

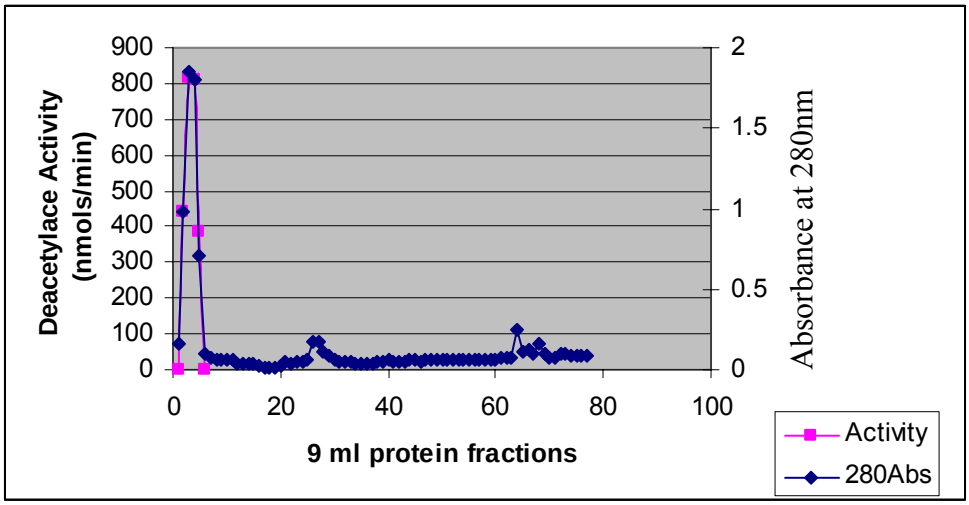

Figure 5.5: The elution pattern of mshB from IMAC column.
The protein content is plotted in blue and the deacetylase activity in red. The activity was found in fractions 2-6.

The deacetylase activity eluted in fractions 2, 3, 4, 5 and 6 (figure 5.5), indicating that the enzyme did not bind to the IMAC resin with Zn but eluted with 1 mM imidazole. The purity of these fractions was assayed by SDS-PAGE (figure 5.6, lanes 5-9) where a molecular mass of 33 000 Da was obtained. Although the fractions were still contaminated with *E. coli* proteins, the affinity chromatography proved useful in separating smaller peaks which eluted between fraction 25 and 30 as well as between fraction 63 and 65 in figure 5.5. 58.16 mg of protein with the total activity of 783.2 nmol/min and a specific activity of 13.5 nmol/min/mg was generated from this purification step.

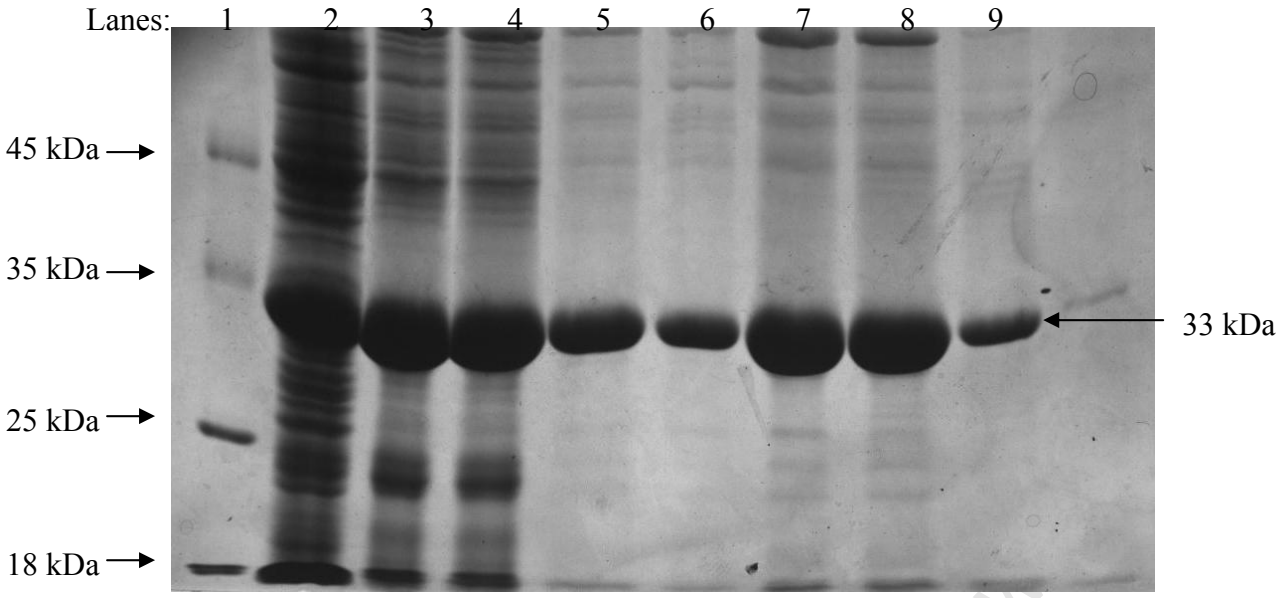

Figure 5.6: SDS-PAGE analysis of mshB with bands stained with Coomassie blue. Lane 1, protein marker; lane 2, crude extract; lane 3, DEAE sepharose before dialysis; lane 4, DEAE after dialysis against 50 mM phosphate buffer, pH 7.0, containing 0.5 M NaCl; lanes 5-9, IMAC active fractions 2, 3, 4, 5 and 6.

The active fractions from the IMAC coumn were pooled and concentrated by ultrafiltration to 8 ml which was loaded on Sephacryl S-300. The deacetylase activity was recovered in fractions 12 to 16 which corresponded to the only protein in the purification profile in figure 5.7.

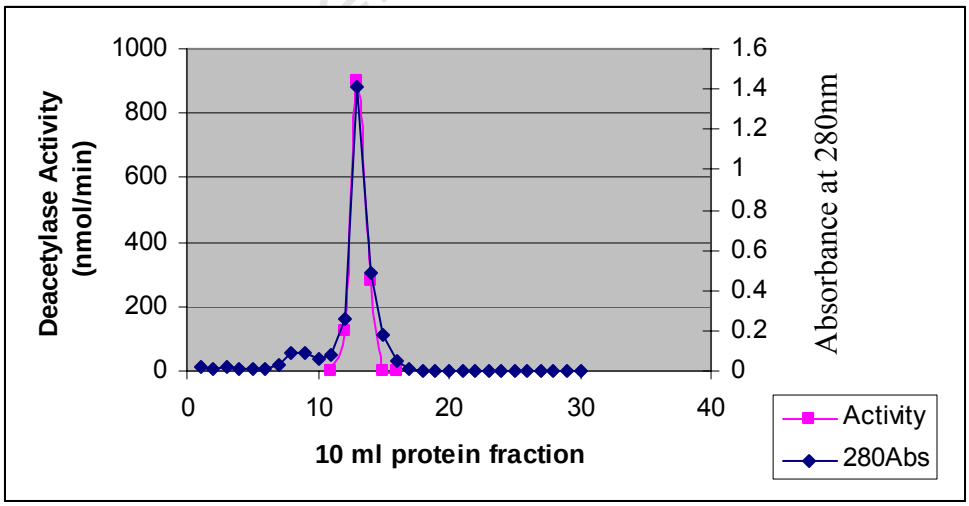

Figure 5.7: Purification of mshB on Sephacryl S-300. The activity, shown in red, eluted in fractions 12 to 16, coinciding with the only protein peak, shown in blue.

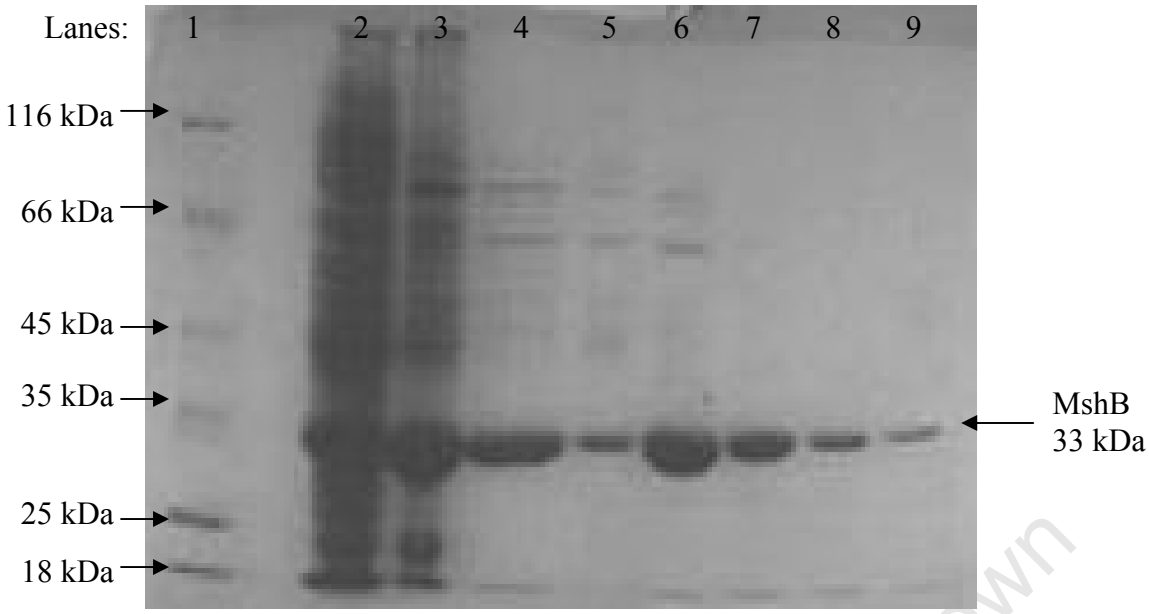

Figure 5.8: SDS-PAGE analysis of *M. tuberculosis* mshB.
Lane 1, protein marker; lane 2, crude extract; lane 3, DEAE sepharose; lane 4, IMAC; lanes 5-9, fractions 12, 13, 14, 15 and 16 from Sephacryl S-300.

SDS-PAGE analysis of fractions from Sephacryl S-300 showed that fractions 12 and 13 were still contaminated with E. coli proteins, but fractions 14, 15 and 16 gave a single band with molecular mass of 33 kDa, indicating that mshB was successfully purified (figure 5.8). The pure fractions were pooled and concentrated by ultrafiltration. The pure mshB was mixed with 20% glycerol and frozen at -20 ^{0}C. The purification of mshB is summarized in table 5.1. There was about 4-fold activation of the enzyme through IMAC and Sephacryl S-300. It is not clear what caused such activation but in their work during the purification of mca from *M. smegmatis,* Newton *et al* in 2000 also saw some activation, but by a factor of 1.5 going through their DEAE and Phenylsepharose steps.

Table 5.1: Purification of recombinant *M. tuberculosis* mshB

Purification Step	Protein Concentration (mg/ml)	Total Volume (ml)	Total Protein (mg)	Total Activity (nmols/min)	Specific Activity (nmol/mg/min)	Yield TA/TA1 %	Purification Factor
Crude Extract	9.88	40	395.2	2544	6.44	100	1
DEAE Sepharose	5.55	18	99.9	1321	13.2	51.9	2.05
IMAC	7.27	8.0	58.16	783.2	13.5	30.8	2.1
Sephacryl S-300	1.63	8.8	14.3	2587	181	101	28

5.3.3. Formation of GlcN-Ins following the deacetylation of Acetyl-GlcN-Ins

The deacetylation of Acetyl-GlcN-Ins with MshB was assayed by normal-phase TLC during purification of the enzyme and by HPLC for quantitative analysis as described in the general materials and methods (section 2.2.8.3). The scheme in figure 5.9 illustrates the derivatization of GlcN-Ins with AccQ-Fluor.

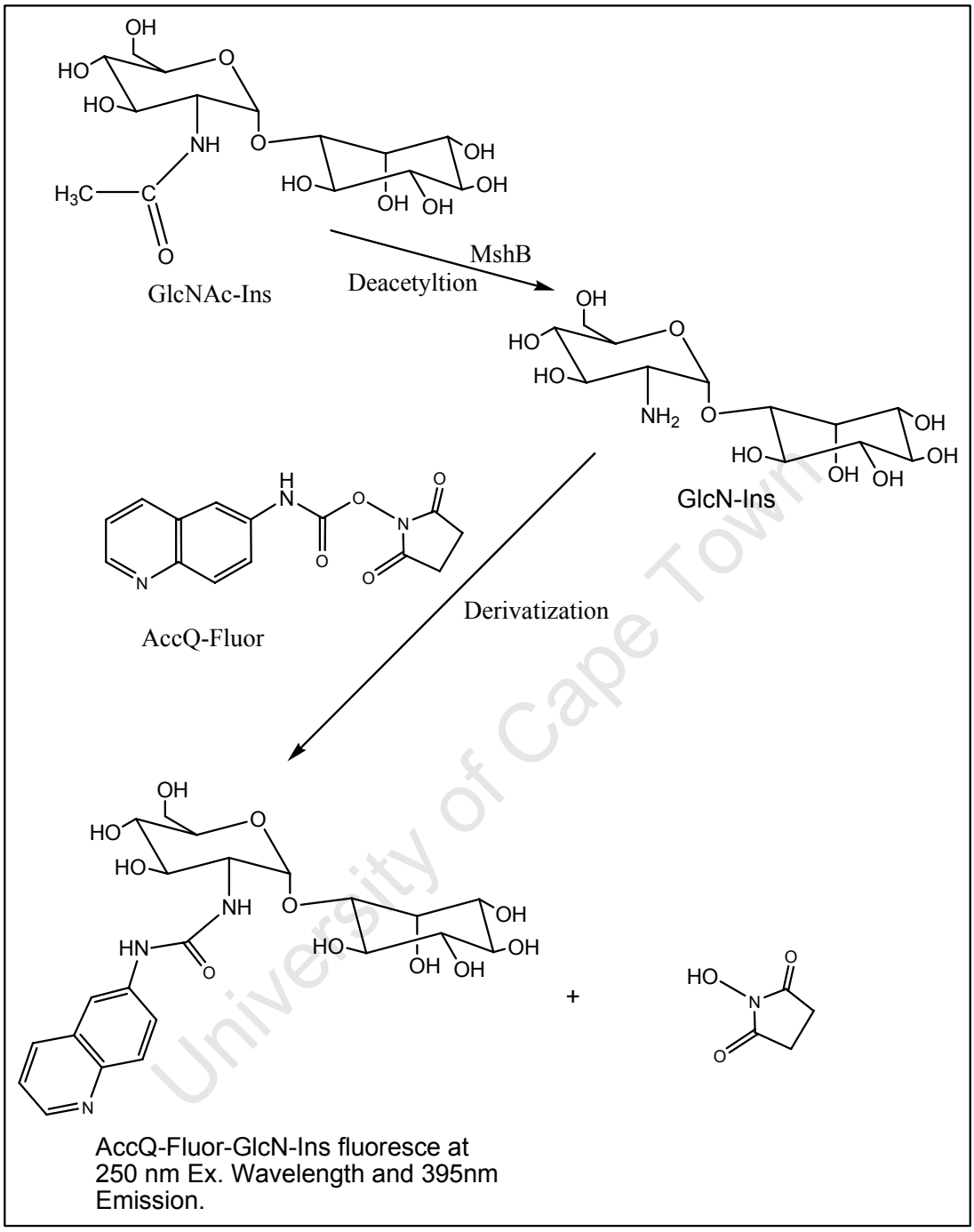

Figure 5.9: Acetyl-GlcN-Ins deacetylase (MshB) assay.

The product of the MshB cleavage, GlcN-Ins, is amino-derivatized with AccQ-Fluor to form a peak which absorbs at 250 nm on HPLC. N-hydroxysuccinimide is the other major fluorescent by-product released during the derivatization.

In a rapid, one step procedure at pH 8.0, AccQ-Fluor attaches to the GlcN-Ins amine group that is exposed after the removal of the acetyl moiety. The resultant GlcN-Ins-AccQ-Fluor derivatives were readily detectable on a reverse-phase HPLC column with excitation at 250 nm and emmision at 395 nm. Using method 2 on C-18 analytical column, the derivatized enzymatic product eluted at 24 minutes and the major fluorescent reaction by-product, AMQ, eluted at 30 minutes with free reagent eluting at 32 and 42 minutes (figure 5.10).

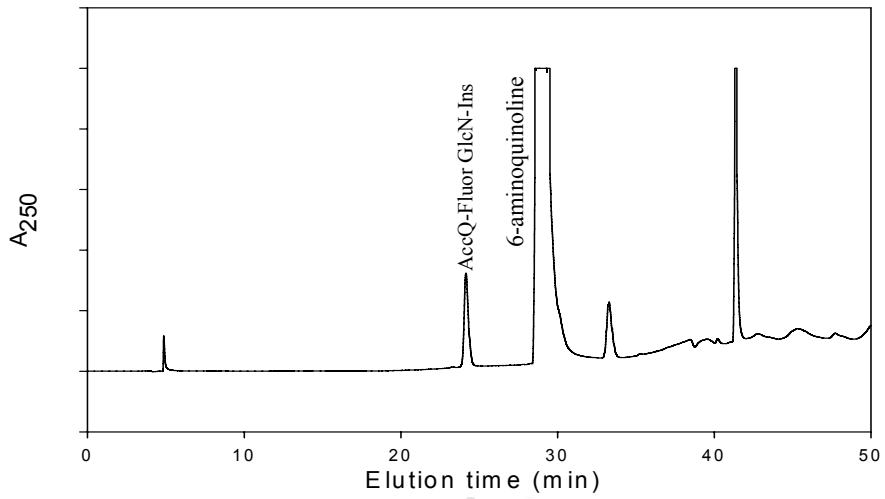

Figure 5.10: The HPLC elution profile of the AccQ-Fluor-derivatized GlcN-Ins.

The MshB deacetylation product, GlcN-Ins, is derivatized with AccQ-Fluor and elutes at 24 minutes. The other derivatization by-product, AMQ, elutes at 30 minutes while the excess free reagent elutes at 32 and 42 minutes.

5.3.4. Kinetic characterization of MshB with Acetyl-GlcN-Ins

The catalytic characterization of MshB with its natural substrate was carried out as previously described by Newton *et al.* (Newton *et al*., 2006). The deacetylation of Acetyl-GlcN-Ins was assayed at 6 substrate concentrations ranging from 50 to 2000 μM and the kinetic constants were obtained from the Lineweaver-Burk plot (figure 5.11). The values were as follows, *K*m = 347.7 ± 27.2 μM, *V*max = 436.6 ± 148 nmol/min/mg, k_{cat} = 0.24 ± 0.08 sec^{-1} and k_{cat}/Km = 690.3 $M^{-1}.sec^{-1}$.

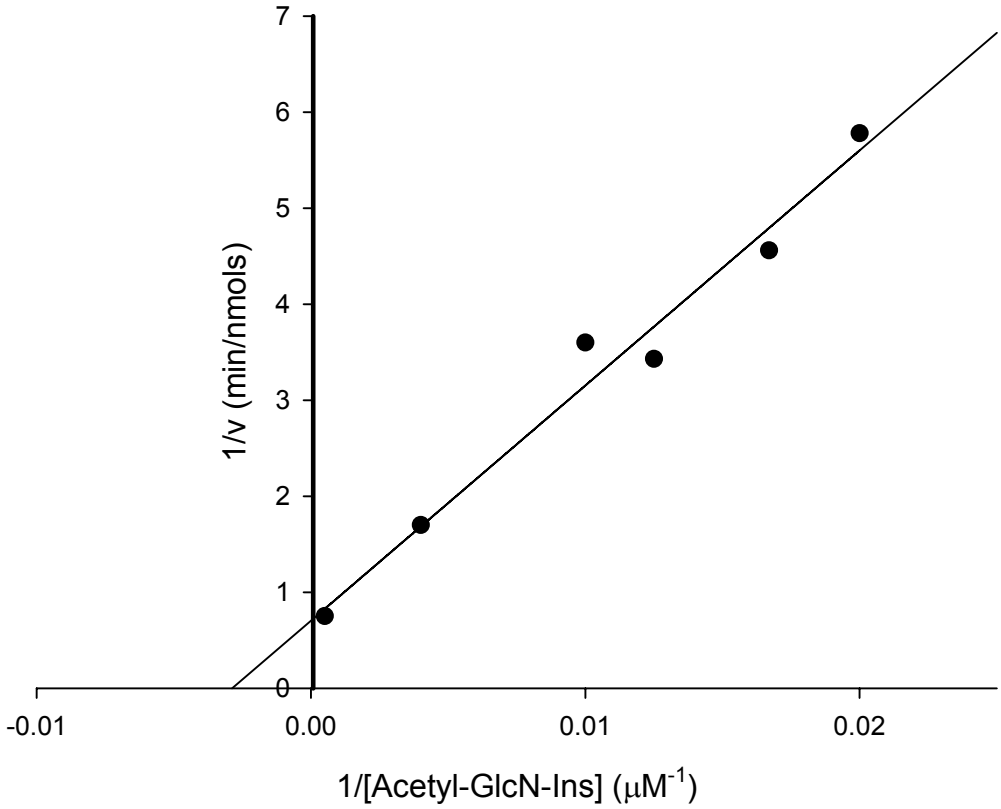

Figure 5.11: Lineweaver-Burk plot of MshB with Acetyl-GlcN-Ins as a substrate. Method 2 was run for the HPLC determination of the kinetic values. The substrate concentrations were 50, 60, 80, 100, 250 and 2000 μM.

The *K*m obtained in this study for Acetyl-GlcN-Ins as a substrate is comparable to the 340 ± 80 μM reported for MshB in Newton *et al.,* 2006. However, the *V*max in the current work is about half the value of 960 ± 150 nmol/min/mg reported by these authors. It is not known whether the higher activity obtained for the His-tagged enzyme is due to the shortened time required for its isolation or due to the presence of the Histag itself; by having either an effect on the activity of the enzyme or on its stability (Newton *et al*., 2006). Protein degradation was not apparent in the present study as witnessed by the pure band obtained at 33 kDa without evidence of a smaller band at 26 kDa (figure 5.8).

5.3.5. Evaluation of structural analogs of Acetyl-GlcN-Ins as MshB substrates

MCL2, J1, JDF1 and JDF2 (figure 5.1) are all structural analogs of Acetyl-GlcN-Ins, which were chemically synthesized to contain thiophenol as aglycon in place of inositol. Because the phenyl group absorbs at 254 nm wavelength, these compounds are readily detectable on HPLC without the need for derivatization. The product resulting from their cleavage with mshB should also give an additional peak on HPLC. Amongst these thiophenyl compounds, MCL2 was the only one which was deacetylated by mshB, and it was therefore further analyzed in detail as a substrate.

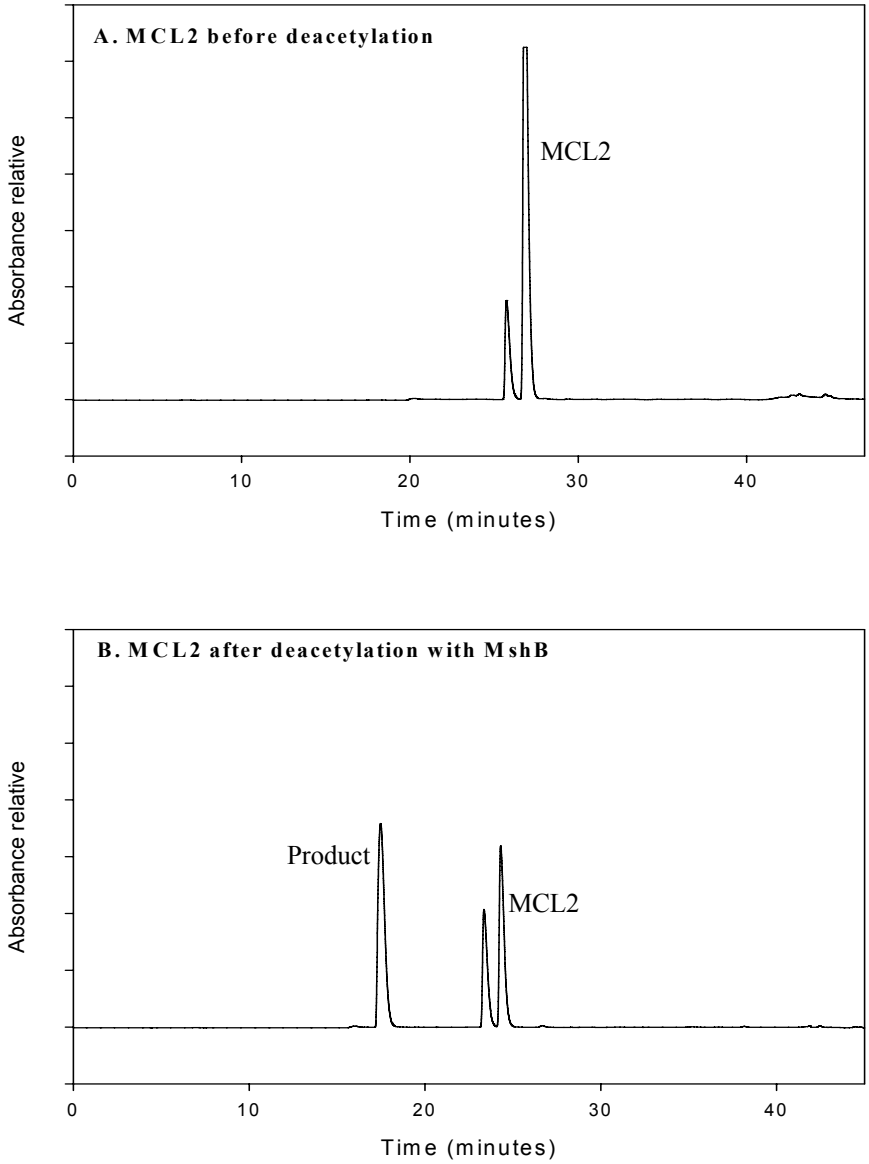

Figure 5.12: HPLC elution profiles showing the cleavage of MCL2 with MshB. C-18 HPLC column (250 x 4.6mm) was eluted with method 1.

In the control experiment (figure 5.12, A), the uncleaved MCL2 gave two sharp peaks between 25 and 30 mins. When the compound was treated with the deacetylase the second large peak was consumed while the first smaller peak remained unchanged. This indicated that MCL2 eluted as the second peak and the first peak may be the β-linked anomer or an uncharacterized contaminant. The deacetylation of MCL2 with mshB resulted in the formation of the product peak at 18 mins as shown in figure 5.12, B. The kinetic parameters of mshB with MCL2 as a substrate were estimated by both Michaelis-Menten and Lineweaver-Burk plots: *K*m value = 1695 ± 151 µM, *V*max = 214 ± 57 nmol/min/mg, k_{cat}= 0.120 ± 0.03 sec^{-1} and k_{cat}/Km = 69.4 $M^{-1}.sec^{-1}$.

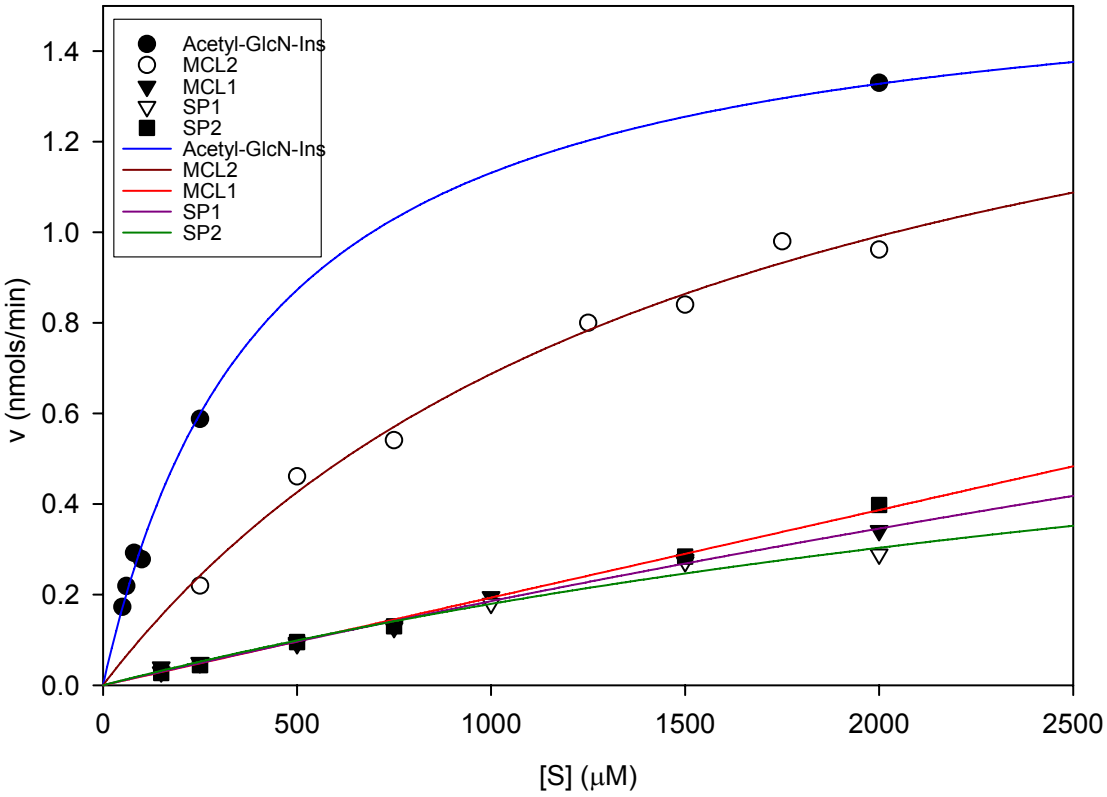

Figure 5.13: Michaelis-Menten plot showing the evaluation of Acetyl-GlcN-Ins, MCL2, MCL1, SP1 and SP2 as substrates for mshB.

Each of the cyclohexane-containing compounds, MCL1, SP1, SP2 and A1120 (figure 5.2), was evaluated separately as a substrate for MshB. The compounds contained a cyclohexane ring as a replacement for *myo*-inositol, present in the natural substrate of mshB. At the end of the incubation with mshB, the reaction mixtures were dansylated

for visualization of the amine formed upon cleavage of the amide bond. The result obtained by HPLC analysis of the dansylated reaction product formed by cleavage of the amide bond in Acetyl-GlcN-Ins is shown in figure 5.14. Dansylated GlcN-Ins eluted at 23 mins, while excess dansyl chloride (DnsCl) eluted at 36 mins. The other by-product of the dansylation, dansyl hydroxide, eluted at 25 mins. Of the four analogs, only A1120 was not cleavable by the deacetylase.

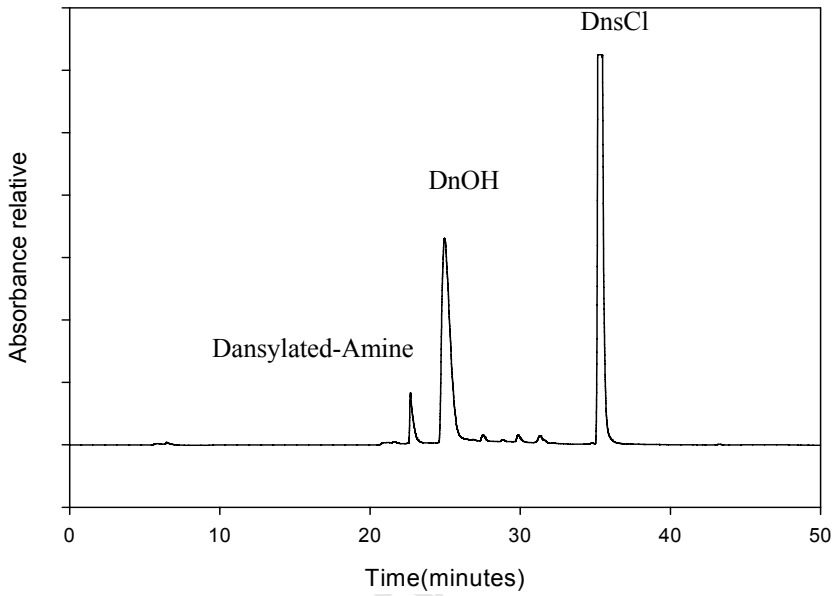

Figure 5.14: Analysis of GlcN-Ins formed during the deacetylation of GlcNAc-Ins by HPLC. Reaction mixtures were dansylated as described in section 2.2.8.2 and analysed by chromatography on a C-18 reversed phase column using a gradient in acetonitrile (Method 1, see Chapter 2).

It seemed that the substrate concentration range used for the evaluation of MCL1, SP1 and SP2 as substrates for mshB was too low to give more accurate kinetic values. The problem is that the compounds are probably not soluble enough to conduct assays in the range that will be suitable for estimation of kinetic parameters. As a result, the comparison between these compounds and the natural substrate was carried out by determining their specific activities. At 250 μM substrate concentration the specific activities were 106, 6.07, 27, 6.11, and 5.45 nmols/min/mg for Acetyl-GlcN-Ins, MCL1, MCL2, SP1 and SP2 respectively.

5.3.6. MshB Inhibition

There are some difficulties associated with chemical synthesis of pseudodisaccharides containing inositol. Some methods involve protecting 5 out of 6 hydroxyl groups, leaving one specific hydroxyl available for substitution with glucosamine (Gammon *et al.,* 2003). The findings in the current study that Acetyl-GlcN-Ins analogs, which contain either a cyclohexane or a phenyl group instead of *myo*-inositol, can serve as substrates of mshB indicate that the inositol moiety is not strictly required for binding to the active site. This therefore inspired the objectives of this study to incorporate testing of compounds containing phenyl and cyclohexyl conjugates as mshB inhibitors. Because the phenyl ring and the glucose moiety of MCL2 are joined by a sulphur atom, some of the potential inhibitors were designed to contain sulphur rather than oxygen. Such compounds are termed thioglycosides.

21 chemically synthesized MSH analogs, grouped as 4 naphthoquinones, 10 various thioglycosides, and 7 *O*-glycosides, were tested as inhibitors of mshB at 500 μM using HPLC assays in the presence of 500 μM Acetyl-GlcN-Ins as a substrate. The inhibion percentages are shown in tables 5.2, 5.3 and 5.4 for thioglycosides, naphthoquinones and *O*-glycosides respectively, and summarized in figure 5.15.

Table 5.2: Inhibition of MshB by Thioglycosides

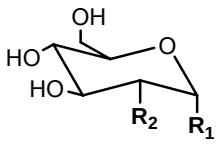

	R_1	R_2	MshB Inhibition
J1	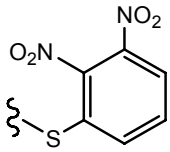	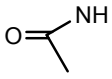	29%
A1120	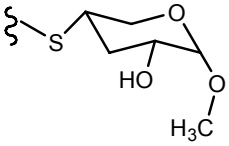	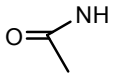	0%
JDF1	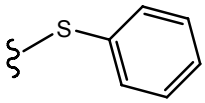	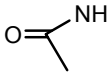	15%
JDF2	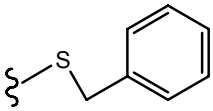	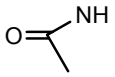	13%
SP2	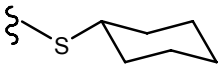	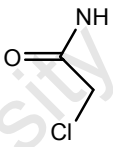	6%
SP3	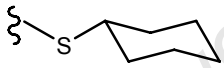		15%
SP4	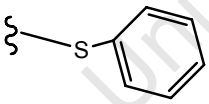		16%
SP5	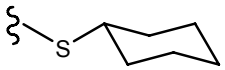	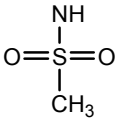	0%
SP6	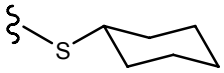	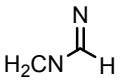	0%
SP7	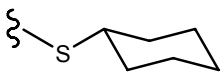	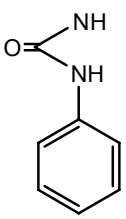	17%

Table 5.3: Inhibition of MshB by Naphthoquinones

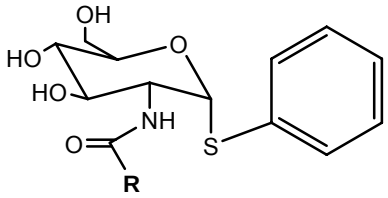

	R	MshB Inhibition
Vu2	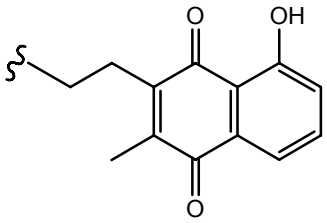	57%
Vu3	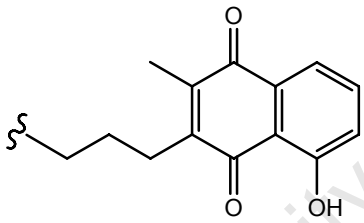	82%
Vu4	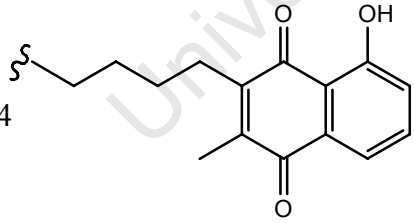	81%
Vu5	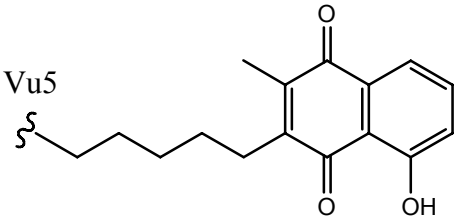	95%

Table 5.4: Inhibition of MshB by *O*-glycosides

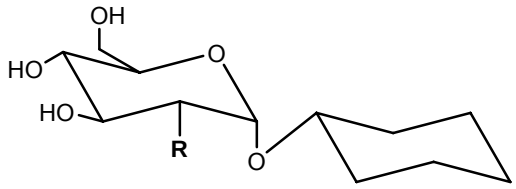

	R	MshB Inhibition
Th1 (β-linkage)	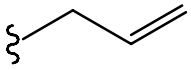	0%
Th2	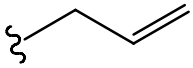	0%
Th3	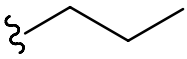	0%
Th4	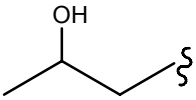	11%
Th5	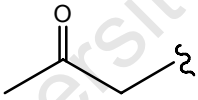	7%
Th6	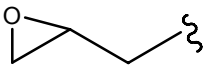	20%
Th7	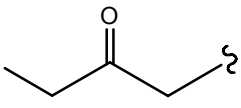	7%

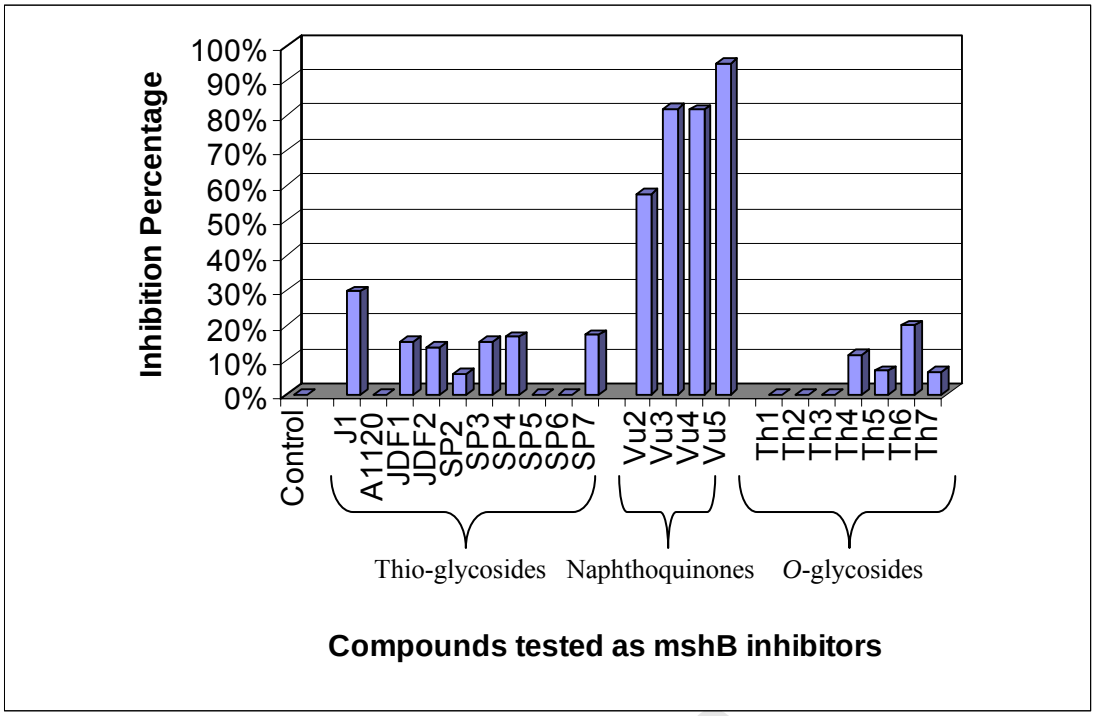

Figure 5.15: The inhibition of mshB. The 21 compounds were tested at 500 μM for inhibition of mshB using HPLC assays. The experiments were performed in the presence of 500 μM Acetyl-GlcN-Ins. The bars represent the average of two assays run in duplicates and the errors were within 10% of the indicated values.

The naphthoquinones displayed the highest inhibition activity against mshB. Vu2, Vu3, Vu4 and Vu5 gave 57%, 82%, 81% and 95% inhibition, respectively, while all other compounds gave less than 30% inhibition. Because of their effectiveness, all the naphthoquinones were selected for a detailed kinetic characterization as mshB inhibitors. The inhibition constants (Ki) of these compounds were determined by HPLC assays using method 2. The assay mixtures contained a constant amount of mshB and varying inhibitor concentrations. The inhibition reactions were performed in presence of varying concentrations of the substrate Acetyl-GlcN-Ins. Figures 5.19a-5.21b present the Lineweaver-Burk plots from which Ki values for Vu2, Vu4 and Vu5, were derived.

Ki determination for Vu2 against MshB

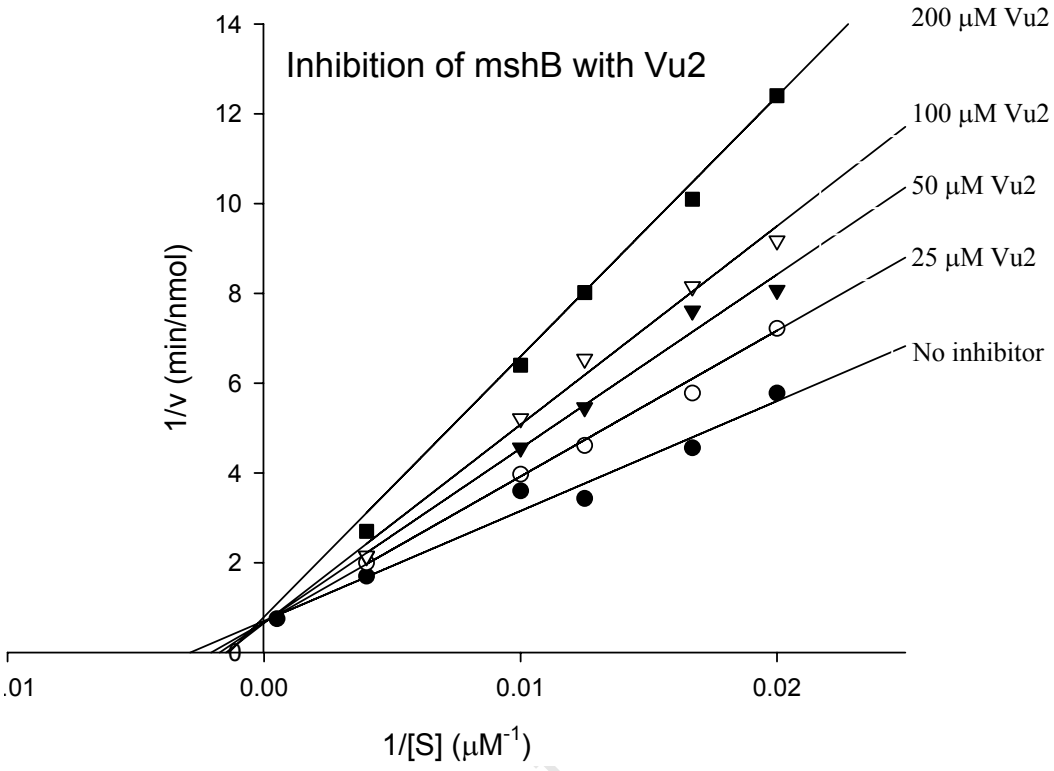

Figure 5.16a: Competitive inhibition of *M. tuberculosis* mshB with Vu2.
The assays were performed by HPLC at the indicated inhibitor concentrations and substrate concentrations of 50, 60, 80, 100 and 250 µM. The 0 µM inhibitor was taken from the values used for mshB *K*m determination for Acetyl-GlcN-Ins where the substrate range was up to 2000 µM.

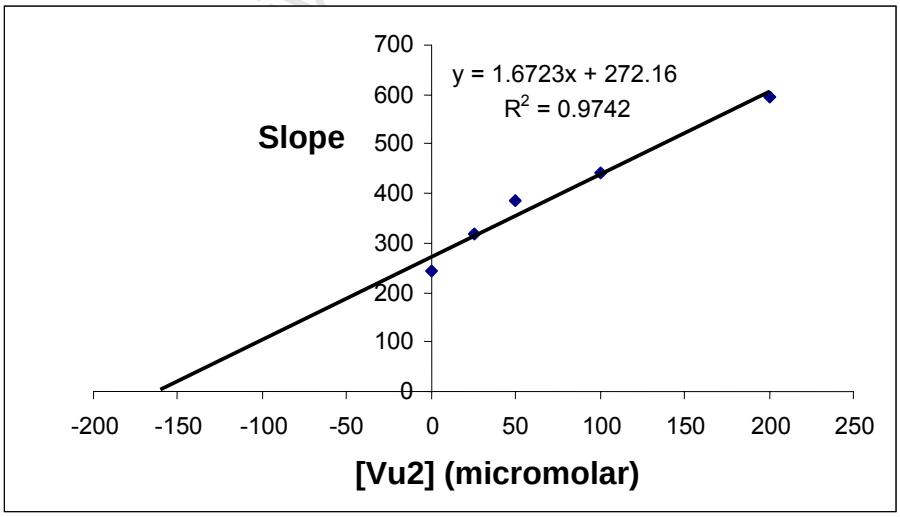

Figure 5.16b: Ki determination for Vu2: Slopes from each inhibitor concentration in the Lineweaver-Burk inhibition plots were plotted against the Inhibitor concentrations (µM). The Ki for mshB is 162.7 ± 15 µM.

Ki determination for Vu4 against MshB

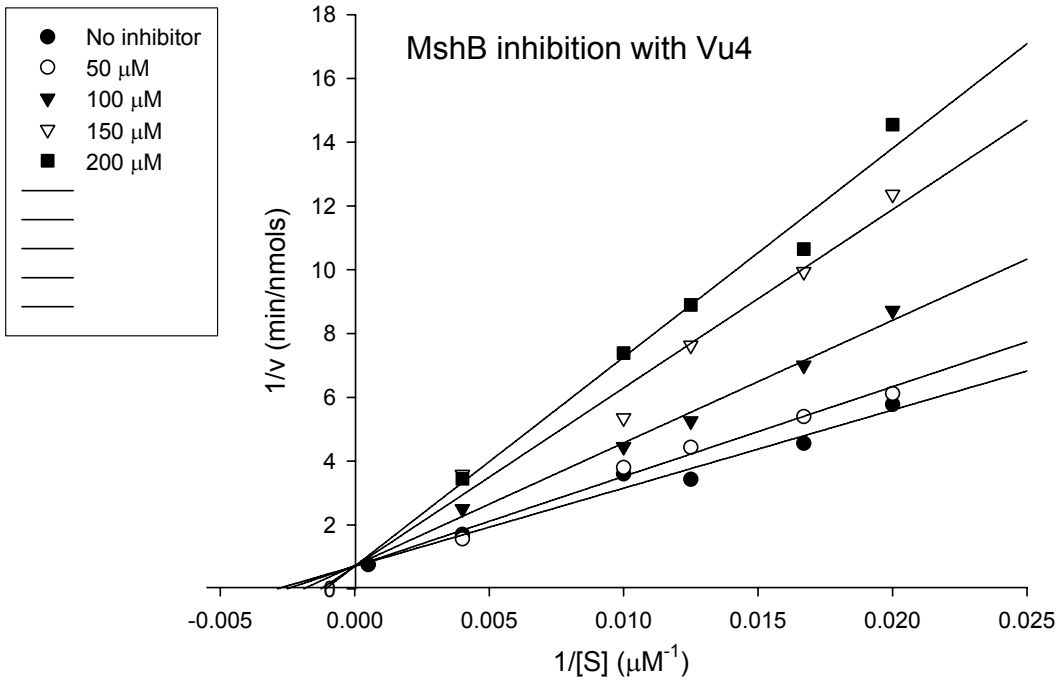

Figure 5.17a: Competitive inhibition of *M. tuberculosis* MshB with Vu4.
The assays were performed by HPLC at the inhibitor concentrations of 50, 100, 150 and 200 μM and the substrate concentration of 50, 60, 80, 100 and 250 μM. The 0 μM inhibitor was taken from the values used for mshB *K*m determination for Acetyl-GlcN-Ins where the substrate range was up to 2000 μM.

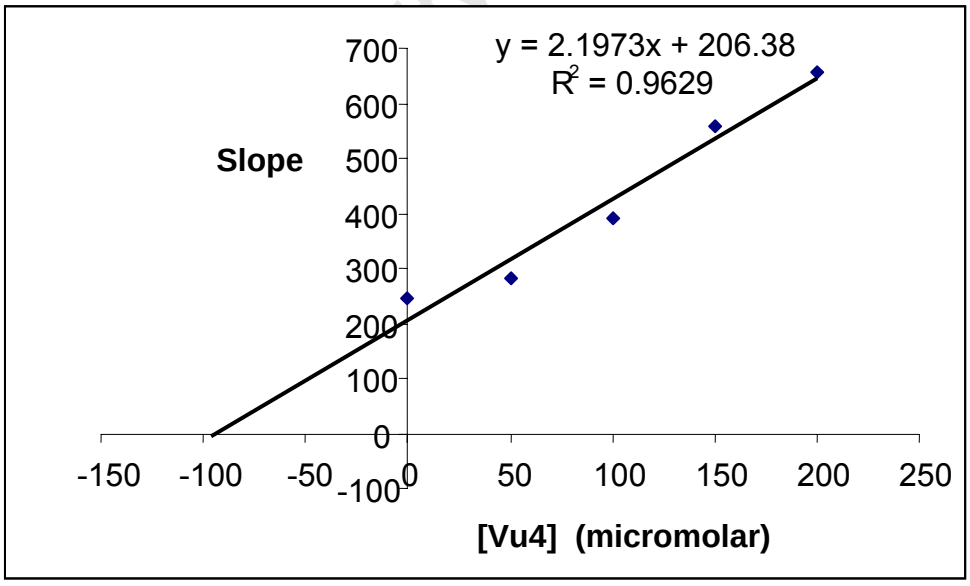

Figure 5.17b: Ki determination for Vu4: Slopes from each inhibitor concentration in the Lineweaver-Burk inhibition plots were plotted against the Inhibitor concentrations (μM). Ki = 93.92 ± 11 μM.

Ki determination for Vu5 against MshB

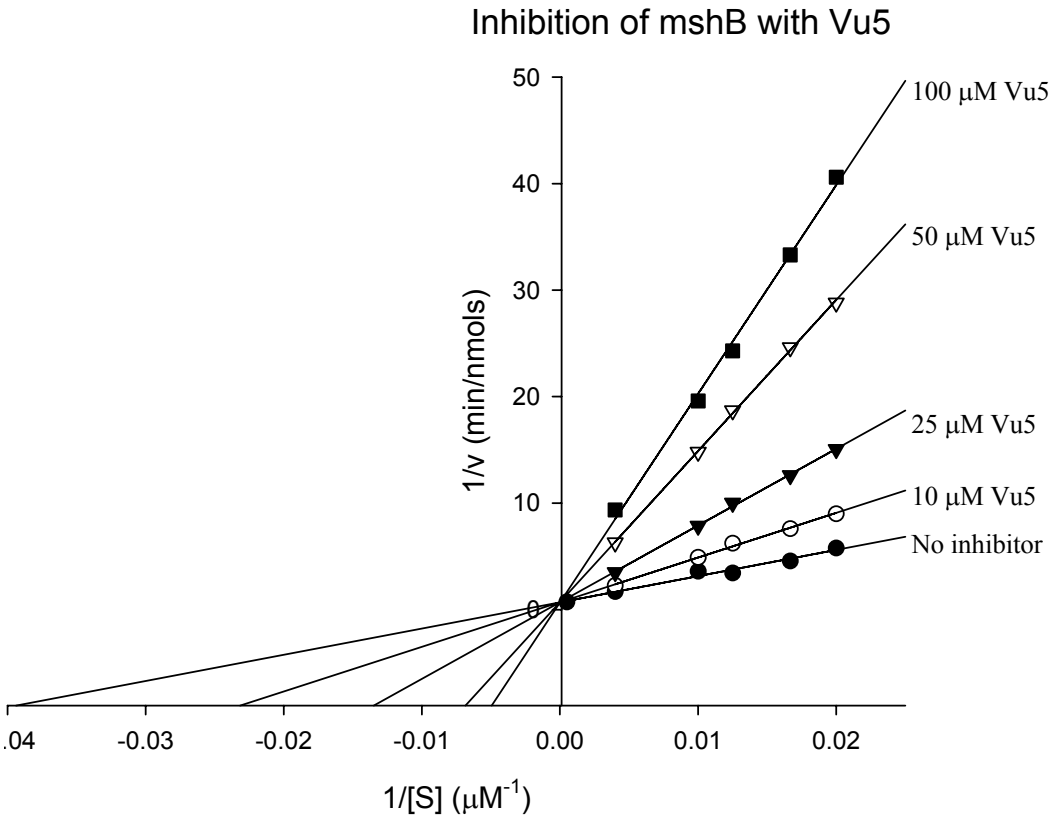

Figure 5.18a: Competitive inhibition of *M. tuberculosis* MshB with Vu5.
The assays were performed by HPLC at the indicated inhibitor concentrations and substrate concentrations of 50, 60, 80, 100 and 250 µM.

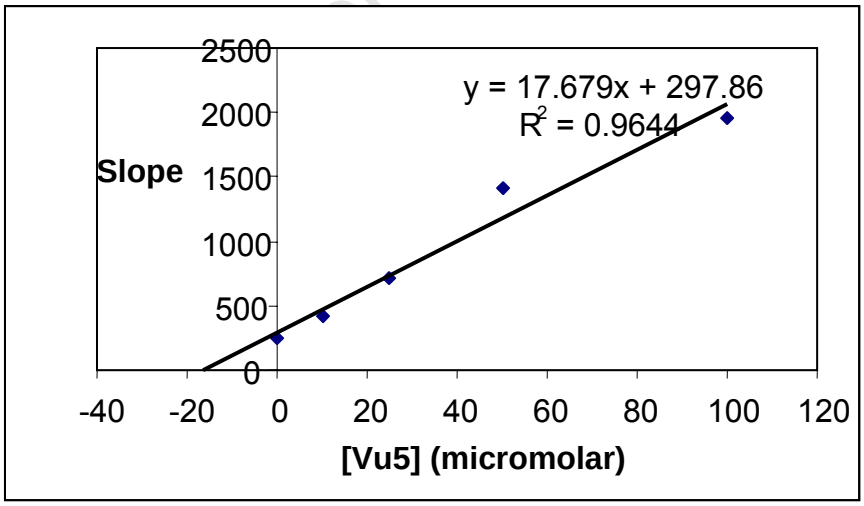

Figure 5.18b: Ki determination for Vu5: Slopes from each inhibitor concentration in the Lineweaver-Burk inhibition plots were plotted against the Inhibitor concentrations (µM). Ki = 16.8 ± 1.9 µM.

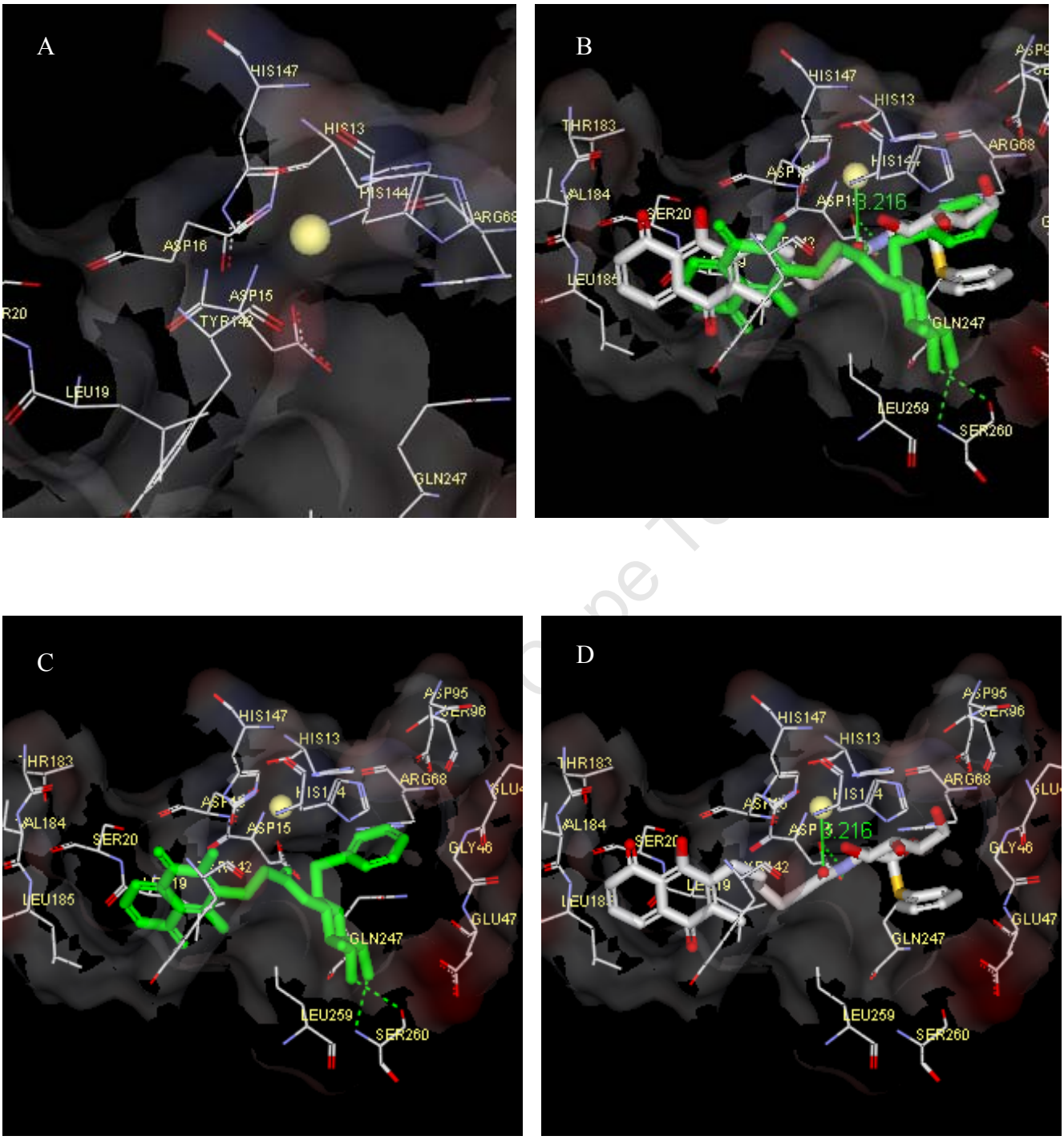

Figure 5.19: Docking of inhibitors Vu2 (green) and Vu5 (white) to MshB.
In all figures Zn^{2+} is shown as a yellow sphere and hydrogen bonding between the ligands and the mshB residues is indicated by dotted green lines. A. The active site of mshB showing the amino acids which play a major role in the catalysis. B. Ligands, Vu2 (green) and Vu5 (white and red), in the active site of mshB. C. Vu2 docked to mshB. D. Vu5 docked to mshB. The distance between Zn^{2+} and Vu5 is 3.216 Å.

The x-ray crystal structure of mshB from *M. tuberculosis* has been solved in presence of the natural substrate in the active site (Maynes *et al*., 2003: McCarthy *et al*., 2004). In order to understand the interaction of the novel inhibitors and mshB, the crystal structure solved by Maynes *et al* was used to dock the naphthoquinones using the Accelrys Discovery Studio 17. Proper zinc coordination geometry is a prerequisite for quality docking of zinc metalloproteinase inhibitors (Hu *et al*., 2004), thus because mshB is also a metalloproteinase, the runs were performed in search of Zn^{2+} as a guide to finding the active site.

The two ligands docked, Vu2 and Vu5, figure 5.22B, occupied the cavity formed by the same residues involved in the binding of Acetyl-GlcN-Ins. The residues in this region include His 13, His 144, His 147, Asp 15, Asp 16, Asp 95, Ser 260, Arg 68 and Gln 45, which were reported to form a cleft-like binding cavity in the active site of mshB (Metaferia *et al*., 2007). These results therefore show that the naphthoquinones bind to the active site of mshB and therefore competitively inhibit the deacetylase as also confirmed by the Lineweaver-Burk plots where *V*max values remained the same before and after the inhibition.

The Ki values of Vu2, Vu4 and Vu5 were found to be 162.7, 93.9 and 16.8 μM against mshB. These values are in agreement with the inhibition percentages of 57%, 81%, and 95% exhibited by the naphthoquinones against the deacetylase as shown in table 5.3 and figure 5.15, indicating that the binding of the compounds to the enzyme increases with the length of the spacer between the naphthoquinone and GlcNAc. In figure 5.22D, the quinone group of Vu5 extends to the non-polar residues, Val 184 and Leu 185, while Vu2, figure 5.22C, cannot stretch towards the residues. This observation is consistent with the observed dependence of active site affinity of the inhibitors on the number of carbon atoms in the spacer. It would therefore be of great interest to evaluate additional naphthoquinones with variable spacer lengths as inhibitors.

CHAPTER 6: GENERAL DISCUSSION

MSH *S*-conjugate amidase, mca, was discovered in the studies aimed at labelling intact *M. smegmatis* with monobromobimane (Newton *et al*., 2000b). In a comparison of different alkylating agents MSmB was found to be the preferred substrate of this enzyme (Steffek *et al*., 2003), but unfortunately monobromobimane is expensive.

In an attempt to discover simple methods for the synthesis of MSH and its precursors, MSSNaph (figure 4.6), which is much less expensive and can be used for the preparation of GlcN-Ins has been identified as an alternate mca substrate. MSSNaph is the immediate product obtained upon the reaction of MSH present in perchlorate extracts of mycobacteria with S-2-(2'-thiopyridyl)-6-hydroxylnaphthyldisulfide and its isolation has been optimized. Although its *K*m is almost 2-fold larger than that of MSmB (table 6.1), mca has a higher affinity for MSSNaph than for 11 out of 12 other compounds previously tested as substrates for mca (Steffek *et al*., 2003), and it can therefore be used as an alternative substrate of the amidase. MSSNaph can be used to assay for mca, without the need to first produce MSH and then MSmB by alkylation with monobromobimane.

Table 6.1: Kinetic constants of mca

Substrate	***K*m**	***V*max**
MSmB	187.6 ± 19.3 μM	64.2 ± 5.5 nmols/min/mg
MSSNaph	328 ± 22 μM	189.6 ± 33 nmols/min/mg

8 structural analogs of Acetyl-GlcN-Ins (figure 5.1 and 5.2), which were chemically synthesized to contain either a spacefilling cyclohexane or a phenyl group instead of *myo*-inositol, were tested as substrates for mshB. Table 6.2 shows the compounds which were cleavable by mshB in the same way that the natural substrate is

deacetylated. At 250 μM substrate concentration, the specific activity for MCL2 was 27 nmols/min/mg, about 4-fold lower than that for Acetyl-GlcN-Ins. At the same substrate concentration the specific activities for MCL, SP1 and SP2 were about 20-fold lower than that of the natural substrate, indicating that the presence of the *myo*-inositol moiety increases the activity or is important for tighter binding to mshB as indicated by a 5-fold increase in the *K*m value when *myo*-inositol is substituted with the phenyl group.

The active site of mshB contains the carboxylate groups (Asp-15, Asp-95, and Asp-146), the hydroxyl groups (Ser-20, Tyr-142, and Ser-260), one amide from the side chain of Gln-247, four main chain carbonyls (Gly-140, Tyr-142, Glu-213, and Ile-214), and two positively charged residues (Arg-68 and His-144), all contributing to the hydrophilic and electronegative nature of the substrate binding pocket (Maynes *et al*., 2003). Carbohydrate-binding molecules containing hydrophilic residues form hydrogen-bonding interactions with the sugar hydroxyl groups (Quiocho, 1993). This therefore explains why the the presence of highly hydrophilic inositol contribute to strong binding to the active site of mshB.

Of all analogs tested MCL2 was the best in terms of binding affinity, giving a *K*m value of 1695 μM. For MCL1, SP1 and SP2 accurate *K*m and *V*max values could not be obtained at the substrate concentration range of 150 to 2000 μM. Because cyclohexane, the substituent on MCL1, SP1 and SP2 is apolar, these compounds were insoluble at higher concentrations where more accurate values can be obtained. The other impediment was that the amount of compounds provided were not enough to evaluate them as substrates at the much higher levels that would have been required.

Table 6.2: Specific activities of mshB with the structural analogs of Acetyl-GlcN-Ins.

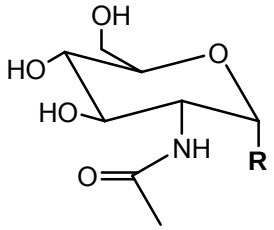

R-substituent	Specific activity at 250 μM substrate concentration (nmols/min/mg)
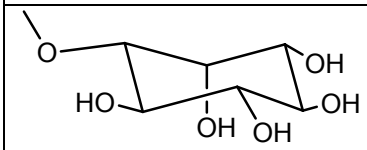 Acetyl-GlcN-Ins	106 nmols/min/mg
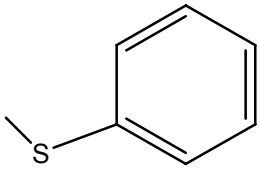 MCL2	27.0 nmols/min/mg
 SP1	6.11 nmols/min/mg
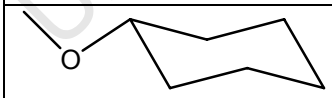 MCL1	6.07 nmols/min/mg
 SP2 Also CH_3 was substituted by Cl on the acetyl moiety	5.45 nmols/min/mg

Newton *et al* showed that the removal of inositol from MSmB also reduces the mca activity by a factor of 45 000 (Newton *et al*., 2006), and elsewhere it was reported that the specific activity of mca for the bimane derivative prepared from the cyclohexane analog of MSH is 7 500 nmol.min^{-1}.mg^{-1}, about half the value of 14 200 nmol.min^{-1}.mg^{-1} for MSmB (Knapp *et al*., 2002).

The disulfide form of des-*myo*-inositol mycothiol was also identified as a substrate of mtr with a *K*m of 400 μM (Patel and Blanchard, 1998), five-fold higher than that for the natural substrate MSSM (*K*m = 73 μM) (Patel and Blanchard, 1999). On the other hand Stewart *et al.* also reported that substituting inositol in MSSM with methyl and benzyl groups increased the *K*m values for the resultant compounds from 113 to 610 and 438 μM, respectively (Stewart *et al*., 2008). Thus, space filling substitutes for inositol within MSSM analogs do not improve the binding of such substrates as compared to des-*myo*-inositol MSSM.

The substitution of inositol with a cyclohexane or a phenyl seems to be an ideal solution in circumventing undesired enzymatic cleavage by glycosidases. The substitution of an oxygen with a sulphur as a linking atom between the rings also provides several possible advantages because R-GlcNAc thioconjugates can be prepared with high anomeric purities and in good yield by *S*-substitution reactions. (Knapp and Myers; 2002), and thioglycosides are more resistant to degradation by glycosidases than *O*-glycosides (Spencer *et al*., 1996; Cohen and Halcomb, 2000; Bousquet *et al*., 2000).
These reports evidently support the advantages of substitution of oxygen with a sulphur atom and thus the thioglycosides, particularly the naphthoquinones, would be more resistant to the degradation by glycosidases if they were to be used as biological inhibitors.

The disruption of the *mshB* gene results in a substantial decrease of MSH production, yielding only 5-10% of the level produced by *M. smegmatis* wild-type mc^{2}155 (Rawat *et al*., 2003). Rv1170, the gene that encodes mshB in *M. tuberculosis*, was first identified as a homolog of *mca* (Newton *et al*., 2000a, b). Both mca and mshB are metalloproteinases depending on zinc for activity and they were both reported to have good activity against MS-acetophenone as a substrate (Steffek *et al*., 2003, Newton *et*

al., 2006). Because of these similarities, it is believed that mca is responsible for the deacetylase activity that produces minute mycothiol in the mshB mutants. Due to the overlapping deacetylase activities of mca and mshB (Newton *et al*., 2006), a complete disruption of MSH production at the deacetylase step can only be achieved by simultaneous inhibition of both these enzymes.

Mtr, the enzyme that maintains MSH at the reduced state, is known to reduce quinones (Patel and Blanchard, 1999). The napthoquinones that have been investigated in this study were initially designed as potential subversive substrates of mtr and it was surprising that they act as the best inhibitors of both mshB and mca. This, seen together with the work of Metafaria *et al*., 2007, which reported the first inhibitors of both mca and mshB, does raise the possibility of designing inhibitors that will inhibit several enzymes to do with mycothiol metabolism.

In the present study 21 MSH analogs were, therefore, tested against both mca and mshB with the goal of finding a single compound that could inhibit both enzymes. The inhibition of mca and mshB with thioglycosides, naphthoquinones and *O*-glycosides is shown in figure 4.9 and 5.15 respectively. The results identified the *O*-glycoside, Th2, as the best inhibitor of mca with 74% inhibition, followed by the naphthoquinones Vu2, 3, 4 and 5, which gave 29, 38, 23 and 44% inhibition. On the other hand, the naphthoquinones, Vu2, 3, 4 and 5 were the best inhibitors against mshB giving inhibition percentages of 57, 82, 81 and 95% respectively, while all other compounds tested, including Th2, gave inhibition of less 30% against mshB.

These results suggest that the naphthoquinoes are suitable lead compounds for the development of more potent inhibitors which could completely abolish the biosynthesis of MSH by inhibition of both mca and mshB. In order to rationalize the differences in potency of the available naphthoquinones a somewhat more detailed kinetic study was undertaken. Vu 2, 4 and 5 were all found to be competitive inhibitors of mshB and their Ki values were markedly dependent on the length of the spacer between the naphthoquinone and glucosamine moieties, as shown in Table 6.3. The Ki value of Vu3 was not determined as it was not expected to be significantly different from that of Vu4; based on their similar inhibition percentage against mshB (figure 5.15).

Table 6.3: Ki values for the most potent inhibitors of MshB

Compounds	Ki (μM)
Vu2	162.7 ± 15
Vu4	93.9 ± 11
Vu5	16.8 ± 1.9

The Ki values of the naphthoquinones indicate that the binding affinity increases with the number of carbon chains. To understand this phenomenon, the naphthoquinones with 2 carbons and 5 carbons, Vu2 and 5, were docked to mshB crystal structure previously published by Maynes *et al*., 2003. The docking results suggest a possible binding of the *S*-phenyl motif of the compounds to a hydrophobic region of mshB. The longer carbon chain of Vu5 extends the molecule such as to allow interaction of naphthoquinone moiety with the hydrophobic dipeptide of Val 184 and Leu 185. The docking of Vu2 and Vu5 into the active site of mshB provided a hypothetical model for the binding mode of the naphthoquinones as inhibitors of mshB. A similar pattern of inhibition was observed where naphthoquinones with longer carbon chains were also better inhibitors of mca.

CONCLUSION

In this study MSH was extracted from *M. smegmatis* and used to synthesize the substrates for mca and mshB. Mca was partially purified from *M. smegmatis* using ion exchange chromatography and hydroxyapatite. MSSNaph was found to be a substrate of mca with a *K*m value better than most of the alternate substrates reported. Although it was not better than MSmB as a substrate, MSSNaph provides an inexpensive alternate assay for mca. MshB was expressed in *E. coli* BL21 DE3 pLysS cells and purified to electrophoretic homogeneity using ion exchange, affinity and size exclusion chromatography. A thiophenyl structural analog of Acetyl-GlcN-Ins, MCL2, was found to be a substrate for mshB, albeit 5-fold higher *K*m value.

The study has also discovered novel compounds which inhibit the MSH-biosynthetic enzyme, mshB, and mca, a key enzyme in the MSH-dependent detoxification pathway in *M. tuberculosis*. The fact that the naphthoquinones, which were *ab initio* designed as potential subversive substrates of mycothioldisulfide reductase, were now found to be also the most potent inhibitors of mshB, and have also some activity against mca, suggest that the design of inhibitors which interfere simultaneously with the function of several different enzymes is a viable objective.

FUTURE RESEARCH

A more detailed comparative study of the inhibition of mca and mshB should be undertaken. An evaluation of compounds bearing apolar groups, attached through spacers of variable length to the glucosamine moiety, as potential inhibitors of both mca and mshB will be especially fruitful. Co-crystals of mshB and mca with such compounds will provide further insights and towards this end the availability of a resolved structure of mca will be invaluable.

Experiments on the effect of the most potent inhibitors on mammalian cell lines could be useful in evaluating their cytotoxicity. The evaluation of the compounds against the growth of *M. tuberculosis* as well as *in vivo* models will also be necessary for future research.

REFERENCES:

Anderberg SJ, Newton GL, Fahey RH. (1998) Mycothiol biosynthesis and metabolism. Cellular levels of potential intermediates in the biosynthesis and degradation of mycothiol in mycobacterium smegmatis. J Biol Chem. 273(46): 30391-7.

Ayvazian LF. (1993) History of tuberculosis. Lung biology in health and disease vol. 66 (2 p.1/2):1-20.

Bacchawat N, Mande SC. (1999) Identification of the INO1 gene of Mycobacterium tuberculosis H37Rv reveals a novel class of inositol-1-phosphate synthase enzyme. J Mol Biol. 291(3): 531-6.

Bloom BR, Murray CJL. (1992) Tuberculosis: commentary on a reemergent killer. *Science* 257(5073):1055-64.

Bornemann C, Jardine MA, Spies HS, Steenkamp. (1997) Biosynthesis of mycothiol: elucidation of the sequence of steps in Mycobacterium smegmatis. Biochem J. 325 (Pt 3): 623-9.

Bousquet E, Spadaro A, Pappalardo M S, Bernardini R, Romeo R, Panza L, Ronisvalle G. (2000) Synthesis and immunostimulating activity of a thioglycolipopeptide glycomimetic as a potential anticancer vaccine derived from Tn antigen *J. Carbohydr. Chem.* 19 : 527-541.

Brennan PJ, Nikaido H. (1995) The envelope of mycobacteria. *Annu Rev Biochem. 64*: 29-63.

Brosch R, Gordon SV, Marmiesse M, Brodin P, Buchrieser C, Eiglmeier K, Garnier T, Gutierrez C, Hewinson G, Kremer K, Parsons LM, Pym AS, Samper S, van Soolingen D, Cole ST. (2002) A new evolutionary scenario for the *Mycobacterium tuberculosis* complex. Proc Natl Acad Sci U S A. 99(6):3684-9.

Bryk R, Lima CD, Erdjument-Bromage H, Tempst P, Nathan C. (2002) Metabolic enzymes of mycobacteria linked to antioxidant defense by a thioredoxin-like protein. *Science*. 295:1073–1077.

Buchmeier N, Fahey RC. (2006). The mshA gene encoding the glycosyltransferase of mycothiol biosynthesis is essential in Mycobacterium tuberculosis Erdman. FEMS Microbiol Lett. 264(1): 74-9.

Buchmeier NA, Newton GL, Fahey RC. (2006) A mycothiol synthase mutant of Mycobacterium tuberculosis has an altered thiol-disulfide content and limited tolerance to stress. J Bacteriol. 188(17):6245-52.

Campbell NF, Hubbard LE, Mazenko RS, Medina MB. (1997) Development of a chromatographic method for the isolation and detection of hygromycin B in biological

fluids. Journal of Chromatography B: Biomedical Sciences and Applications. Vol 692, Issue 2: 367-374**.**

Camus JC, Pryor MJ, Médigue C, Cole ST. (2002) Re-annotation of the genome sequence of Mycobacterium tuberculosis H37Rv. Microbiology.148(Pt 10): 2967-73.

Centers for Disease control and prevention. (2006) Emergence of *Mycobacterium tuberculosis* with extensive resistance to second-line drugs--worldwide, 2000-2004. MMWR Morb Mortal Wkly Rep. 55(11):301-5.

Chae HZ, Chung SJ, Rhee SG. (1994) Thioredoxin-dependent peroxide reductase from yeast. J. Biol. Chem. Vol. 269, Issue 44: 27670-27678.

Christianson DW, Lipscomb NW. (1989) Carboxypeptidase A. *Acc. Chem. Res.* 22: 62-69.

Chua J, Deretic V. (2004) Mycobacterium tuberculosis reprograms waves of phosphatidylinositol 3-phosphate on phagosomal organelles. J Biol Chem. 279(35): 36982-92.

Clark-Curtiss JE, Haydel SE. (2003) Molecular genetics of *Mycobacterium tuberculosis* pathogenesis. Annu Rev Microbiol. 57: 517-49.

Clerici M, Sarin A, Coffman RL, Wynn TA, Blatt SP, Hendrix CW, Wolf SF, Shearer GM, Henkart PA. (1994) Type 1/type 2 cytokine modulation of T-cell programmed cell death as a model for human immunodeficiency virus pathogenesis. Proc Natl Acad Sci U S A. 91(25): 11811-5.

Cohen SA, Michaud DP. (1993) Synthesis of a fluorescent derivatizing reagent, 6-aminoquinolyl-N-hydroxysuccinimidyl carbamate, and its application for the analysis of hydrolysate amino acids via high-performance liquid chromatography. Anal Biochem. 211(2): 279-87.

Cohen SB, Halcomb RL. (2000) Synthesis and Characterization of an Anomeric Sulfur Analogue of CMP-Sialic Acid *J. Org. Chem. 65*: 6145-6152.

Colditz GA, Brewer TF, Berkey CS, Wilson ME, Burdick E, Fineberg HV, Mosteller F. (1994) Efficacy of BCG vaccine in the prevention of tuberculosis. Meta-analysis of the published literature. Jama. 271(9): 698-702.

Cole ST, **Brosch R**, **Parkhill J**, **Garnier T**, **Churcher C**, **Harris D**, **Gordon SV**, **Eiglmeier K**, **Gas S**, **Barry CE 3rd**, **Tekaia F**, **Badcock K**, **Basham D**, **Brown D**, **Chillingworth T**, **Connor R**, **Davies R**, **Devlin K**, **Feltwell T**, **Gentles S**, **Hamlin N**, **Holroyd S**, **Hornsby T**, **Jagels K**, **Krogh A**, **McLean J**, **Moule S**, **Murphy L**, **Oliver K**, **Osborne J**, **Quail MA**, **Rajandream MA**, **Rogers J**, **Rutter S**, **Seeger K**, **Skelton J**, **Squares R**, **Squares S**, **Sulston JE**, **Taylor K**, **Whitehead S**, **Barrell BG**. **(1998)** Deciphering the biology of *Mycobacterium tuberculosis* from the complete genome sequence. Nature. 393, 537–544.

Collins KR, Quinones-Mateu ME, Toossi Z, Arts EJ. (2002) Impact of tuberculosis on HIV-1 replication, diversity, and disease progression.AIDS Rev. 4(3):165-76.

Dalton, D. K., S. Pitts-Meek, Keshav S, Figari IS, Bradley A, Stewart TA. **(1993)** Multiple defects of immune cell function in mice with disrupted interferon-gamma genes. Science. 259(5102): 1739-42.

Das B, Thirupathi P, Kumar RA, Laxminarayana K. (2007) Part 148 in the Series Studies on Novel Synthetic Methodologies: Selective Acetylation of Alcohols, Phenols and Amines and Selective Deprotection of Aromatic Acetates using Silica-Supported Phosphomolybdic Acid. Advanced Synthesis & Catalysis. Vol 349, Issue 17-18: 2677 – 2683.

Ducati RG, Ruffino-Netto A, Basso LA, Santos DS. (2006) The resumption of consumption-A review on tuberculosis. *Mem Inst Oswaldo Cruz,* Rio de Janeiro, Vol. *101*(7): 697-714.

Ehlers S, Kutsch S, Benni J, Cooper A, Hahn C, Gerdes J, Orme I, Martin C, Rietschel E. (1999) NOS2-derived nitric oxide regulates the size, quantity and quality of granuloma formation in Mycobacterium avium-infected mice without affecting bacterial loads. Immunology. 98(3): 313-23.

Feng J, Che Y, Milse J, Yin YJ, Liu L, Rückert C, Shen XH, Qi SW, Kalinowski J, Liu SJ. (2006) The gene ncgl2918 encodes a novel maleylpyruvate isomerase that needs mycothiol as cofactor and links mycothiol biosynthesis and gentisate assimilation in Corynebacterium glutamicum. J Biol Chem. 281(16): 10778-85.

Fetterolf B, Bewley CA. (2004) Synthesis of a bromotyrosine-derived natural product inhibitor of mycothiol-S-conjugate amidase. Bioorganic & Medicinal Chemistry Letters. Vol 14, Issue 14: 3785-3788.

Fox W, **Ellard GA**, **Mitchison DA. (1999)** Studies on the treatment of tuberculosis undertaken by the British Medical Research Council tuberculosis units, 1946-1986, with relevant subsequent publications. Int J Tuberc Lung Dis. 3(10 Suppl 2):S231-79.

Gammon DW, Hunter R, Steenkamp DJ, Mudzunga TT. (2003) Synthesis of 2-deoxy-2-C-alkylglucosides of myo-inositol as possible inhibitors of a N-deacetylase enzyme in the biosynthesis of mycothiol. Bioorg Med Chem Lett. 13(12): 2045-9.

Gandhi NR, Moll A, Sturm AW, Pawinski R, Govender T, Lalloo U, Zeller K, Andrews J, Friedland G. (2006) Extensively drug-resistant tuberculosis as a cause of death in patients co-infected with tuberculosis and HIV in a rural area of South Africa. Lancet 368: 1575–80.

Glickman MS, Jacobs Jr WF. (2001) Microbial pathogenesis of Mycobacterium tuberculosis: dawn of a discipline. Cell. 104(4): 477-85.

Gros C, Labouesse B. (1969) Study of the dansylation reaction of amino acids, peptides and proteins. Eur J Biochem. 7(4):463-70.

Grund E, Denecke B, Eichenlaub R. (1992) Naphthalene degradation via salicylate and gentisate by Rhodococcus sp. strain B4. Appl Environ Microbiol. 58(6): 1874–1877.

Hand CE, Honek JF. (2005) Biological chemistry of naturally occurring thiols of microbial and marine origin. J Nat Prod. 68(2): 293-308.

Handa N, Terada T, Kamewari Y, Hamana H, Tame JRH, Park SY, Kinoshita K, Ota M, Nakamura H, Kuramitsu S, Shirouzu M, Yokoyama S. (2003) Crystal structure of the conserved protein TT1542 from *Thermus thermophilus* HB8. *Protein Science*. 12:1621-1632.

Hu X, Balaz S, Shelver WH. (2004) A practical approach to docking of zinc metalloproteinase inhibitors. *J. Mol. Graph. Model. 22*: 293–307.

Isabelle D, Simpson DR, Daniels L. (2002) Large-Scale Production of Coenzyme F_{420}-5,6 by Using *Mycobacterium smegmatis*. Applied and Environmental Microbiology. Vol. 68, No. 11: 5750-5755.

Jardine MA, Spies HS, Nkambule CM, Gammon DW, Steenkamp DJ. (2002) Synthesis of mycothiol, 1D-1-O-(2-[N-acetyl-L-cysteinyl]amino-2-deoxy-alpha-D-glucopyranosyl)-myo- inositol, principal low molecular mass thiol in the actinomycetes. Bioorg Med Chem. 10(4): 875-81.

Jawahar MS. (2004) Current trends in chemotherapy of tuberculosis. Indian J Med Res. 120:398-417.

Jones KD, Hesketh T, Yudkin J. (2008) Extensively drug-resistant tuberculosis in sub-Saharan Africa: an emerging public-health concern. Trans R Soc Trop Med Hyg. 102(3): 219-24.

Jungbauer A, Machold C, Hahn R. (2005) Hydrophobic interaction chromatography of proteins.III Unfolding of proteins upon adsorption. *J Chromatog.A*.1079: 221-228.

Keil B. (1992) *Specificity of Proteolysis*. Springer-Verlag: Berlin, Germany.

Ketterer B. (1988) Protective role of glutathione and glutathione transferases in mutagenesis and carcinogenesis. *Mutation Res.* 202: 343−361.

Knapp S, Gonzalez S, Myers DS, Eckman LL, Bewley CA. (2002) Shortcut to mycothiol analogues. Org Lett. 4(24): 4337-9.

Knapp S, Myers DS. (2002) Synthesis of alpha-GalNAc thioconjugates from an alpha-GalNAc mercaptan. J Org Chem. 67(9): 2995-9.

Knapp S, Vocadlo D, Gao Z, Kirk B, Lou J, Withers SG. (1996) NAG-thiazoline, an N-acetyl-b-hexosaminidase inhibitor that implicates acetamido participation. *J. Am. Chem. Soc.* 118: 6804-6805.

Koledin T, Newton GL, Fahey RC. (2002) Identification of the mycothiol synthase gene (mshD) encoding the acetyltransferase producing mycothiol in actinomycetes. Arch Microbiol. 178(5): 331-7.

Koledin T, Newton, GL, Fahey RC. (2002) Identification of the mycothiol synthase gene (mshD) encoding the acetyltransferase producing mycothiol in actinomycetes. Arch Microbiol. 178(5): 331-7.

Kosower NS, Kosower E M, Newton GL, Ranney HM. (1979) Bimane fluorescent labels: labeling of normal human red cells under physiological conditions. Proc Natl Acad Sci U S A. 76(7): 3382–3386.

Laemmli UK. (1970) Cleavage of Structural Proteins during the Assembly of the Head of Bacteriophage T4. Nature. 227: 680-685.

Lefevre C, Kang HC, Haugland RP, Malekzadeh N, Arttamangkul S, Haugland RP. (1996) Texas Res-X and rhodamine Red-X, new derivatives of sulforhodamine 101 and lissamine rhodamine B with improved labeling and fluorescence properties. Bioconjug Chem. 7(4): 482-9.

Lin JK, Chang JY. (1975) Chromophoric labeling of amino acids with 4-dimethylaminoazobenzene-4'-sulfonyl chloride. Anal Chem. 47(9): 1634-8.
Lohmann-Matthes ML, Steinmuller C, Franke-Ullmann G. **(1994)** Pulmonary macrophages. Eur Respir J. 7(9): 1678-89.

Mahapatra A, Mativandlela SP, Binneman B, Fourie PB, Hamilton CJ, Meyer JJ, van der Kooy F, Houghton P, Lall N. (2007) Activity of 7-methyljuglone derivatives against *Mycobacterium tuberculosis* and as subversive substrates for mycothiol disulfide reductase. Bioorg Med Chem**.** 15(24): 7638-46.

Mannervik B, Danielson UH, Ketterer B. (1988) Glutathione transferases-structure and catalytic activity. Critical Reviews in Biochemistry and Molecular Biology, Vol, 23,(3): 283 – 337.

Mathema B, Kurepina NE, Bifani PJ, Kreiswirth BN. (2006) Molecular epidemiology of tuberculosis: current insights. Clin Microbiol Rev. 19(4):658-85.

Maynes, J. T.,Garen C, Cherney MM, Newton G, Arad D, Av-Gay Y, Fahey RC, James MN. (2003) The crystal structure of 1-D-myo-inosityl 2-acetamido-2-deoxy-alpha-D-glucopyranoside deacetylase (MshB) from *Mycobacterium tuberculosis* reveals a zinc hydrolase with a lactate dehydrogenase fold. J Biol Chem. 278(47): 47166-70.

McCarthy AA, Peterson NA, Knijff R, Baker EN. (2004) Crystal structure of MshB from *Mycobacterium tuberculosis*, a deacetylase involved in mycothiol biosynthesis. J Mol Biol. 335(4): 1131-41.

Meinnel T, Mechulam Y, Blanquet S. (1995) in *tRNA: Structure, Biosynthesis, and Function.* ASM Press, Washington, DC (RajBhandary, D. S. a. U., Editor) pp 251-292.

Metaferia BB, Fetterolf BJ, Shazad-Ul-Hussan S, Moravec M, Smith JA, Ray S, Gutierrez-Lugo MT, Bewley CA. (2007) Synthesis of natural product-inspired inhibitors of *Mycobacterium tuberculosis* mycothiol-associated enzymes: the first inhibitors of GlcNAc-Ins deacetylase. J Med Chem. 50(25): 6326-36.

Misset-Smits M, van Ophem PW, Sakuda S, Duine JA. (1997) Mycothiol, 1-O-(2'-[N-acetyl-L-cysteinyl]amido-2'-deoxy-alpha-D-glucopyranosyl)-D- myo-inositol, is the factor of NAD/factor-dependent formaldehyde dehydrogenase. FEBS Lett. 409(2): 221-2.

Nathan C, Shiloh MU. (2000) Reactive oxygen and nitrogen intermediates in the relationship between mammalian hosts and microbial pathogens. Proc Natl Acad Sci U S A. 97(16): 8841-8.

Newton GL, Arnold K, Price MS, Sherrill C, Delcardayre SB, Aharonowitz Y, Cohen G, Davies J, Fahey RC, Davis C. (1996) Distribution of thiols in microorganisms: mycothiol is a major thiol in most actinomycetes. J Bacteriol 178(7): 1990-5.

Newton GL, Av-Gay Y, Fahey RC. (2000) N-Acetyl-1-D-myo-inosityl-2-amino-2-deoxy-alpha-D-glucopyranoside deacetylase (MshB) is a key enzyme in mycothiol biosynthesis. J Bacteriol. 182(24): 6958-63.

Newton GL, Av-Gay Y, Fahey RC. **(2000b)** A novel mycothiol-dependent detoxification pathway in mycobacteria involving mycothiol S-conjugate amidase. Biochemistry.39(35):10739-46.

Newton GL, Bewley CA, Dwyer TJ, Horn R, Aharonowitz Y, Cohen G, Davies J, Faulkner DJ, Fahey RC. (1995) The structure of U17 isolated from *Streptomyces clavuligerus* and its properties as an antioxidant thiol. Eur J Biochem. 230:821–825.

Newton GL, Dorian R, Fahey RC. (1981) Analysis of biological thiols: derivatization with monobromobimane and separation by reverse-phase high-performance liquid chromatography. Anal Biochem 114(2): 383-7.

Newton GL, Fahey RC, Cohen G, Aharonowitz Y. (1993) Low molecular weight thiols in streptomycetes and their potential role as antioxidants. J Bacteriol. 175:2734–2742.

Newton GL, Fahey RC. (2002) Mycothiol biochemistry. Arch Microbiol. 178(6): 388-94.

Newton GL, Ko M, Ta P, Av-Gay Y, Fahey RC. (2006) Purification and characterization of Mycobacterium tuberculosis 1D-myo-inosityl-2-acetamido-2-deoxy-alpha-D-glucopyranoside deacetylase, MshB, a mycothiol biosynthetic enzyme. Protein Expr Purif. 47(2): 542-50.

Newton GL, Koledin T, Gorovitz B, Rawat M, Fahey RC, Av-Gay Y. (2003) The glycosyltransferase gene encoding the enzyme catalyzing the first step of mycothiol biosynthesis (mshA). J Bacteriol.185(11): 3476-9.

Newton GL, Ta P, Bzymek KP, Fahey RC. (2006) Biochemistry of the initial steps of mycothiol biosynthesis. J Biol Chem. 281(45): 33910-20.

Newton GL, Ta P, Fahey RC. (2005) A mycothiol synthase mutant of *Mycobacterium smegmatis* produces novel thiols and has an altered thiol redox status. J Bacteriol.187(21): 7309-16.

Ng VH, Cox JS, Sousa AO, MacMicking JD, McKinney JD. (2004) Role of KatG catalase-peroxidase in mycobacterial pathogenesis: countering the phagocyte oxidative burst. *Mol. Microbiol.* 52:1291–1302.

Nicholas GM, Eckman LL, Newton GL, Fahey RC, Ray S, Bewley CA. (2003) Inhibition and kinetics of *Mycobacterium tuberculosis* and *Mycobacterium smegmatis* mycothiol-S-conjugate amidase by natural product inhibitors. Bioorg Med Chem. 11(4): 601-8.

Nicholas GM, Kovác P, Bewley CA. (2002) Total synthesis and proof of structure of mycothiol bimane.J Am Chem Soc. 124(14): 3492-3.

Nicholas GM, Newton GL, Fahey RC, Bewley CA. (2001) Novel bromotyrosine alkaloids: inhibitors of mycothiol S-conjugate amidase. Org Lett**.** 3(10): 1543-5.

Norin A, Van Ophem PW, Piersma SR, Persson B, Duine JA, Jörnvall H. (1997) Mycothiol-dependent formaldehyde dehydrogenase, a prokaryotic medium-chain dehydrogenase/reductase, phylogenetically links different eukaroytic alcohol dehydrogenases--primary structure, conformational modelling and functional correlations. Eur J Biochem**.** 248(2): 282-9.

Ohmoto T, Sakai K, Hamada N, Ohe T. (1991) Salicylic Acid Metabolism through a Gentisate Pathway by *Pseudomonas* sp. TA-2. Agricultural and Biological Chemistry. Vol.55, No.7:1733-1737.

Olsen JV, Ong SE, Mann M. (2004) Trypsin cleaves exclusively C-terminal to arginine and lysine residues. Mol Cell Proteomics. 3: 608-14.

Park JH, Cha CJ, Roe JH. (2006) Identification of genes for mycothiol biosynthesis in Streptomyces coelicolor A3(2). J Microbiol. 44(1): 121-5.

Patel MP, Blanchard JS. (1999) Expression, purification, and characterization of *Mycobacterium tuberculosis* mycothione reductase. Biochemistry. 38(36): 11827-33.

Patel MP, Blanchard JS. 1998 Synthesis of des-*myo*-inositol mycothiol and demonstration of a mycobacterial specific reductase activity. J. Am. Chem. Soc. 120:11538-11539

Patel, MP, Blanchard JS. (2001) *Mycobacterium tuberculosis* mycothione reductase: pH dependence of the kinetic parameters and kinetic isotope effects. Biochemistry. 40(17): 5119-26.

Pérez-Martínez I, Ponce-De-León A, Bobadilla M, Villegas-Sepúlveda N, Pérez-García M, Sifuentes-Osornio J, González-y-Merchand JA Estrada-García T. (2008) A novel identification scheme for genus Mycobacterium complex, and seven mycobacteria species of human clinical impact. Eur J Clin Microbiol Infect Dis. 27(6):451-9.

Pick N, Rawat M, Arad D, Lan J, Fan J, Kende AS, Av-Gay Y. (2006) In vitro properties of antimicrobial bromotyrosine alkaloids. J Med Microbiol. 55(Pt 4): 407-15.

Quiocho FA. (1993) Probing the atomic interactions between proteins and carbohydrates. *Biochem. Soc. Trans.* 21**,** 442–448.

Ramaswamy S, Musser JM. (1998) Genotypic analysis of multidrug-resistant *Mycobacterium tuberculosis* isolates from Monterrey, Mexico. Diagnostics, typing and identification. Journal of Medical Microbiology. 53(2):107-113.

Rawat M, Av-Gay Y. (2007) Mycothiol-dependent proteins in actinomycetes. FEMS Microbiol Rev. 31(3): 278-92.

Rawat M, Kovacevic S, Billman-Jacobe H, Av-Gay Y. (2003) Inactivation of mshB, a key gene in the mycothiol biosynthesis pathway in *Mycobacterium smegmatis*. Microbiology. 149(Pt 5): 1341-9.

Rawat M, Newton GL, Ko M, Martinez GJ, Fahey RC, Av-Gay Y. (2002) Mycothiol-deficient *Mycobacterium smegmatis* mutants are hypersensitive to alkylating agents, free radicals, and antibiotics. Antimicrob Agents Chemother. 46(11): 3348-55.

Rawat M, Uppal M, Newton G, Steffek M, Fahey RC, Av-Gay Y. (2004) Targeted mutagenesis of the Mycobacterium smegmatis mca gene, encoding a mycothiol-dependent detoxification protein. J Bacteriol. 186(18): 6050-8.

Rodriguez J, Gupta N, Smith RD, Pevzner PA. (2008) Does Trypsin Cut Before Proline? *J. Proteome Res. 7* (01): 300–305.

Roitt I, Brostoff J, Male D. (2001) Immunology text book. 6th edition, Mosby international LTD.

Rook GA, Hernandez-Pando R. (1996) The pathogenesis of tuberculosis. Annu Rev Microbiol 50: 259-84.

Russell DG. (2007) Who puts the tubercle in tuberculosis? Nature Reviews Microbiology. vol 5: 39-47.

Sacchettini JC, Rubin EJ, Freundlich JS. (2008) Drugs versus bugs: in pursuit of the persistent predator Mycobacterium tuberculosis. Nat Rev Microbiol. 6(1):41-52.

Sakuda S, Zhou ZY, Yamada Y. (1994) Structure of a novel disulfide of 2-(N-acetylcysteinyl)amido-2-deoxy-alpha-D-glucopyranosyl-myo-inositol produced by Streptomyces sp. Biosci Biotechnol Biochem. 58(7):1347-8

Salgame P, Abrams JS, Clayberger C, Goldstein H, Convit J, Modlin RL, Bloom BR. (1991) Differing lymphokine profiles of functional subsets of human CD4 and CD8 T cell clones. Science. 254(5029): 279-82.

Sareen D, Newton GL, Fahey RC, Buchmeier NA. (2003) Mycothiol is essential for growth of Mycobacterium tuberculosis Erdman. J Bacteriol. 185(22): 6736-40.

Sareen D, Steffek M, Newton GL, Fahey RC. (2002) ATP-dependent L-cysteine:1D-myo-inosityl 2-amino-2-deoxy-alpha-D-glucopyranoside ligase, mycothiol biosynthesis enzyme MshC, is related to class I cysteinyl-tRNA synthetases. Biochemistry. 41(22): 6885-90.

Sassetti CM, Boyd DH, Rubin EJ. (2003) Genes required for mycobacterial growth defined by high density mutagenesis. Mol Microbiol. 48(1): 77-84.

Sassetti CM, Rubin EJ. (2003) Genetic requirements for mycobacterial survival during infection. Proc Natl Acad Sci U S A. 100(22): 12989-94.

Schatz A, Bugie E, Waksman SA. (1944) Streptomycin, a substance exhibiting antibiotic activity against gram-positive and gram-negative bacteria. *Proc. Soc. Exptl. Biol. Med.* 55:66-69.

Schatz A, Waksman SA. (1944) Effect of streptomycin and other antibiotic substances upon *Mycobacterium tuberculosis* and related organisms. *Proc. Soc. Exptl. Biol. Med.* 57:244-248.

Sharma SK, Mohan A, Kadhiravan T. (2005) HIV-TB co-infection: Epidemiology, diagnosis & management. Indian J Med Res. 121: 550-567.

Sharma SK, Mohan A. (2004) Multidrug-resistant tuberculosis. Indian J Med Res.120(4):354-76.

Shen XH, Jiang CY, Huang Y, Liu ZP, Liu SJ. (2005) Functional Identification of Novel Genes Involved in the Glutathione-Independent Gentisate Pathway in *Corynebacterium glutamicum.* Applied and Environmental Microbiology. 71: 3442–3452.

Slättegård R, Gammon DW, Oscarson S. (2007) Synthesis of fused bicyclic thioglycosides of N-acylated glucosamine as analogues of mycothiol. Carbohydr Res. 342(12-13): 1943-6.

Spies HS, Steenkamp DJ. (1994) Thiols of intracellular pathogens. Identification of ovothiol A in Leishmania donovani and structural analysis of a novel thiol from Mycobacterium bovis. Eur J Biochem. 224(1): 203-13.

Steenkamp DJ, Vogt RN. (2004) Preparation and utilization of a reagent for the isolation and purification of low-molecular-mass thiols. Anal Biochem 325(1): 21-7.

Steffek M, Newton GL, Av-Gay Y, Fahey RC. (2003) Characterization of Mycobacterium tuberculosis mycothiol S-conjugate amidase. Biochemistry. 42(41): 12067-76.

Stevens JL, Jones DP. (1989) The mercapturic acid pathway: biosynthesis, intermediary metabolism, and physiological disposition. D Dolphin, R Poulson, O Avramovic, editors, In *Glutathione: Chemical, Biochemical and Medical Aspects*, Wiley Interscience, New York: pp. 46–84.

Stewart MJ, Jothivasan VK, Rowan AS, Wagg J, Hamilton CJ. (2008) Mycothiol disulfide reductase: solid phase synthesis and evaluation of alternative substrate analogues. Org Biomol Chem. 6(2): 385-90.

Ung KSE, Av-Gay Y. (2006) Mycothiol-dependent mycobacterial response to oxidative stress. FEBS Letters. 580: 2712–2716.

Vergne I, Chua J, Deretic V. (2003) *Mycobacterium tuberculosis* phagosome maturation arrest: selective targeting of PI3P-dependent membrane trafficking. Traffic. 4(9): 600-6.

Vetting MW, S de Carvalho LP, Yu M, Hegde SS, Magnet S, Roderick SL, Blanchard JS. (2005) Structure and functions of the GNAT superfamily of acetyltransferases. Arch Biochem Biophys. 433(1): 212-26.

Victor, TC, Streicher EM, Kewley C, Jordaan AM, van der Spuy GD, Bosman M, Louw, H, Murray M, Young D, van Helden PD, Warren RM. (2007) Spread of an emerging *Mycobacterium tuberculosis* drug-resistant strain in the Western Cape of South Africa. INT J TUBERC LUNG DIS. 11(2):195–201.

Vogt RN, Steenkamp DJ, Zheng R, Blanchard JS. (2003) The metabolism of nitrosothiols in the Mycobacteria: identification and characterization of S-nitrosomycothiol reductase. Biochem J. 374(Pt 3): 657-66.

Volmink J, Garner P. (2003) Directly observed therapy for treating tuberculosis. Cochrane Database Syst Rev. (1): CD003343.

Voskuil MI, Schnappinger D, Visconti KC, Harrell MI, Dolganov GM, Sherman DR, Schoolnik GK. (2006) Inhibition of Respiration by Nitric Oxide Induces a *Mycobacterium tuberculosis* Dormancy Program. J. Exp. Med. 198 (5): 705-713.

Wang R, Yin YJ, Wang F, Li M, Feng J, Zhang HM, Zhang JP, Liu SJ, Chang WR. (2007) Crystal structures and site-directed mutagenesis of a mycothiol-

dependent enzyme reveal a novel folding and molecular basis for mycothiol-mediated maleylpyruvate isomerization. J Biol Chem. 282(22): 16288-294.

Weir RE, Gorak-Stolinska P, Floyd S, Lalor MK, Stenson S, Branson K, Blitz R, Ben-Smith A, Fine P EM, Dockrell HM. (2008) Persistence of the immune response induced by BCG vaccination. BMC Infect Dis. 8: 9

Werwath J, Arfmann H, Pieper DH, Timmis KN, Wittich R. (1998) Biochemical and Genetic Characterization of a Gentisate 1,2-Dioxygenase from *Sphingomonas* sp. Strain RW5. Journal of Bacteriology. Vol. 180, No. 16: 4171-4176.

White JL, Hackert M L, Buehner M, Adams MJ, Ford GC, Lentz PJ, Smiley IE, Steindel SJ, Rossmann M G. (1976) A comparison of the structures of apo dogfish M4 lactate dehydrogenase and its ternary complexes. *J. Mol. Biol.* 102: 759–779

Williams MJ. (2007) Conditions Affecting Ergothioneine Levels in *Mycobacterium smegmatis* & The Attempted Isolation of ⟨-*N, N, N*-Histidine Methyltransferase, the First Enzyme in Ergothioneine Biosynthesis. PhD Thesis. University of Cape Town. Pages: 1-158.

Zhou NY, Fuenmayor SL, Williams PA. (2001) *nag* genes of *Ralstonia* (formerly *Pseudomonas*) sp. strain U2 encoding enzymes for gentisate catabolism. *J Bacteriol.* 183, 700-708.

Zink AR, Sola C, Reischl U, Grabner W, Rastogi N, Wolf H, Nerlich1 HG. (2003) Characterization of *Mycobacterium tuberculosis* Complex DNAs from Egyptian Mummies by Spoligotyping. Journal of Clinical Microbiology.Vol. 41, No. 1: 359–367.

Internet References:

www.hivforum.org. (accessed in 2007)

MRC-SA. (2006) Extensively Drug-Resistant Tuberculosis (XDR-TB). http://www.mrc.ac.za/public/fact7.htmhivforum.org, 2007

Todar textbook online. (2008) Kenneth Todar University of Wisconsin Madison Department of Bacteriology http://www.textbookofbacteriology.net/tuberculosis.html

usaid.gov. (2008) HIV/AIDS and Tuberculosis Co-Infection. http://www.usaid.gov/our_work/global_health/id/tuberculosis/techareas/tbhiv.html

WHO global tuberculosis report. (2008) fact sheet no. 104, revised in March 2007. http://www.who.int/mediacentre/factsheets/fs104/en/

WHO Report. (2006) Global Tuberculosis Control: Surveillance, Planning, Financing. Accessed in March 2008. www.who.int/tb

APPENDIX

Appendix A: Standard Curves

A.1. GlcN-Ins standard curve:

Amount of GlcN-Ins (nmols)	Area of the absorbance peak
0.00	0.00
1.167	266414
2.33	557191
4.67	1189342
5.83	1259233

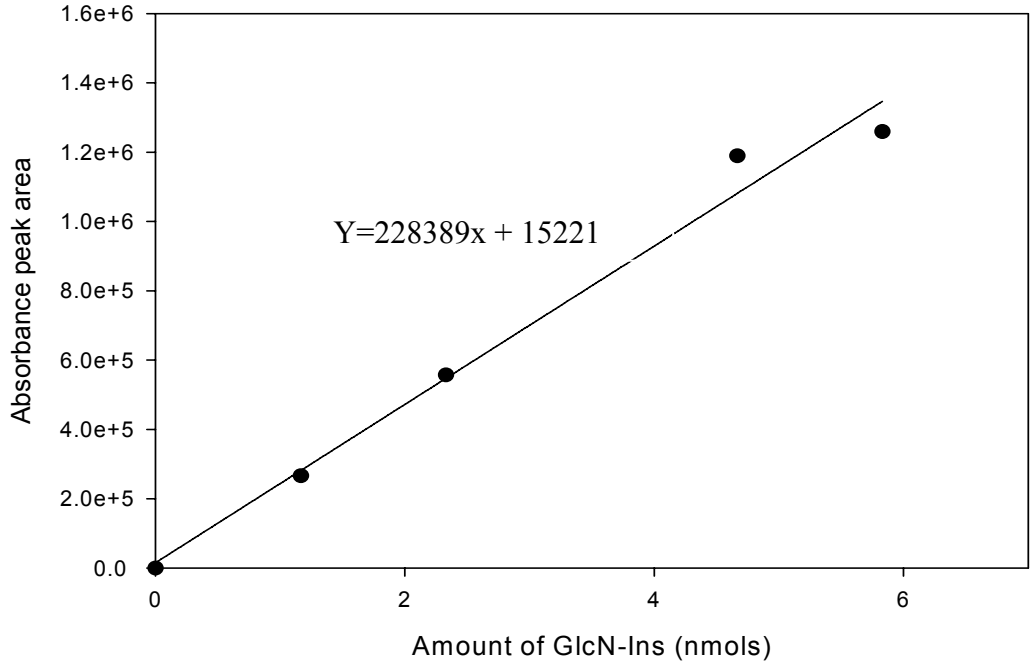

Figure A: Standard curve of GlcN-Ins

A.2. N-Acetyl-L-Cysteine-Bimane standard curve:

Amount of N-Acetyl-L-Cysteine-Bimane (nmols)	Area of the absorbance peak
0	0
2.5	322497
5.0	647321
10	1370537
15	1834788
20	2540788

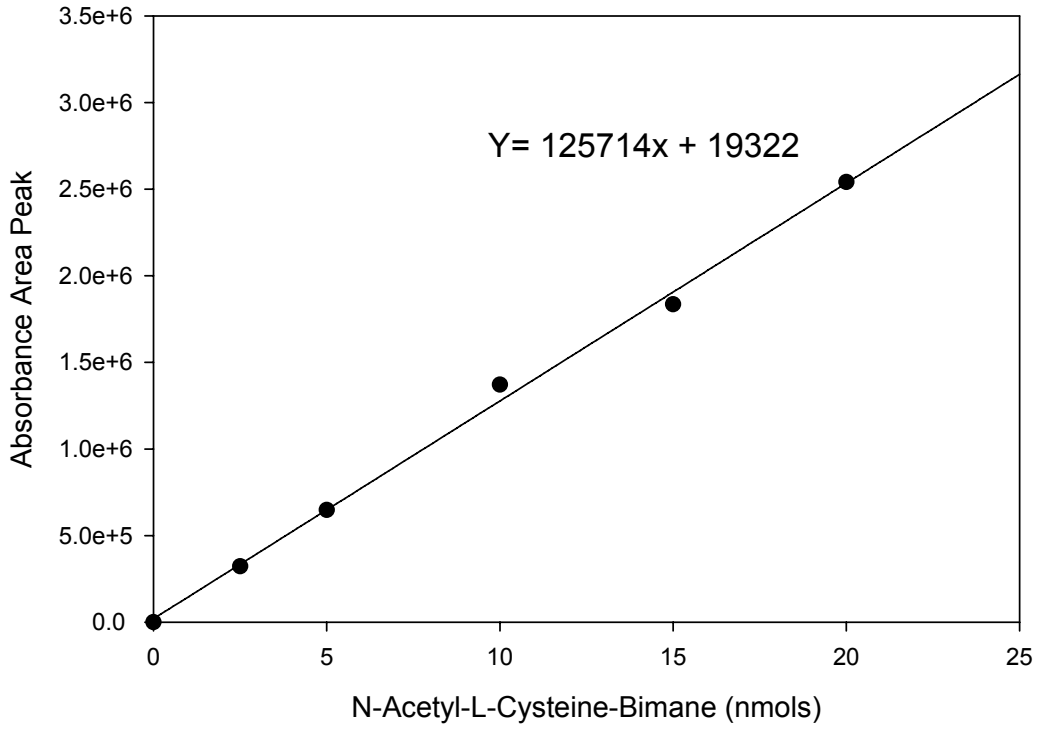

Figure B: Standard curve of N-Acetyl-L-Cysteine-Bimane

A.3. Standard curve for BIORAD protein assay: (Williams M.J, PhD Thesis, 2007).

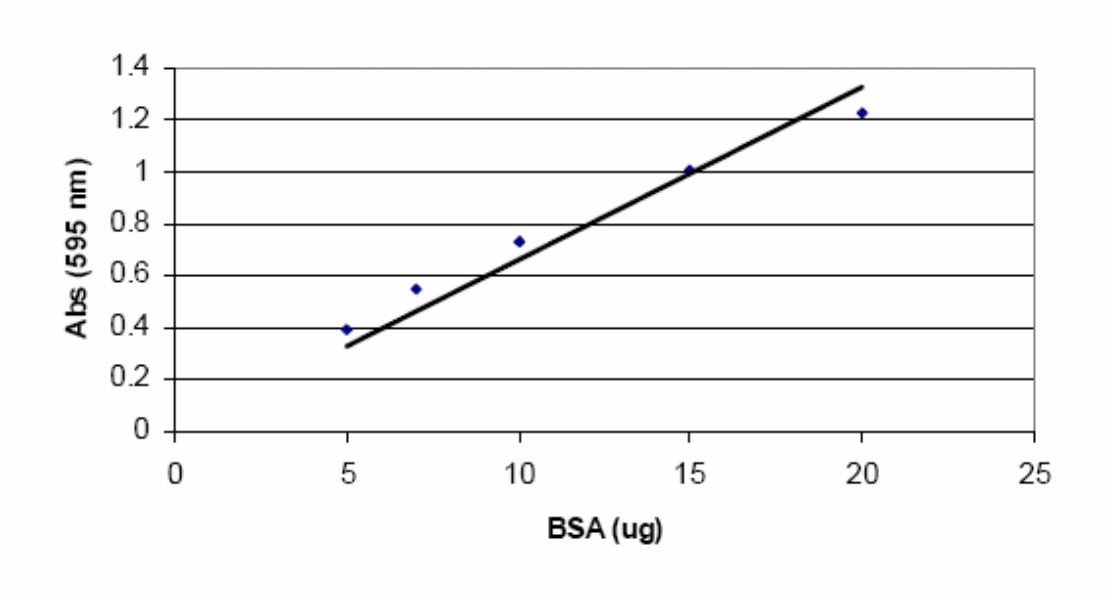

Equation: $Absorbance_{595}$ = BSA (µg) x 0.0662

Figure C: Standrad curve for BIORAD protein assay.

A.4. Protein determination using BIORAD protein assay

- Sample diluted appropriately in 800µl of water
- Assay blank was prepared with 800 µl of either water or buffer
- Added 200 µl of Dye Reagent Concentrate to each sample
- Incubation at room temperature for 5min
- Absorbance measured for samples and blank at 595nm
- Protein concentration was determined by the equation: [protein] = Abs595 x C
- C is determined experimentally using a Bovine Serum albumin standard curve.

A.5. Protein Molecular Weight Markers:

The Electrophoresis Calibration Kit (Pharmacia) used contained the following protein standards:

Phosphorylase b	94 000 Da
Bovine Serum Albumin	67 000
Ovalbumin	43 000
Carbonic Anhydrase	30 000
Soybean Trypsin Inhibitor	20 100
α-Lactalbumin	14 400

The Protein Molecular weight Marker (Fermentas) contains the following protein Standards

β-galactosidase	116 000 Da
Bovine Serum Albumin	66 200
Ovalbumin	45 000
Lactate dehydrogenase	35 000
Restriction Endonuclease Bsp981	25 000
β-lactoglobulin	18 400
lysozyme	14 400

Appendix B: Tables of data used for kinetic plots

Table B1: Data used for the 1/v against 1/[S] plot of mca with MSmB as a substrate

1/[MSmB] (μM^{-1})	1/v (min/nmols)
0.00667	4.53
0.005	4.07
0.004	3.33
0.002	2.93
0.00133	2.45

Table B2: Data used for the 1/v against 1/[S] plot of mca with MSSNaph as a substrate

1/[MSSNaph] (μM^{-1})	1/v (min/nmols)
0.0106	3.03
0.00935	2.79
0.00772	2.55
0.00617	2.00
0.00309	1.38

Table B3: Data used for the 1/v against 1/[S] plot of mshB with Acetyl-GlcN-Ins as a substrate

1/[Acetyl-GlcN-Ins] (μM^{-1})	1/v (min/nmols)
0.0200	5.78
0.0167	4.56
0.0125	3.43
0.0100	3.60
0.0040	1.70
0.0005	0.752

Table B4: Data used for the v against [S] plot of mshB with MCL2 as a substrate

[MCL2] (μM)	v (nmol/min)
250	0.2198
500	0.4608
750	0.5405
1000	0.4808
1250	0.8000
1500	0.8403
1750	0.9804
2000	0.9615

Table B5: Data used for the v against [S] plot of mshB with MCL1 as a substrate

[MCL1] (μM)	v (nmols/min)
250	0.0495
500	0.0912
750	0.1271
1000	0.1949
1500	0.2770
2000	0.3413

Table B6: Data used for the v against [S] plot of mshB with SP1 as a substrate

[SP1] (μM)	v (nmols/min)
150	0.0290

250	0.0498
500	0.0943
750	0.1318
1000	0.1802
1500	0.2717
2000	0.2890

Table B7: Data used for the v against [S] plot of mshB with SP2 as a substrate

[Sp2] (μM)	v (nmols/min)
150	0.0271
250	0.0444
500	0.0954
750	0.1300
1500	0.2841
2000	0.3984

Table B8a: Data for Ki determination of Vu2 against mshB, 1/v versus 1/[S]

1/[Acetyl-GlcN-Ins] (μM^{-1})	No inhibitor 1/v (min/nmols)	25μM Vu2 1/v (min/nmols)	50μM Vu2 1/v (min/nmols)	100μM Vu2 1/v (min/nmols)	200μM Vu2 1/v (min/nmols)
0.0200	5.78	7.22	8.07	9.17	12.4
0.0167	4.56	5.78	7.61	8.15	10.1
0.0125	3.43	4.61	5.46	6.54	8.02
0.0100	3.60	3.97	4.56	5.21	6.40
0.0040	1.70	2.00	2.14	2.15	2.70
0.0005	0.752				

Table B8b: Data for Ki determination of Vu2 against mshB, slope versus [I]

[Vu2] (μM)	Slope
0	245
25	316
50	387
100	442
200	597

Table B9a: Data for Ki determination of Vu4 against mshB, 1/v versus 1/[S]

1/[Acetyl-	No inhibitor	50μM Vu4	100μM Vu4	150μM Vu4	200μM Vu4

GlcN-Ins] (μM^{-1})	1/v (min/nmols)	1/v (min/nmols)	1/v (min/nmols)	1/v (min/nmols)	1/v (min/nmols)
0.0200	5.78	6.12	8.72	12.4	14.6
0.0167	4.56	5.40	7.00	9.94	10.6
0.0125	3.43	4.43	5.26	7.63	8.90
0.0100	3.60	3.80	4.45	5.35	7.39
0.0040	1.70	1.56	2.50	3.58	3.45
0.0005	0.752				

Table B9b: Data for Ki determination of Vu4 against mshB, slope versus [I]

[Vu4] (μM)	Slope
0	245
50	281
100	390
150	559
200	655

Table B10a: Data for Ki determination of Vu5 against mshB, 1/v versus 1/[S]

1/[Acetyl-GlcN-Ins] (μM^{-1})	No inhibitor 1/v (min/nmols)	10μM Vu5 1/v (min/nmols)	25μM Vu5 1/v (min/nmols)	50μM Vu5 1/v (min/nmols)	100μM Vu5 1/v (min/nmols)
0.0200	5.78	9.00	15.0	28.8	40.6
0.0167	4.56	7.60	12.6	24.6	33.3
0.0125	3.43	6.23	10.0	18.7	24.3
0.0100	3.60	4.90	7.85	14.8	19.6
0.0040	1.70	2.26	3.50	6.28	9.36
0.0005	0.752				

Table B10b: Data for Ki determination of Vu5 against mshB, slope versus [I]

[Vu5] (μM)	Slope
0	245

10	419
25	720
50	1418
100	1958

Appendix C: Laboratory Suppliers Contacts

Beckman Coulter Inc.
4300 N. Harbor Boulevard
P.O. Box 3100
Fullerton, CA 92834-3100 USA
www.beckmancoulter.com

BDH Laboratory Suppliers
Poole, Dorset
England BH15 1TD
BioRAD Laboratories
1000 Alfred Nobel Drive
Hercules, CA 94547
www.bio-rad.com

Biospec Products
POB 788
Bartlesville
OK 74005
www.biospec.com

BioTechnology Institute
University of Minnesota
1479 Gortner Avenue
St. Paul, MN55108
http://cbs.umn.edu/bti/

Boehringer Ingelheim
Dept. Fine Chemicals
Binger Straße 173
D-55216 Ingelheim
Germany
www.boehringer-ingelheim.com/finechem

Fermentas International Inc.
830 Harrington Court
Burlington
Ontario L7N 3N4
www.fermantas.com

Grace Vydac
17434 Mojave Street
Hesperia, CA 92345 USA
www.vydac.com

Invitrogen Ltd.
3 Fountain Drive
Inchinnan Business Park
Paisley, UK
PA4 9RF
www.invitrogen.com

KIMIX
P.O. Box 93
7475 Eppindust
South Africa
www.chemicalsupplier.co.za

Merck
Frankfurter StraBe 250
D-6100 Darmstadt 1
www.merck.co.za

Oxoid Limited
Wade Road, Basingstoke
Hampshire RG24 8PW
United Kingdom
www.oxoid.com

Perkin-Elmer
940 Winter Street
Waltham
Massachusetts 02451 USA
www.perkinelmer.com

PhamaTech International
21 Just Rd. Fairfield
New Jersey 07004 USA
www.oriondevel.com/pharmatech/index.aspx

Phenomenex
2320 W. 205th Street
Torrance
California 90501 USA
www.phenomenex.com

Research Organics Inc.

4353 East 49th Street
Cleveland, OH. 44125
http://resorg.com/body.cfm

Roche Ltd.
Group Headquarters
Grenzacherstrasse 124
CH-4070 Basel
Switzerland
www.roche.com

Sigma-Aldrich / Fluka / Riedel-de Haën
Box 14508, St. Louis
Missouri 63178, USA
www.sigma-aldrich.com

The Nest Group Inc.
45 Valley Road
Southborough
MA 01772-1323
www.nestgrp.com

Waters Corporation
34 Maple Street
Milford Massachusetts
01757 USA
www.waters.com

Whatman
info@whatman.com
www.whatman.com